34307

National Library of Canada
Bibliothèque nationale du Canada

CANADIAN THESES ON MICROFICHE

THÈSES CANADIENNES SUR MICROFICHE

NAME OF AUTHOR/*NOM DE L'AUTEUR* David F. Cape

TITLE OF THESIS/*TITRE DE LA THÈSE* An Investigation of the Radioactivity of the Pilot lake Area, N.W.T.

UNIVERSITY/*UNIVERSITÉ* University of Alberta

DEGREE FOR WHICH THESIS WAS PRESENTED/ *GRADE POUR LEQUEL CETTE THÈSE FUT PRÉSENTÉE* Master of Scienc

YEAR THIS DEGREE CONFERRED/*ANNÉE D'OBTENTION DE CE GRADE* 1977

NAME OF SUPERVISOR/*NOM DU DIRECTEUR DE THÈSE* Dr. R.A. Burwash

Permission is hereby granted to the NATIONAL LIBRARY OF CANADA to microfilm this thesis and to lend or sell copies of the film.

The author reserves other publication rights, and neither the thesis nor extensive extracts from it may be printed or otherwise reproduced without the author's written permission.

L'autorisation est, par la présente, accordée à la BIBLIOTHÈQUE NATIONALE DU CANADA de microfilmer cette thèse et de prêter ou de vendre des exemplaires du film.

L'auteur se réserve les autres droits de publication; ni la thèse ni de longs extraits de celle-ci ne doivent être imprimés ou autrement reproduits sans l'autorisation écrite de l'auteur.

DATED/*DATÉ* Oct 14/77 SIGNED/*SIGNÉ* David Cape

PERMANENT ADDRESS/*RÉSIDENCE FIXE*
1786 Dacotah Dr
Windsor, Ontario

NL-91 (3-74)

National Library of Canada

Cataloguing Branch
Canadian Theses Division

Ottawa, Canada
K1A 0N4

Bibliothèque nationale du Canada

Direction du catalogage
Division des thèses canadiennes

NOTICE

The quality of this microfiche is heavily dependent upon the quality of the original thesis submitted for microfilming. Every effort has been made to ensure the highest quality of reproduction possible.

If pages are missing, contact the university which granted the degree.

Some pages may have indistinct print especially if the original pages were typed with a poor typewriter ribbon or if the university sent us a poor photocopy.

Previously copyrighted materials (journal articles, published tests, etc.) are not filmed.

Reproduction in full or in part of this film is governed by the Canadian Copyright Act, R.S.C. 1970, c. C-30. Please read the authorization forms which accompany this thesis.

THIS DISSERTATION
HAS BEEN MICROFILMED
EXACTLY AS RECEIVED

AVIS

La qualité de cette microfiche dépend grandement de la qualité de la thèse soumise au microfilmage. Nous avons tout fait pour assurer une qualité supérieure de reproduction.

S'il manque des pages, veuillez communiquer avec l'université qui a conféré le grade.

La qualité d'impression de certaines pages peut laisser à désirer, surtout si les pages originales ont été dactylographiées à l'aide d'un ruban usé ou si l'université nous a fait parvenir une photocopie de mauvaise qualité.

Les documents qui font déjà l'objet d'un droit d'auteur (articles de revue, examens publiés, etc.) ne sont pas microfilmés.

La reproduction, même partielle, de ce microfilm est soumise à la Loi canadienne sur le droit d'auteur, SRC 1970, c. C-30. Veuillez prendre connaissance des formules d'autorisation qui accompagnent cette thèse.

LA THÈSE A ÉTÉ
MICROFILMÉE TELLE QUE
NOUS L'AVONS REÇUE

NL-339 (3/77)

THE UNIVERSITY OF ALBERTA

AN INVESTIGATION OF THE RADIOACTIVITY OF THE PILOT LAKE AREA, N.W.T.

by

© DAVID F. CAPE

A THESIS
SUBMITTED TO THE FACULTY OF GRADUATE STUDIES AND RESEARCH
IN PARTIAL FULFILMENT OF THE REQUIREMENTS FOR THE DEGREE
OF MASTER OF SCIENCE

DEPARTMENT OF GEOLOGY

EDMONTON, ALBERTA
FALL, 1977

THE UNIVERSITY OF ALBERTA

FACULTY OF GRADUATE STUDIES AND RESEARCH

The undersigned certify that they have read, and recommend to the Faculty of Graduate Studies and Research, for acceptance, a thesis entitled AN INVESTIGATION OF THE RADIOACTIVITY OF THE PILOT LAKE AREA, N.W.T. submitted by DAVID F. CAPE in partial fulfilment of the requirements for the degree of Master of Science

R A Burwash
....
Supervisor

G L Cumming
....

J. Krupicka
....

....

Date ..Aug..31.....1977

DEDICATION

To members of my immediate family: my grandparents, Mr. and Mrs. Frank Cape, who have always been a source of inspiration; my parents, Frank and Mary Cape, whose encouragement and understanding have allowed me to achieve one of the most important goals of my life, and to my lovely sisters Lynne, Kathy and Suzanne.

ABSTRACT

An airborne radiometric survey flown by the Geological Survey of Canada (Darnley annd Grasty, 1970) showed a large anomalous area in the Fort Smith-Great Slave Lake region, N.W.T. Above average radioactivity occurs in a north-trending belt 260 km by 48 km in extent. The eastern margin of this belt crosses Pilot Lake, 55 km northeast of Fort Smith.

In the Pilot Lake region detailed petrologic investigations reveal a foliated, granitic augen gneiss (the Pilot Lake Gneiss) and metasedimentary rock lithologies. These form part of a crystalline basement that has been subjected to high grade metamorphism and polyphase deformation. Outcrop scintillometer surveys indicate the Pilot Lake Gneiss to be some 4.5 times more radioactive than the average metasedimentary rock. Analysis by delayed neutron activation give the following averages: 1.64 ppm uranium and 14.94 ppm thorium for the paragneisses and 11.21 ppm uranium and 105.21 ppm thorium for the Pilot Lake Gneiss.

Also disclosed, were four small lenticular zones of highly radioactive rock within the gneissic complex. Monazite was found to vary from 1 to greater than 3 percent with the following associations recognized in the first three zones: Zone 1, monazite-zircon-apatite-plagioclase; Zone 2, monazite-zircon-apatite-biotite; Zone 3, monazite-

zircon-ilmenite-hematite-anatase-biotite.

Mineralogical and textural relationships suggest an accumulation of monazite as a heavy mineral in placer deposits in an original clastic sequence. In these zones uranium often exceeds 100 ppm and thorium 2000 ppm. Thorium shows an excellent negative correlation with silica and positive correlations with high percentages of total iron and thorium.

Incorporation of these, and similar monazite-bearing sediments, into a granitic magma (melt?) prior to, or during emplacement, has resulted in the above average radioactivity for the Pilot Lake Gneiss. Redistribution of uranium by oxidation during magmatic activity results in the poor correlation of uranium with all major oxides.

Late, very local metasomatism within the Pilot Lake Gneiss may be responsible for the enrichment of uranium to the 100 ppm level in a fourth zone.

ACKNOWLEDGEMENTS

The author wishes to thank Dr. R.A. Burwash for suggestion of this topic, his encouragement and supervision during the preparation and writing of this thesis, and for his thoughtfulness throughout the writer's tenure at the University of Alberta.

The writer is indebted to Dr. Burwash, Dr. J. Kupicka and Mr. Tom Donaghy for their assistance and meaningful discussions while in the field.

Financial support was derived from Department of Energy Mines and Resources and National Research Council of Canada grants to Dr. R.A. Burwash.

I wish to thank my wife, Cindy, for her able assistance in the final preparations of this manuscript. Finally I would like to declare my deepest appreciaton to Mr. and Mrs. C. V. Davies for their warm hospitality and generosity during our stay in Edmonton.

TABLE OF CONTENTS

Page

DEDICATION

ABSTRACT

ACKNOWLEDGEMENTS

CHAPTER ONE-INTRODUCTION

Statement of the problem and location 1

Previous studies 5

Regional geology 6

CHAPTER TWO-PETROLOGY OF THE PILOT LAKE AREA

Geological setting 9

Discussion of map units 12

Pilot Lake Gneiss 12

Petrography 15

Major element analysis 20

Regional extent 30

Metadiorite 31

Variable paragneiss 33

Impure quartzite 35

Porphyroblastic garnet-cordierite gneiss and garnet-cordierite-andalusite gneiss 38

Muscovite-biotite schist 39

Quartzo-feldspathic gneiss 41

Amphibolite 41

CHAPTER THREE-RADIOACTIVITY

Methods and data used 46

Results of the airborne radiometric surveys 49

Investigations in the Pilot Lake area 56

Page

Outcrop scintillometer results 56

Results of U and Th determinations 57

Variable paragneiss 64

Pilot Lake Gneiss 66

Variation in U and Th contents and their geographic distribution 67

Anomalous radioactivity 74

Zone one 78

Petrography and chemistry 81

Zone two 86

Petrography and chemistry 88

Zone three 94

Petrography 99

Chemistry 108

Chemical and mineralogical changes about zone 3 112

Zone four 118

Petrography and chemistry 118

CHAPTER FOUR-DISCUSSION OF RESULTS

Structure and metamorphism 121

Chemical correlatons 125

Petrogenesis of uranium and thorium rich rocks .. 134

Zones one, two and three 134

Pilot Lake Gneiss and Zone four 137

Summary 141

SELECTED BIBLIOGRAPHY 143

APPENDIX I - METHOD FOR DELAYED NEUTRON ACTIVATION

ANALYSIS 149

APPENDIX II- IDENTIFICATION OF RADIOACTIVE MINERALS ... 154

LIST OF TABLES

Page

Table 1. Results of chemical and modal analysis for selected Pilot Lake Gneiss samples 22

Table 2. CIPW normative calculations for Pilot Lake Gneiss samples with key to abbreviations 25

Table 3. Results of chemical and modal analysis for a metadiorite sample 32

Table 4. Results of chemical analysis for selected paragneiss samples 40

Table 5. Results of chemical and normative analysis for an amphibolite sample 45

Table 6. Uranium and thorium contents and Th to U ratios for selected Pilot Lake paragneisses and amphibolite 58

Table 7. Uranium and thorium contents and Th to U ratios for selected Pilot Lake Gneiss samples 59

Table 8. Average uranium and thorium abundances for common sedimentary rocks, granites and the Canadian Shield 68

Table 9. Uranium and thorium contents and Th to U ratios for anomalously radioactive samples .. 79

Table 10. Results of chemical and modal analysis for Zone 1 85

Table 11. Results of chemical and modal analysis for Zone 2 92

Table 12. Results of chemical and modal analysis for Zone 3 106

Table 13. Results of chemical and modal analysis for trench samples Zone 3 114

Table 14. Results of chemical and normative analysis for a sample from Zone 4. 119

Table 15. Results of chemical and modal analysis for two granulite samples. 124

LIST OF FIGURES

Page

Figure 1. Map of the Fort Smith-Great Slave Lake Region 3

Figure 2. Enlarged map of the Fort Smith-Great Slave Lake region 4

Figure 3. Geological sketch map of the Pilot Lake area 10

Figure 4. Total alkalies vs. silica (wt %) diagram 29

Figure 5. An-Or-Ab normative projections of subalkaline rocks 29

Figure 6. Thorium isorad map from G.S.C. Open File Report Number 101, showing the core of the Fort Smith-Great Slave Lake 'high' 52

Figure 7. Flight profiles for the Pilot Lake area from G.S.C. Open File Report Number 101 54

Figure 8. Histogram showing the distribution of uranium for the Pilot Lake paragneisses 60

Figure 9. Histogram showing the distribution of uranium for the Pilot Lake Gneiss 61

Figure 10. Histogram showing the distribution of thorium for the Pilot Lake paragneisses 62

Figure 11. Histogram showing the distribution of thorium for the Pilot Lake Gneiss 63

Figure 12. Histogram showing the distribution of Th to U ratios for the Pilot Lake paragneisses 65

Figure 13. Histogram showing the distribution of Th to U ratios for the Pilot Lake Gneiss 70

Figure 14. Uranium content vs. thorium content for the Pilot Lake Gneiss 71

Figure 15. Uranium content vs. Th to U ratios for the Pilot Lake Gneiss 72

Figure 16. Thorium content vs. Th to U ratios for the Pilot Lake Gneiss 72

Figure 17. Sample collection site map 75

Figure 18. Trends of peak thorium values, peak uranium page

values and an aeromagnetic high 76

Figure 19. Aeromagnetic map of the Pilot Lake area 77

Figure 20. Scintillometer profile for Zone 1 80

Figure 21. Scintillometer profile for Zone 2 87

Figure 22. Scintillometer profile about the main showing in Zone 3 95

Figure 23. Scintillometer profile about the trench south of the main showing in Zone 3 100

Figure 24. Chemical variations in the Pilot Lake Gneiss about a radioactive lens in Zone 3 ... 116

Figure 25. Mineralogical variations in the Pilot Lake Gneiss about a radioactive lens in Zone 3 ... 117

Figure 26. Relation of uranium to SiO2 128

Figure 27. Relation of thorium to SiO2 128

Figure 28. Relation of total iron to SiO2 129

Figure 29. Relation of TiO2 to SiO2 129

Figure 30. Relation of uranium to K2O 130

Figure 31. Relation of thorium to K2O 130

Figure 32. Relation of uranium to total iron 131

Figure 33. Relation of thorium to total iron 131

Figure 34. Relation of uranium to TiO2 132

Figure 35. Relation of thorium to TiO2 132

Figure 36. Relation of TiO2 to total iron 133

Figure 37. Relation of thorium to uranium 133

LIST OF PLATES

Page

Plate 1. Pilot Lake Gneiss 14

Plate 2. Pilot Lake Gneiss 19

Plate 3. Variable Paragneiss 37

Plate 4. Variable Paragneiss 43

Plate 5. Anomalous Zone 1 84

Plate 6. Anomalous Zones 1 and 2 90

Plate 7. Anomalous Zone 3 98

Plate 8. Anomalous Zone 3 103

Plate 9. Mineral Separates and Metamorphic Mineral Relationships 111

CHAPTER I

INTRODUCTION

Statement of the Problem and Location

In the summer of 1969 the Geological Survey of Canada flew a cross-country gamma-ray spectrometry survey between Ottawa, Ontario and Yellowknife, Northwest Territories (Darnley *et al*. 1971). This survey was undertaken to look for broad scale variations in radioactivity levels and to identify previously unreported areas of high radioactivity. The flight between Uranium City, Saskatchewan and Yellowknife became important when a major radiometric 'high' to the east of Fort Smith, Northwest Territories, was discovered.

Several flight lines over this area showed the 'high' to be about 48 km (30 miles) wide and to extend more than 240 km (150 miles) from the LaLoche fault system, which parallels the south side of the East Arm of Great Slave Lake, to south of latitude 60°N.

As a result of this discovery the Geological Survey of Canada in the following summer flew a more detailed radiometric survey (Darnley 1970) covering approximately 39,000 km^2 (15,000 sq. miles) in the Fort Smith - Great Slave Lake region. The area covered is bounded approximately by latitudes 59°45' N and 62°25' N and longitudes 110°00' W and 112°00' W, (see Figs. 1 and 2). This survey, released as

Open File Report Number 101, further outlined the extensive 'high' to have a length of 260 km (160 miles) and an average east to west width of about 48 km (30 miles), its boundaries approximately are; longitudes 111°W and 112°W.

The southeastern corner of the radiometric 'high' crosses Pilot Lake, a rather circular body of water some 7 km (4.3 miles) in diameter, located 55 km (35 miles) northeast of Fort Smith. The lake has been named Pilot Lake because its circular shape in an area of structurally controlled linear bodies of water is an aid in pilot navigation. The south central shore of the lake is located approximately at latitude 60°15' N. and longitude 111°00' W.

As only light follow up ground investigations were carried out by the Geological Survey (Charbonneau 1971) it was decided to undertake a detailed but local petrographic and geochemical study in the Pilot Lake area to determine the cause of the Fort Smith-Great Slave Lake 'high'.

After travelling from Fort Smith by float equipped aircraft, geological investigations were carried out during June of 1975 from a base camp on the shore of Pilot Lake. Radioactive measurements were taken using portable scintillometers along the shores of Pilot Lake and in a second area some 7 to 8 km (4.6 miles) further north. Since the exposure in the area is excellent (over 75 percent excluding water cover) extensive outcrop sampling was carried out. All major lithological rock types encountered,

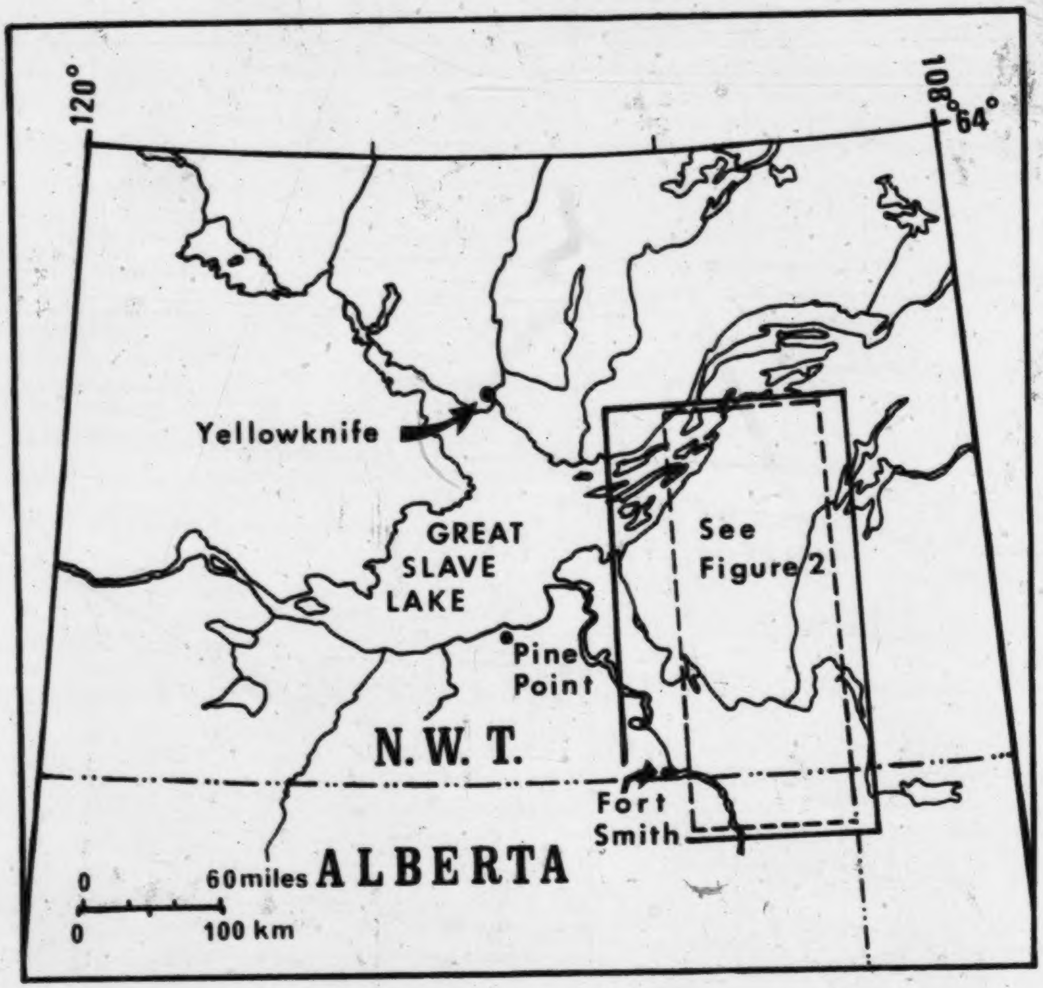

Fig. 1. Map of the Fort Smith-Great Slave Lake region. Area outlined is that enlarged in Fig. 2.

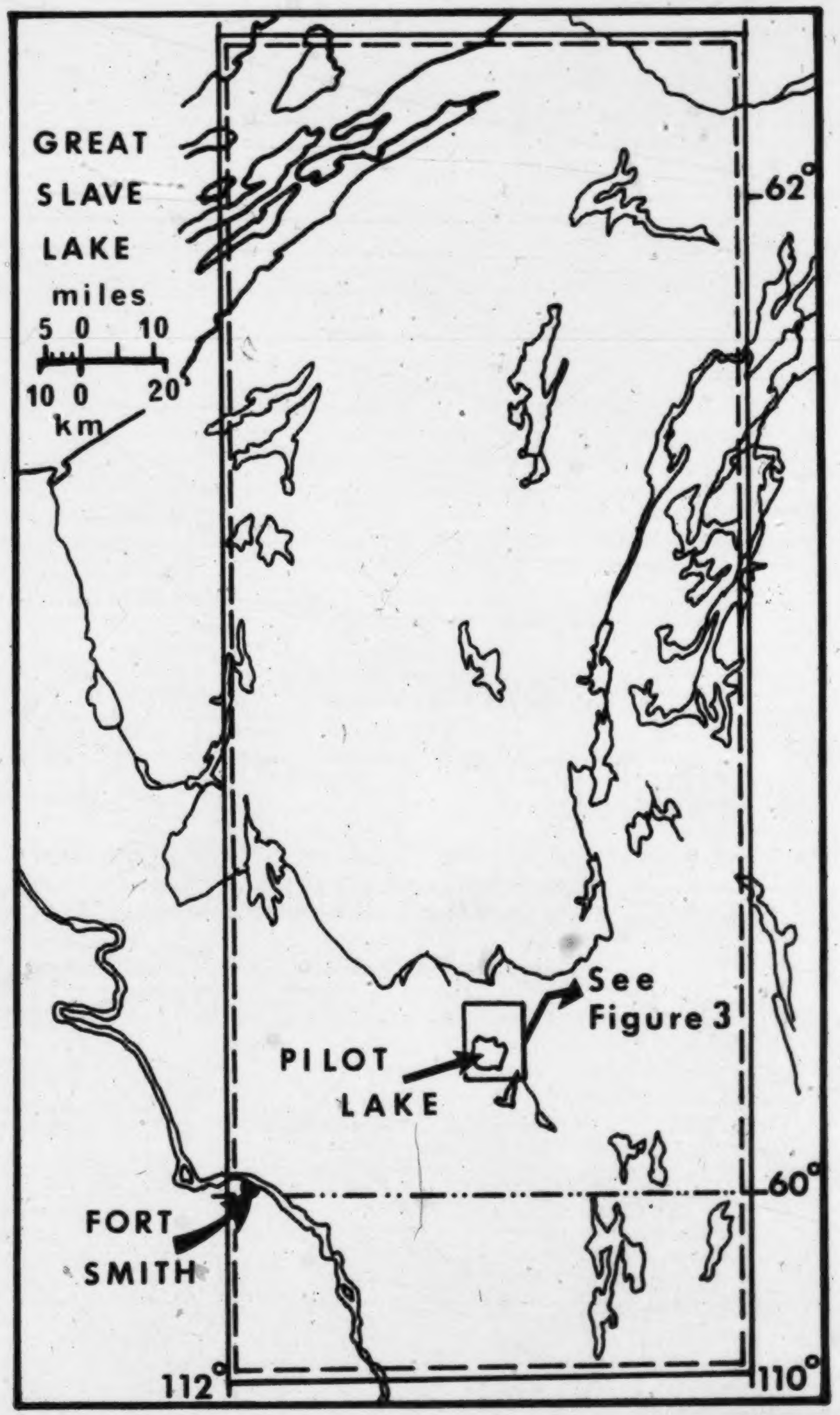

Fig. 2. Enlarged map of the Fort Smith-Great Slave Lake region. Dashed lines outline the boundaries of G.S.C.'s airborne radiometric survey. Pilot Lake area is enlarged in Fig. 3.

with as wide a range of scintillometer values as possible, were collected. Upon returning from the field detailed petrography and uranium and thorium determinations were performed on over 100 samples. Whole rock chemical analysis was undertaken on a selected suite to further aid in the petrogenetic interpretation of the Pilot Lake area.

Previous Studies

Although Samuel Hearne was reported to have visited the Tazin and Talston rivers' area in the early part of 1772 it wasn't until Charles Camsell of the Geological Survey of Canada, travelled down the two rivers between Lake Athabasca and Great Slave Lake in the summer of 1914, that the first geological account was recorded (Camsell 1916).

A lengthy time elapsed before J. Tuzo Wilson in 1941 published a four mile to the inch reconnaissance map of the Fort Smith area, north of the Northwest Territories-Alberta border. G.C. Riley produced a similar geological map in 1960 for the Fort Fitzgerald area, south of the Sixtieth Parallel.

J.D. Godfrey has been mapping the Shield area of northeastern Alberta for the Research Council of Alberta since the late 1950's. Reports have been published on the Charles, Andrew and Colin Lake districts in the extreme northeastern corner of the province, (Godfrey, 1961, 1963, 1964 and 1966).

The two airborne radiometric surveys flown by the

Geological Survey of Canada in 1969 and 1970 have spurred the private search for uranium deposits throughout the area, the extent of which are unknown.

Regional Geology

The rocks of the Pilot Lake area are all Precambrian in age and form part of the western edge of the Churchill Structural Province of the Canadian Shield. Foliated gneisses and metasedimentary rock lithologies make up a polymetamorphic crystalline basement that extends to the south and southwest into the Province of Alberta where it is eventually unconformably overlaid by Paleozoic cover rocks. The belt continues northward toward the fault systems that mark the boundary between the Churchill Province and the East Arm fold belt of Great Slave Lake. The north - south structural trend exhibited by all the major rock types in the area is typical of the Hudsonian structural grain found in this extreme western part of the exposed Churchill Province.

Paralleling the northwestern shore of Lake Athabasca and then turning towards the north to pass through the Charles Lake area of Alberta is a boundary, indicated by Riley (1960), between granitic and porphyroblastic gneisses to the east and equigranular and strongly lineated porphyritic granites to the west. The eastern gneisses have an abundance of sedimentary material associated with them and appear to be part of a true supracrustal paragneissic complex. To the west of the boundary Riley has mapped plutonic granites and granites possibly derived by the granitization of pre-existing sedimentary rocks.

In Alberta, Godfrey and Langenberg (1977) have termed these eastern and western terrains, the Andrew Lake domain and the Leland Lake domain respectively. They suggest that the dominantly granitoid terrain of the Leland Lake domain is the result of remobilization of infrastructure materials (accompanied by reconstitution of supracrustals) during metamorphism.

This boundary appears to continue northward through the Pilot Lake area where well lineated granitic gneiss is found to the west of porphyroblastic gneisses of sedimentary origin.

Aeromagnetic data correlates well with this boundary. The paragneiss generally displays a higher magnetic expression than does the granitic terrain, which correlates well with a prominent magnetic low shown on the 1 to 5,000,000 magnetic anomaly map of Canada (G.S.C. Map 1255A). The Fort Smith radiometric 'high' also coincides with the magnetic low.

The only related published age dates are those that exist for the Andrew Lake domain in northeastern Alberta, (Baadsgaard and Godfrey 1966,1972). This area is some 40 km (25 miles) to the southeast of Pilot Lake. Baadsgaard and Godfrey (1966) suggest that the K-Ar dates on mica and hornblende group closely together and give the time of the latest diastrophic event in the Andrew Lake area at 1790 ± 40 million years. This is coeval with the 1735 million year date given to the Hudsonian orogeny by Stockwell (1970). However, they also suggest (Baadsgaard and Godfrey, 1972) that these are 'reset' dates as pegmatites cutting the gneissic complex give Rb-Sr ages of 2524 ± 27 million years, revealing a much older Archean history.

CHAPTER II

PETROLOGY OF THE PILOT LAKE AREA

Geological Setting

The Pilot Lake geology can be very generally divided into two units, a pink weathering texturally distictive augen gneiss of granitic composition and banded porphyroblastic gneisses of variable composition derived from sedimentary material. A small metadiorite instrusion appears to cut the paragneisses in the extreme southwest corner of Pilot Lake, (Fig. 3). The granitic augen gneiss is termed the Pilot Lake Gneiss. Within the study area it has a known width of 5 km and trends approximately N 15°W across Pilot Lake. All rock types other than the augen gneiss and the metadiorite have been mapped under the broad term variable paragneiss. The paragneisses comprise a variety of rock types including: impure quartzites, mica schists, garnet and cordierite gneisses and quartzo-feldspathic gneisses. Minor amphibolite is also present within the study area.

The Pilot Lake Gneiss is well foliated and quite homogeneous when xenolithic material is not considered. Within the main body, this rock type is easily recognizable and where textures and chemical compositions differ drastically between the augen gneiss and the paragneisses, contacts are found to be sharp. However, where chemical compositions between the two units are similar and textures

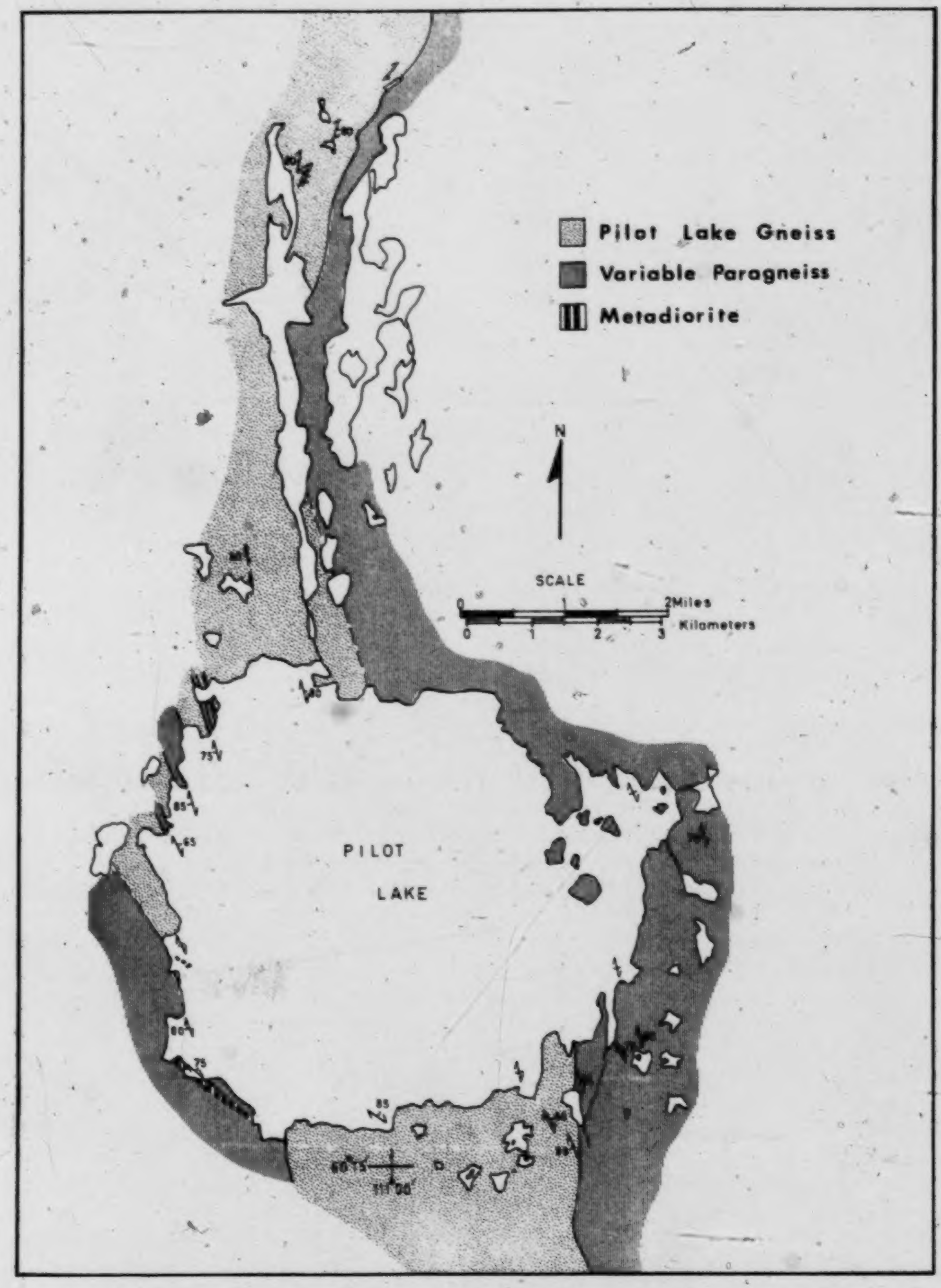

Fig. 3. Geological sketch map of the Pilot Lake area.

appear gradational due to deformation and metamorphism boundaries are obscured and appear transitional. The Pilot Lake Gneiss, however, was found to be four times more radioactive than the paragneisses and contacts were often delineated with the aid of scintillometers.

Inclusions ranging in size from meters to hundreds of meters in length are quite common within the Pilot Lake Gneiss. All appear to be of sedimentary origin and are aligned with their long axes parallel to the main foliation trend. Length to width ratios are usually 10 to 1 or greater. Both frequency and size of the xenoliths increase towards the western edge of the study area, until it becomes evident that extremely large blocks of supracrustals are surrounded by the Pilot Lake Gneiss. This is best seen along the northwestern shores of Pilot Lake (Fig. 3).

Although boundaries between the Pilot Lake Gneiss and bordering paragneisses are often obscured, contacts with the sedimentary inclusions are usually very sharp and distinct. In one instance the Pilot Lake Gneiss was found to truncate older structures, possibly bedding, within a large inclusion of sediment. A small three inch wide reddened zone of Pilot Lake Gneiss at the contact with this inclusion is devoid of the characteristic large feldspars found in the gneiss and appears to be the chilled zone of an intrusive contact (Plate 1,a).

The tectonic history of the Pilot Lake area has been a complex one. All rock types show a strong north-south foliation, and exhibit varying degrees of cataclasis due to deformation and metamorphism. Surface exposures show that there have been at least two and possibly three periods of deformation. The penetrative north-south foliation is indicative of an early phase. A second deformation period gives rise to fine dark gray mylonite zones a few meters wide within the Pilot Lake Gneiss that cross-cut the main foliation trend at angles up to 35 degrees. Lubricated flow is demonstrated by the rotation of microclines in the direction of mylonitization (Plate 1,b). An isolated case of a brittle upper crustal level breccia is indicative of a yet later stage of deformation.

Discussion of Map Units

Pilot Lake Gneiss

As previously mentioned, Pilot Lake Gneiss is the name given to a texturally distinctive augen gneiss trending roughly N 15°W across Pilot Lake.

The features making this rock type easily recognizable in the field are: a pale reddish brown colour, a good foliation with the parallel alignment of large feldspar prophyroclasts* and radioactivity some four times greater than the surrounding paragneiss.

---

* Porphyroclast - a large grain surviving in an otherwise granulated or mylonitized rock (Moorhouse, 1959, p.409) Megacryst used to denote the same.

PLATE 1. PILOT LAKE GNEISS

a. Field photograph. Pilot Lake Gneiss (at bottom of photograph) in contact with an inclusion of spinel-cordierite-andalusite gneiss (sample 4-6). Note the truncation of structures (cross-bedding?) and quartz vein (lower centre) in the paragneiss by the Pilot Lake Gneiss.

b. Field photograph. Cross-cutting mylonite in the Pilot Lake Gneiss. Note rotation of the microclines into the direction of mylonitization.

PLATE 1

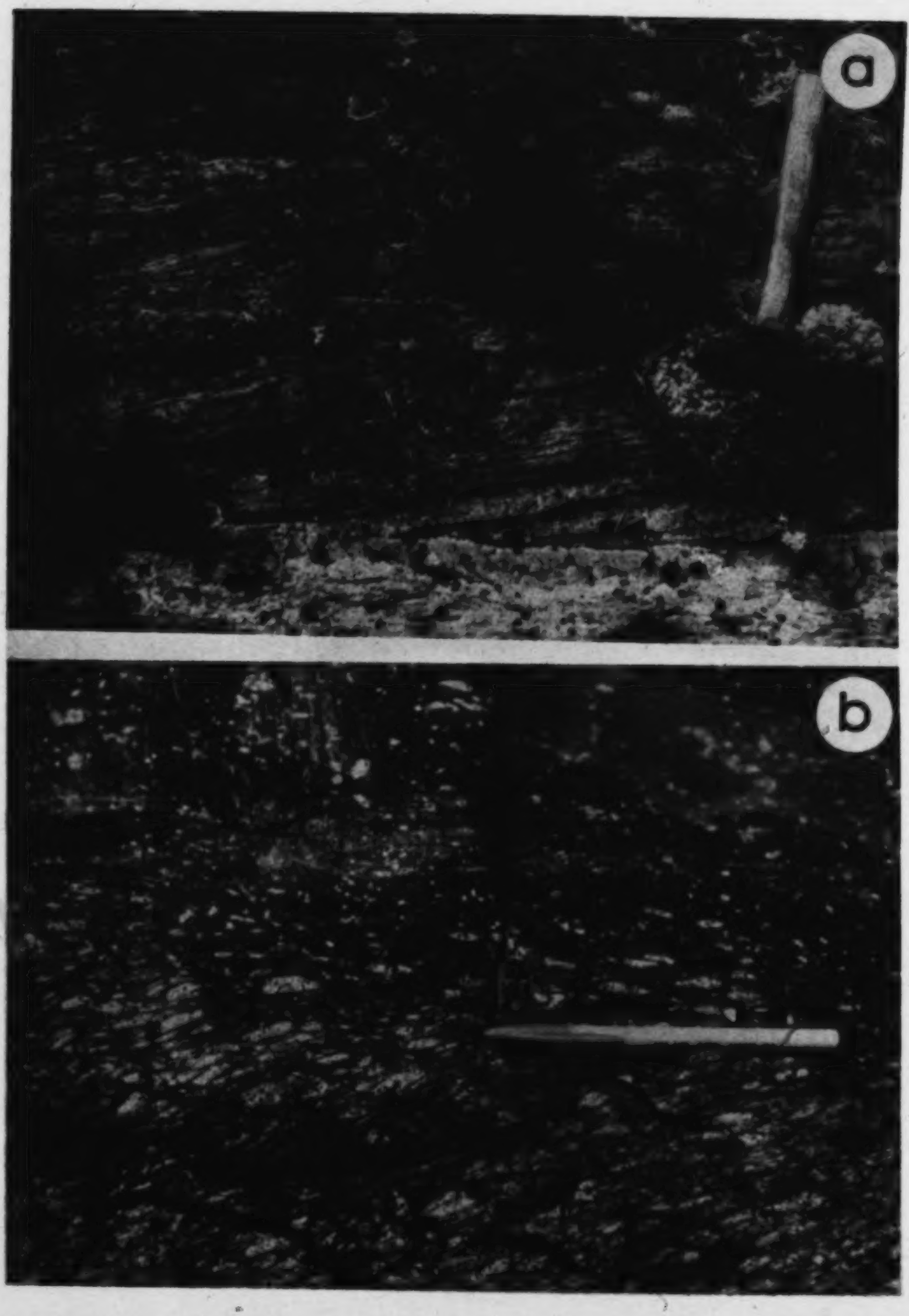

A weathered outcrop of Pilot Lake Gneiss is generally lighter in colour than the overall pale reddish brown colour** of a fresh surface. A steeply dipping penetrative foliation is well marked by the consistent parallel alignment of large white to pink porphyroclasts of microcline. These prophyroclasts comprise from 30 to 50 percent of the rock and have an average length of 1.5 to 2 cm. However, microclines exceeding 5 cm (2 in.) are quite common. They are set in a fine to medium grained, streaky to foliated matrix of feldspar, dusted red by hematite, distinctive bluish ribbon quartz and minor biotite. The megacrysts are always separated from one another by the matrix, which has a tendency to wrap around the large microclines producing the augen-like structure (Plate 2,a).

In total quartz and feldspar often exceed 85 percent of the rock. Mafic minerals are of minor proportion with the most prominent being garnet up to 1 cm in diameter. The rounded garnet is found in very fresh form or as retrograded clusters of biotite and chlorite. Where the garnets or softer retrograded products have weathered at the surface the gneiss takes on a pitted appearance.

Petrography

In thin section the Pilot Lake Gneiss comprises large, abraded, subhedral microcline porphyroclasts and rounded

---

** All the listed rock colours in this study have been referenced to the Geological Society of America's Rock-Colour Chart, 1951.

garnets set in a foliated, highly sheared and crushed matrix of quartz, microcline, plagioclase, biotite and muscovite.

Examination of over 45 thin sections indicates that deformation has played an important role in the development of the Pilot Lake Gneiss.

The highly perthitic microcline porphyroclasts are usually elongate-subhedral to ovoid in shape. Significant postcrystalline stress is indicated by shadowy extinction, bent composition planes of Carlsbad twin crystals and abraded, often highly irregular crystal margins. Embayment of the microcline by quartz, plagioclase, myrmekite and recrystallized microcline is common, (Plate 2,b). Minerals included within the larger microclines are: quartz, less severely strained than in the matrix; biotite, often retrograding to chlorite; rare plagioclase, small opaques and accessories such as zircon.

The microclines are usually immediately surrounded by fine granulated microcline and crushed, polycrystalline, untwinned plagioclase laced with well foliated muscovite. This in turn is bordered by sutured or polygonally recrystallized bands or streaks of quartz exhibiting a high degree of strain, (Plate 2,c). Other than the alignment of the megacrysts, it is the streaks of quartz and the lineation of the muscovite that define the foliation within the thin sections.

The matrix of plagioclase, quartz, potassium feldspar and micas is subequigranular to highly inequigranular depending on the degree of cataclasis. Average grain size ranges from less than 0.1 mm to 0.5 mm. However, thorough recrystallization has often resulted in equigranular sections with grain size approaching 1 mm. The crushed matrix wraps around the ends of the large microcline porphyroclasts in augen-like fashion with uncrushed matrix or recrystallized microcline and quartz forming within the pressure shadows of the megacrysts.

Large (1-2 mm) abraded, anhedral to subhedral crystals of plagioclase are rare but when present are highly deformed, fractured and moderately altered to sericite. Compositions determined by the Michel-Levy method are between An25 and An30 on both the larger crystals and plagioclase within the crush.

Garnet up to 1 cm in diameter usually appears within the recrystallized bands of quartz. It is massive anhedral, rounded or in slightly irregular form. A poikilitic texture is exhibited with the inclusions being the same as those found within the large microclines. The garnet can be extremely fresh and fractured but more often is partially to totally retrograded to biotite and chlorite. Muscovite appears late in the history of the gneiss taking the place of some of the biotite associated with the garnet. In rarer cases small euhedral crystals of andalusite are found replacing biotite, (Plate 2,d).

PLATE 2. PILOT LAKE GNEISS

a. Field photograph. Typical exposure of Pilot Lake Gneiss. Note elongated lineated microclines.

b. Pilot Lake Gneiss. Photomicrograph. Sample 6-2. Microcline porphyroclast with Carlsbad and gridiron twinning being invaded by myrmekite. Crossed nicols. Bar scale is 0.5 mm.

c. Pilot Lake Gneiss. Photomicrograph. Sample 4-3. Perthitic microcline in typical crushed matrix. Note the protected quartz and biotite inclusion in the microcline, also the thin granulated microcline margin laced with muscovite and the sutured boundaries between recrystallized quartz grains (upper left). Crossed nicols. Bar scale is 0.5 mm.

d. Pilot Lake Gneiss. Photomicrograph. Sample 8.2. Garnet (high relief) has been retrograded to biotite (dark) which hosts a late euhedral crystal of andalusite (upper right). Plane light. Bar scale is 0.1 mm.

PLATE 2

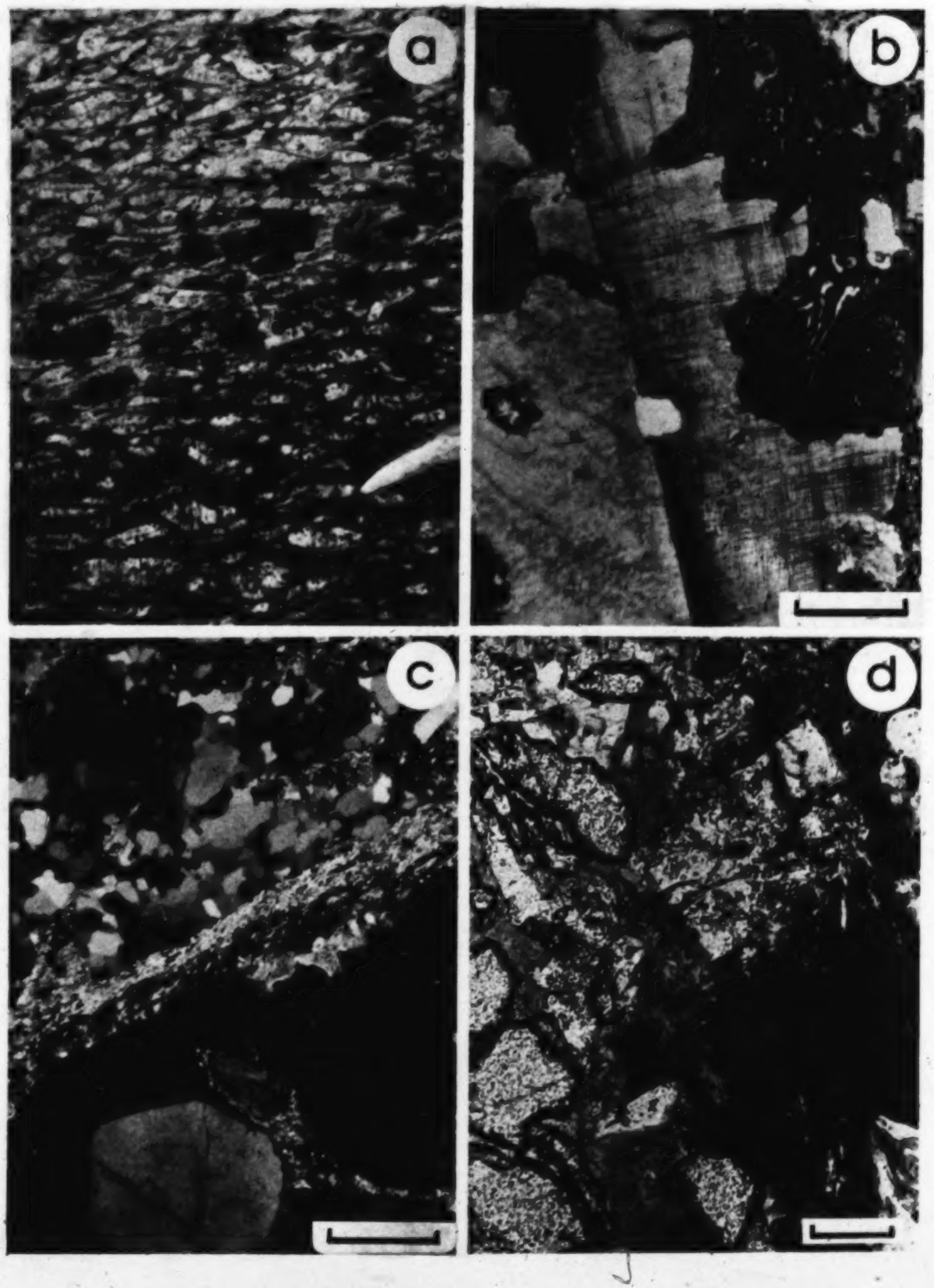

Biotite, other than that associated with the garnet, is found as frayed irregular often randomly orientated crystals scattered throughout the matrix.

Accessories include: opaque minerals, most-likely hematite and ilmenite altered to leucoxene and sphene, apatite, well rounded zircon, and monazite.

Five modal and 12 chemical analyses of Pilot Lake Gneiss are presented in Table 1.

The average mineralogical composition comprises: 51 percent microcline, 6 percent plagioclase, 29 percent quartz, 8 percent biotite, 5 percent muscovite, less than 1 percent garnet and traces of the accessories; opaque minerals, apatite, zircon and monazite. This classifies the rock mineralogically as a granite according to Moorhouse (1959). Because of the coarse grain-size of the microcline and garnet the modal compositions are not always representative and differences may not represent marked changes in bulk chemical composition. This is especially true in the case of garnet which is randomly distributed compared to microcline. Samples of Pilot Lake Gneiss run as high as 15 percent garnet and a more appropriate average should include 5 to 8 percent garnet.

Major Element Analysis

Results of major element analysis and CIPW normative calculations for 12 Pilot Lake Gneiss samples are presented in Tables 1 and 2. All major element analyses in this study were done by Xral Laboratories, Toronto, Ontario, by standard x-ray fluorescence and atomic absorption techniques. FeO determinations, using titration methods, were carried out by the author at the University of Alberta. Uranium and thorium results by delayed neutron activation analysis are presented here to complete the data but will be discussed in chapter three.

All the Pilot Lake Gneiss samples fall well within the subalkaline field as presented by Irvine and Baragar's (1971) total alkalies vs. silica (wt%) diagram (Fig. 4). Subalkaline is used to include the calc-alkaline field of rocks. The average of all 12 samples of Pilot Lake Gneiss compares favourably with Nockolds (1954) average calc-alkaline granite.

The two plot closely together on the alkalies vs. silica diagram. Although total alkalies of the two averages match closely, the Pilot Lake Gneiss has a higher potassium and lower sodium content. This can be seen on the normative anorthite-albite-orthoclase plot (Fig. 5). Eleven of the samples group together towards the Or corner. Nockolds average granite plots with sample 6-1A near the provisional boundaries for average rocks. Sample 6-1A is a finer grain sample than the normal Pilot Lake Gneiss. It occurs at the contact with the eastern paragneiss and possesses a similar mineralogical composition to the augen granite, but is devoid of the large microcline porphyroclasts. The chemical composition, including the potassium and sodium content, is

TABLE 1

Results of chemical and modal analyses for selected Pilot Lake Gneiss samples

SAMPLE NUMBER	4-3	5-1	5-6	6-1A	6-2
SiO_2	70.7	69.1	72.5	73.0	69.4
Al_2O_3	13.5	14.2	13.6	13.4	14.6
CaO	0.85	0.97	0.63	1.06	1.06
MgO	0.95	0.99	0.68	0.85	1.15
Na_2O	1.98	2.22	1.74	2.65	2.10
K_2O	6.12	5.98	7.3	5.13	5.75
FeO	4.35	3.45	2.31	2.25	3.25
Fe_2O_3	0.21	0.17	0.2	0.4	0.54
MnO	0.07	0.04	0.02	0.03	0.03
TiO_2	0.36	0.62	0.3	0.32	0.62
LOI	1.02	1.17	0.79	0.75	1.22
Total	100.11	98.91	100.07	99.84	99.72
Uppm	10.86	13.02	14.11	5.46	18.39
Thppm	127.84	140.44	82.57	39.85	132.25
MODAL ANALYSIS					
Q	24.5		31.8	34.0	26.7
Kfel	57.5		48.0	50.6	50.9
Pg	5.3		3.7	4.5	4.0
Bi	7.4		7.6	5.7	11.1
Mu	2.2		8.4	4.6	6.7
Gt	2.7		---	---	---
Ch	Tr		---	Tr	Tr
Op	0.5		Tr	0.5	0.3
Ap	Tr		0.35	Tr	0.2
Zr	Tr		} 0.1	} 0.13	} 0.13
Mz	Tr				
Total Counts	1500		2000	2000	1500

TABLE 1 (cont'd)

Results of chemical and modal analyses for selected Pilot Lake Gneiss samples

SAMPLE NUMBER	8-2	9-1	9-6	9-18	12-10
SiO_2	67.8	71.6	72.0	71.9	75.2
Al_2O_3	14.6	13.9	14.2	13.9	12.8
CaO	1.4	0.63	0.64	0.89	0.32
MgO	1.15	0.42	0.65	0.62	0.55
Na_2O	2.05	2.18	2.18	1.79	1.89
K_2O	6.05	7.43	6.64	6.48	7.30
FeO	4.44	2.00	1.96	3.21	1.14
Fe_2O_3	0.43	0.13	0.25	0.11	0.18
MnO	0.05	0.02	0.02	0.05	0.02
TiO_2	0.74	0.74	0.24	0.56	0.08
LOI	0.62	1.02	0.58	0.44	0.44
Total	98.03	100.07	99.36	99.95	99.92
Uppm	6.10	2.04	29.65	7.84	18.36
Thppm	152.55	23.15	51.08	113.93	10.59

TABLE 1 (cont'd)

Results of chemical and modal analyses for selected Pilot Lake Gneiss samples

SAMPLE NUMBER	12-11	13-2	AVG. PLG	AVG. CALC-ALKALI GRANITE (NOCKOLDS, 1954)
SiO_2	73.3	70.7	71.43	72.08
Al_2O_3	13.4	13.8	13.82	13.86
CaO	0.6	0.83	0.82	1.33
MgO	0.52	0.88	0.78	0.52
Na_2O	2.26	1.93	1.93	3.08
K_2O	5.75	6.32	6.35	5.46
FeO	1.71	2.85	2.74	1.67
Fe_2O_3	0.06	0.24	0.24	0.86
MnO	0.02	0.04	0.03	0.06
TiO_2	0.16	0.52	0.44	0.37
LOI	0.59	0.89	0.79	0.53
Total	98.37	99.00	99.37	99.82
Uppm	28.24	9.83	13.66	4.8
Thppm	63.97	105.99	87.01	17.0
MODAL ANALYSIS				
Q		26.2	28.6	
Kfel		51.2	51.1	
Pg		11.8	5.9	
Bi		8.2	8.0	
Mu		2.0	4.8	
Gt		---	0.6	
Ch		---	Tr	
Op		0.3	0.3	
Ap		Tr	Tr	
Zr		Tr	} 0.1	
Mz		Tr		
Total Counts		2000		

TABLE 2

CIPW Normative calculations (in wt %) for Pilot Lake Gneiss samples

SAMPLE NUMBER	4-3	5-1	5-6	6-1A	6-2
Q	29.42	27.96	30.62	33.18	29.54
Cor	2.09	2.36	1.69	1.57	3.03
Or	36.53	36.19	43.49	30.62	34.53
Ab	16.91	19.22	14.83	22.63	18.04
An	4.26	4.92	3.15	5.31	5.34
En	2.39	2.52	1.71	2.14	2.91
Fs	7.42	5.37	3.64	3.36	4.62
Mt	0.31	0.25	0.29	0.58	0.79
Il	0.69	1.20	0.57	0.61	1.19

TABLE 2 (cont'd)

CIPW Normative calculations (in wt %) for Pilot Lake Gneiss samples

SAMPLE NUMBER	8-2	9-1	9-6	9-18	12-10
Q	25.27	27.66	30.53	31.72	34.07
Cor	2.15	1.13	2.28	2.33	1.21
Or	36.25	44.37	39.76	38.52	43.40
Ab	17.57	18.62	18.67	15.22	16.07
An	7.04	3.15	3.21	4.44	1.60
En	2.90	1.06	1.64	1.55	1.38
Fs	6.76	2.40	3.07	5.00	1.86
Mt	0.63	0.19	0.37	0.16	0.26
Il	1.42	1.42	0.46	1.07	0.15

TABLE 2 (cont'd)

CIPW Normative calculations (in wt %) for Pilot Lake Gneiss samples

SAMPLE NUMBER	12-11	13-2	AVG. PLG	AVG. CALC-ALK. GR.
Q	35.55	30.82	31.51	28.98
Cor	2.41	2.31	2.31	0.46
Or	34.78	38.10	38.10	32.53
Ab	19.55	16.64	16.56	26.24
An	3.04	4.20	4.13	6.64
En	1.32	2.23	1.97	1.30
Fs	2.93	4.33	4.22	1.87
Mt	0.09	0.35	0.35	1.26
Il	0.31	1.01	0.85	0.71

Key for abbreviations used in this thesis

Minerals

Modal Analysis

Q	Quartz
Kfel	Potassium Feldspar
Pg	Plagioclase
Bi	Biotite
Mu	Muscovite
Gt	Garnet
Ch	Chlorite
Op	Opaques
Ap	Apatite
Zn	Zircon
Mz	Monazite
Sp	Spinel
Py	Pyrite
Lx	Leuxocene
Ant	Anatase
Hy	Hypersthene

CIPW Normative Analysis

Q	Quartz
Ccr	Corundum
Or	Orthoclase
Ab	Albite
An	Anorthite
Dp	Diopside
He	Hedenbergite
En	Enstatite
Fs	Ferrosilite
Fo	Forsterite
Fa	Fayalite
Mt	Magnetite
Il	Ilmenite

Chemistry

U	Uranium
Th	Thorium
L.O.I.	Loss on ignition

Miscellaneous

ppm	parts per million
Tr	trace
cps	counts per second
MW	mega watts
A	amperes
PLG	Pilot Lake Gneiss
AVG.	Average
Total Counts	Modal Point Counts

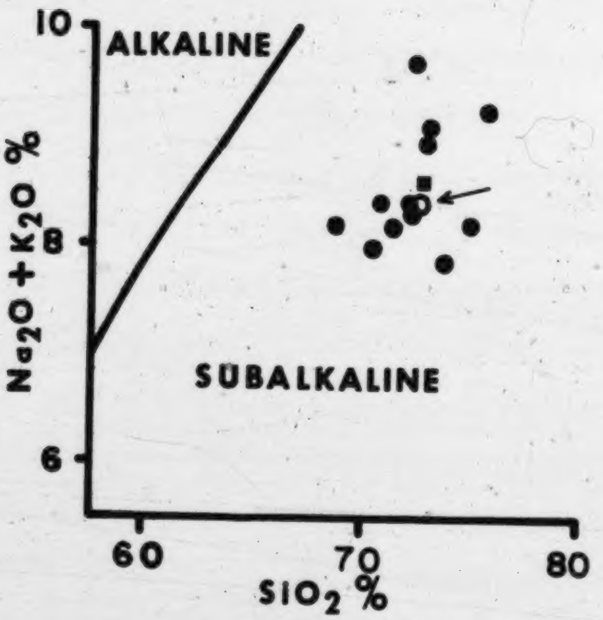

Fig. 4. Total alkalies vs. silica (wt. %) diagram. Dividing line after Irvine and Baragar (1971).

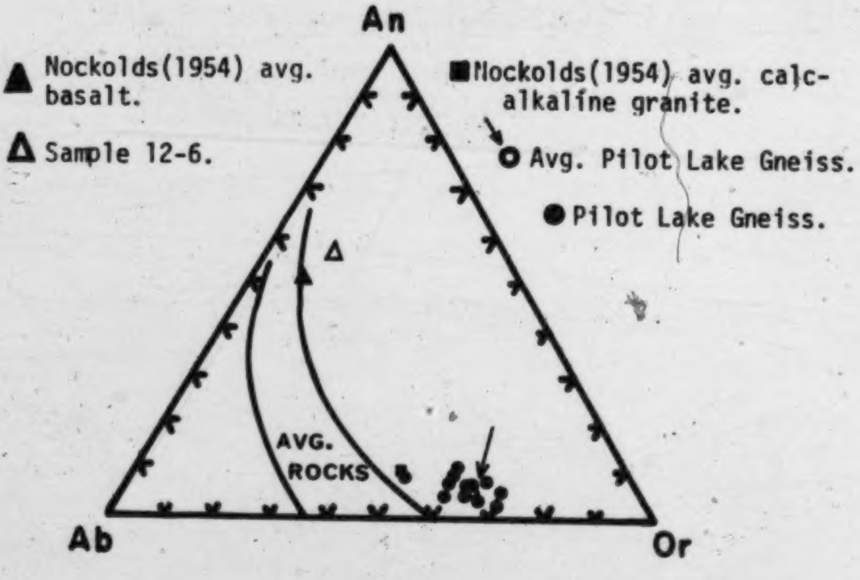

Fig. 5. An-Or-Ab normative projections of subalkaline rocks. Provisional boundaries for average rocks after Irvine and Baragar (1971).

very similar to the average calc-alkaline granite. It is postulated that this and other samples from this zone represent a slightly chilled margin of the Pilot Lake Gneiss.

Regional extent of the Pilot Lake Gneiss

Godfrey (1965, p.26) has described a rock type he terms the Arch Lake Granite in the Charles Lake area of northern Alberta as consisting of:

> "... white to pink, subhedral, elongate, feldspar megacrysts from one-half to one inch in size, aligned in a medium-grained streaky to foliated matrix of blue quartz, biotite, feldspar, and minor muscovite."

This description appears to be very similar to that of the Pilot Lake Gneiss. There are slight differences in modal plagioclase and garnet contents. Godfrey suggests that the Arch Lake Granite (a field term) is petrographically a quartz monzonite and Watanabe (1966) indicates 29 percent plagioclase and only traces of garnet. Godfrey, (personal communication, 1977) however, has confirmed by comparing hand specimens that the two rock types appear to be mineralogically and definitely texturally the same.

Godfrey and Langenberg (1977) show the Arch Lake Granite to be a large pear shaped body of rock at least 50 km in length varying from 13 to 50 km in width. This seems to indicate that the granitic-augen gneiss found in the Pilot Lake area is just a small part of an extremely large body of rock that extends from Alberta to possibly well north of Pilot Lake.

Metadiorite

An extremely massive, medium to coarse grained crystalline rock was encountered at two localities on the extreme southwestern shore of Pilot Lake. A weathered surface shows pink to bleached white feldspar resisting erosion. A fresh surface shows the equigranular rock to be medium dark gray with the feldspars white or shaded light red. A somewhat coarse salt and pepper texture, with intergrown feldspars and mafic minerals characteristic of many diorites, is well displayed. The rock appears very homogeneous and massive with a difference in grain size as the only varying feature.

Boundaries of the metadiorite were not investigated fully beyond the shoreline of the lake and actual contacts with other lithologies were not found. However, a dike-like form trending roughly N 55° W seems most probable, since rocks of sedimentary origin were found both north and south of the metadiorite exposures (see Fig. 3).

In thin section the rock is seen to be hypidiomorphic granular. Some shearing and granulation of the plagioclase has taken place but is minor when compared to the Pilot Lake Gneiss. The plagioclase is anhedral to subhedral with an average composition of An_{45}. This calcic andesine varies from approximately 1 mm to an average size of 5 mm in the coarsest sample. Carlsbad, albite and pericline twinning have developed but untwinned crystals are common with all

TABLE 3

Results of chemical and modal analysis for a metadiorite sample

SAMPLE NUMBER	9-12B	HORN-BI DIORITE (NOCKOLDS, 1954)	9-8	9-12C
SiO_2	54.0	52.97		
Al_2O_3	21.3	18.19		
CaO	4.64	7.61		
MgO	2.60	4.75		
Na_2O	4.81	3.50		
K_2O	3.40	1.65		
FeO	3.84	6.29		
Fe_2O_3	1.26	1.97		
MnO	0.04	0.13		
TiO_2	1.10	1.60		
P_2O_5	0.53	0.34		
LOI	1.22	1.00		
Total	98.74	100.00		
Uppm	13.74		3.67	3.63
Thppm	630.60		209.04	82.79
MODAL ANALYSIS				
Q	0.45			
Kfel	3.05			
Pg	63.1			
Bi	30.75			
Mu	1.55			
Zr+Mz	0.4			
Ap	0.7			
Op	Tr			
Total counts	2000			

having been slightly altered to sericite.

Potassium feldspar is extremely minor and occurs interstially to the plagioclase or as small exsolved masses of microcline within the andesine.

Biotite, interstial to the felsic minerals, is either dark pleochroic brown or olive green. A preferred orientation is exhibited by only the finest grained sample.

A point count indicates the following mineral percentages: plagioclase, 63; biotite, 31; microcline, 3; muscovite, 1.5; quartz, apatite, opaques, zircon and monazite as accessories. According to Moorhouse (1959) this rock type should mineralogically be classified as a diorite.

A chemical analysis of one sample is shown in Table 3. Although somewhat higher in aluminum, potassium, and sodium and lower in total mafic content, the analysis compares best with Nockolds (1954) average hornblende-biotite diorite.

Variable Paragneiss

As previously mentioned all main rock types other than the Pilot Lake Gneiss and metadiorite have been grouped under the term variable paragneiss. This unit contains all the metamorphic equivalents of the insitu sedimentary material of Precambrian age, as well as the metasedimentary inclusions found within the Pilot Lake Gneiss.

As seen from Fig. 3, the bulk of paragneissic material is found to the east of the Pilot Lake Gneiss and continues outside the study area for an undetermined distance. A large volume of metasedimentary rock outcrops along the western shore of Pilot Lake as large blocks surrounded by Pilot Lake Gneiss.

The paragneisses are a mixture of rock types which include: impure quartzites, biotite and muscovite schists, porphyroblastic garnet and cordierite gneiss, and quartzo-feldspathic rocks. Minor amphibolite, probably volcanic in origin, is associated with the paragneisses and will be grouped here.

Alternation of the metasedimentary rock types on a large scale, or slight changes of mineral content or colour on a small scale has produced marked banding or layering, (Plate 3,a). This may be interpreted as relict sedimentary stratification. Banding or layering can be on a scale of centimeters or less or may be visible as fairly homogeneous, massive units meters wide. Except for the layering, primary sedimentary features, are uncommon.

Small scale deformational structures such as folds and crenulations are visible in the well banded rock types. Mylonitic bands have developed locally.

As previously mentioned contacts between the metasedimentary rocks and the Pilot Lake Gneiss are gradational to sharp and are concordant with the gneissic structure.

Following are descriptions of the main metasedimentary rock types found in the Pilot Lake area. Because of the intermixing of many of the metasedimentary lithologies on a small scale division into units on the geological map was not possible.

Impure Quartzite

The impure quartzites are a relatively minor rock type in the study area. They are massive, fine to medium grained and display a sugary texture. They are usually dark gray to grayish red on a fresh surface and a somewhat lighter colour on a weathered exposure.

In thin section they display a granoblastic texture. Quartz has been recrystallized resulting in polygonal or sutured grain boundaries. Porphyroblastic garnets are usually present in amounts varying from 1 to 25 percent. They are xenoblastic but massive containing many rounded inclusions of quartz, (Plate 3,d). Biotite and plagioclase with a composition of An35 to 40 combine in layers to form the remainder of the rock.

Spinel and andalusite are not uncommon in the paragneisses. One particular sample (4-5) found as an inclusion in the Pilot Lake Gneiss displays irregular masses of dark green spinel often enclosing small amounts of a very high relief, colourless mineral, identified as corundum. The spinels are rimmed by a thin zone of andalusite which in turn is bordered by biotite (Plate 3,b,c). Together this

PLATE 3. VARIABLE PARAGNEISS

a. Field photograph. Exposure of thinly banded metasediments. Garnetiferous biotite layers (dark) alternating with feldspar rich layers (light) may represent original sedimentary stratification. Site number 14-1.

b. Impure quartzite. Photomicrograph. Sample 4-5. An inclusion in the Pilot Lake Gneiss with irregular shaped spinel grains (dark) mantled by a thin rim of andalusite in turn bordered by biotite. Light minerals are quartz. Plane light. Bar scale is 0.5 mm.

c. Photomicrograph. Close-up of zoned mineral relationships in Plate 3b (sample 4-5) with a core of green spinel (dark) and corundum (high relief) surrounded by andalusite (light) in turn enclosed by biotite. Plane light. Bar scale is 0.1 mm.

d. Photomicrograph. Sample 7-3. Typical garnet porphyroblast in the Pilot Lake paragneisses. Note massiveness, roundness of margins and protected quartz inclusions. Garnets are pre-tectonic as foliation wraps between them. Plane light. Bar scale 0.5 mm.

PLATE 3

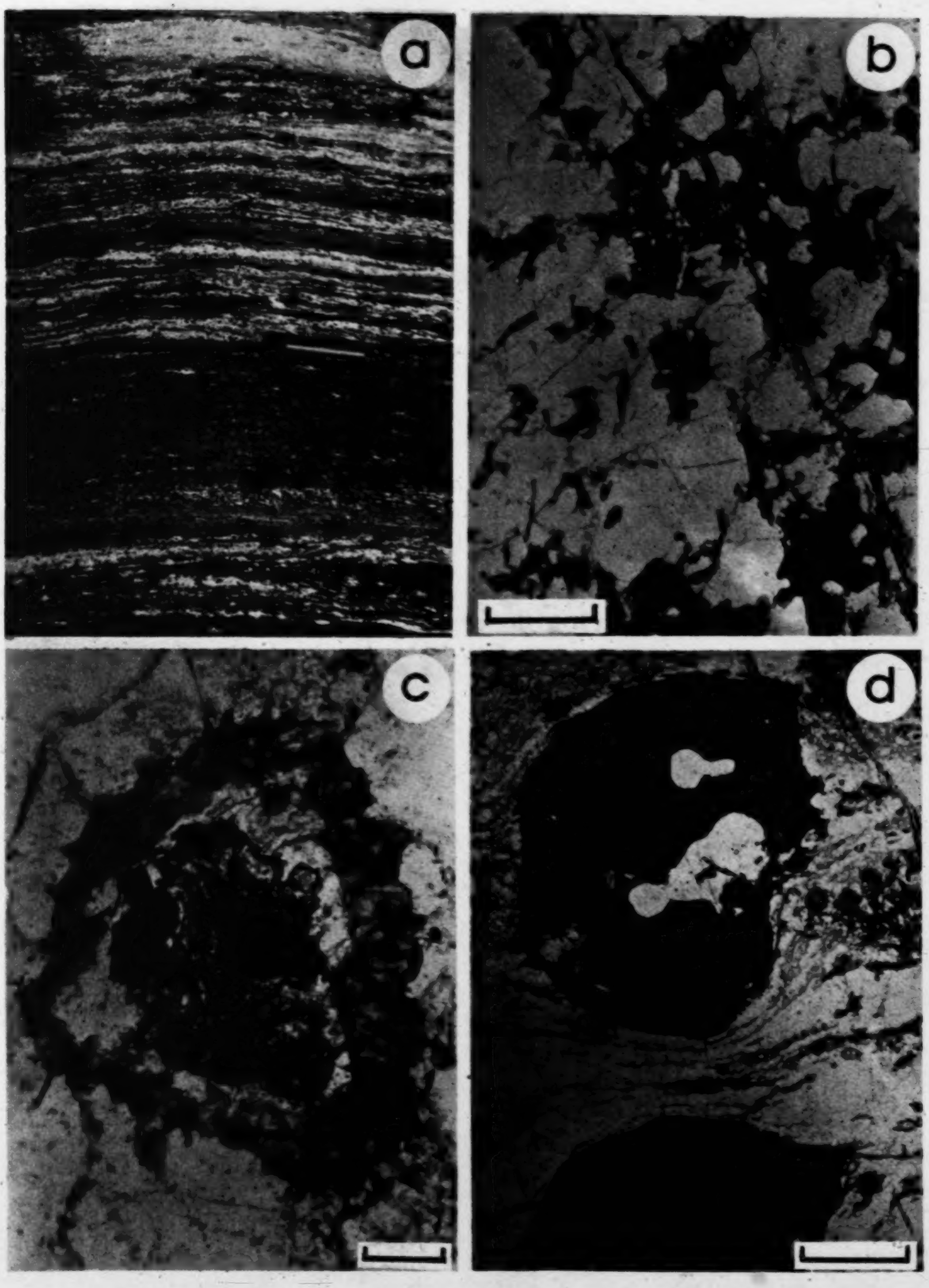

unique combination comprises from 15 to 20 percent of the sample.

Porphyroblastic Garnet-Cordierite Gneiss and Garnet-Cordierite-Andalusite Gneiss

These two rock types are the most common of all the paragneisses. In the field they are easily confused and were often identified as impure quartzites. They occur with the micaceous schists or as xenoliths within the Pilot Lake Gneiss. Generally, they are fine to medium grained, medium gray to dark gray on a fresh surface and massive to thinly banded. Thin sections show a variety of textures and features, many the result of retrogressive metamorphism and varying degrees of deformation. Spinel is found as small highly irregular, green isotropic masses enclosed by poikiloblastic andalusite (Plate 4,c). Also included in the andalusite are small opaques and rare corundum. Biotite occurs as extremely fine grains or as coarse clusters and mats that are multi-crystal pseudomorphs replacing garnet. The andalusite has formed at the expense of biotite and the amount and grain size in each sample is dependent on the amount and grain size of the original biotite.

Spinel in samples devoid of andalusite is scattered throughout, interstial to the cordierite and plagioclase or as small broken fragments within the cordierite.

Cordierite is usually found as anhedral aggregates or as ill-defined or pseudohexagonal porphyroblasts.

Polysynthetic and sectored twinning is quite common making distinction from plagioclase difficult (Plate 4,a). A few samples contain greater than 50 percent cordierite.

Garnets up to 5 mm in diameter often form in layers or aggregates. They can be extremely fresh or broken and altered to biotite. Quartz, if present, is usually associated with the garnet. Other constituents include muscovite, plagioclase and minor potassium feldspar.

Sample 4-6, found as an inclusion within the Pilot Lake gneiss, containing spinel, andalusite, biotite, muscovite, cordierite and plagioclase has been analysed and presented in Table 4.

Muscovite-Biotite Schist

Muscovite - biotite schists do not occur extensively in the Pilot Lake area. They are found as small bands meters wide mixed with the cordierite bearing assemblages. Usually medium gray to brownish gray in colour they exhibit a definite schistosity due to the parallelism of the micas.

Thin sections show the schists to be quartz-rich with the quartz occurring as small grains with the biotite. Garnet and plagioclase porphyroblasts are sometimes present and are often broken down and replaced by biotite and sericite respectively (Plate 4,b). Muscovite wraps around the porphyroblasts forming augen-like structures. Andalusite is found replacing biotite at a few localities.

TABLE 4

Results of chemical analysis for selected paragneiss samples

SAMPLE NUMBER	4-6	16-1	16-3
SiO_2	59.5	76.0	75.8
Al_2O_3	20.8	12.4	13.5
CaO	0.47	0.59	0.82
MgO	2.36	1.54	0.82
Na_2O	1.02	4.50	6.50
K_2O	3.76	1.66	0.78
FeO	6.56	2.01	1.20
Fe_2O_3	0.86	0.10	0.00
MnO	0.03	0.02	0.02
TiO_2	0.68	0.24	0.18
LOI	3.00	1.02	0.31
Total	99.04	100.08	99.93
Uppm	2.35	0.97	0.34
Thppm	23.75	30.46	4.72

Quartzo-Feldspathic Rocks

Many massive, leucocratic bands several centimeters to a few meters thick occur within the Pilot Lake metasediments. These bands often alternate with the more melanocratic gneisses previously described. They are distinctive and contacts with other rock types are usually sharp. Colour is sometimes a light gray but more commonly a moderate orange pink. Hand specimens often indicate a rather coarse grain size but thin sections reveal varying amounts of finely crushed feldspar. The main components, quartz and feldspar, usually exceed 95 percent of the total. Large crystals (1.5 cm) of microcline and plagioclase sometimes exist in the fine crush and bands of recrystallized quartz. This situation is similar to that found in the Pilot Lake Gneiss, however, the microclines are neither as large or aligned as in the augen gneiss. Biotite, muscovite and garnet usually comprise 3 to 10 percent of the rock. Sample 9-9 contains abundant sillimanite blades (Plate 4,d).

Two samples (16-1, 16-3) taken from an area east of Pilot Lake have been chemically analysed (Table 4) and show high $SiO2$ and $Na2O$ contents along with low $K2O$. These samples have been extremely crushed and investigation revealed a major fault trending N 25° W just to the east of the sample location.

Amphibolite

The amphibolite found within the Pilot Lake area is

PLATE 4. VARIABLE PARAGNEISS

a. Spinel-cordierite gneiss. Photomicrograph. Sample 8-10. Cordierite porphyroblast in a matrix of feldspar and spinel. Note pseudohexagonal form and sectored twinning. Crossed nocols. Bar scale is 0.5 mm.

b. Biotite-muscovite schist. Photomicrograph. Sample 7-8. Muscovite and biotite replace a pre-tectonic porphyroblast of feldspar. Finer biotite-muscovite and quartz layers wrap around the end of the blast. Plane light. Bar scale is 0.5 mm.

c. Spinel-andalusite-cordierite gneiss. Photomicrograph. Sample 4-6. Mineral relationships showing poikiloblastic andalusite (center and lower right), with a core of green spinel (dark), replacing brown biotite. Bar scale is 0.5 mm.

d. Quartzo-feldspathic gneiss. Photomicrograph. Sample 9-9. Large garnet (bottom of photograph) in a matrix of muscovite and feldspar containing abundant sillimanite (small squared grains) and spinel (dark). Note that the sillimanite crystals are all cut parallel to (001) and enclose or cluster around the spinel. Plane light. Bar scale is 0.5 mm.

PLATE 4

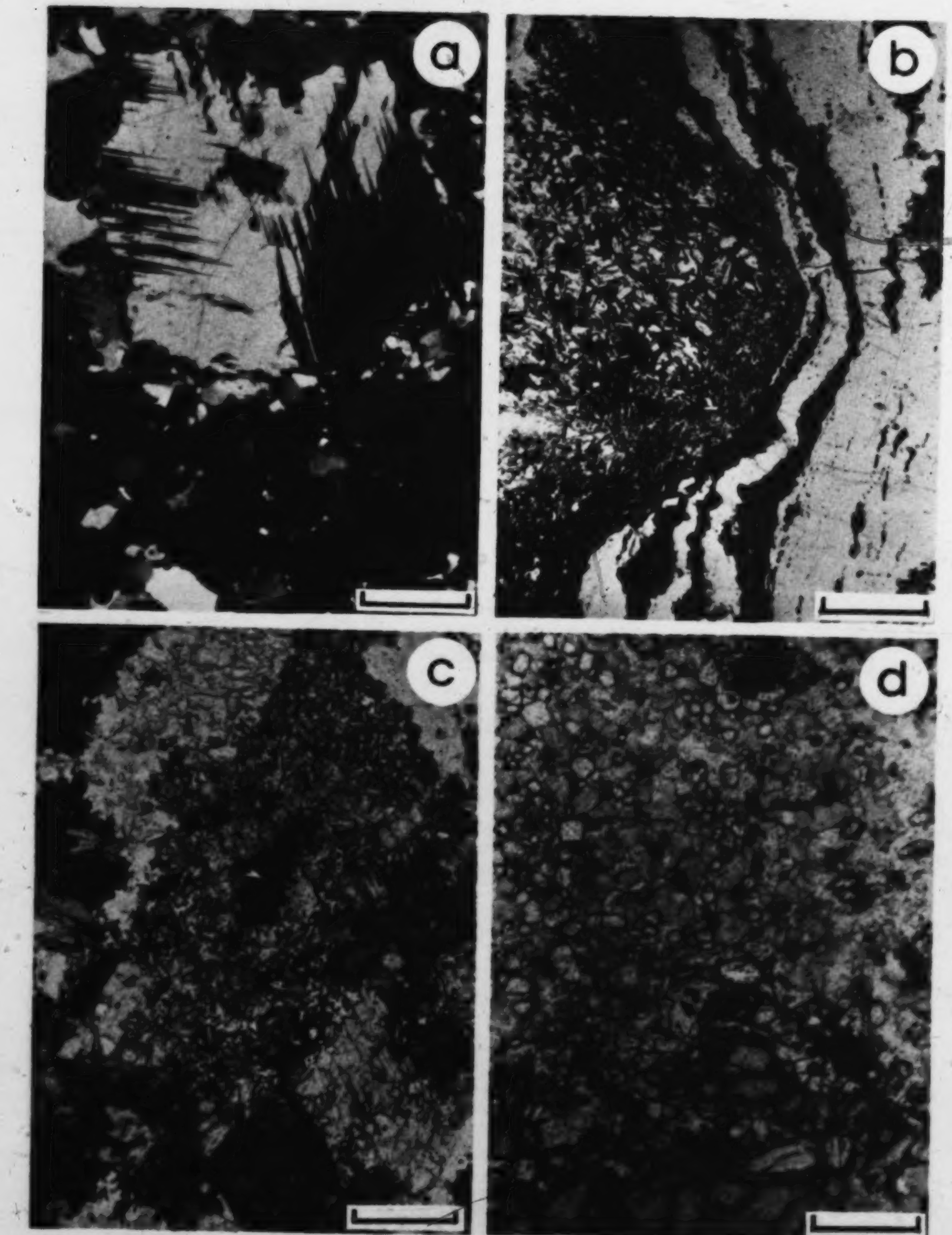

certainly not of sedimentary origin. However, it is found in such minor proportions that it seemed inappropriate to classify it as a separate unit. Its uniqueness within the Pilot Lake geology does warrant a brief description.

Amphibolite is found mixed with the paragneisses at two localities east of the Pilot Lake Gneiss. This rock type is fine grained, greenish black, and massive to slightly foliated. Thin sections exhibit small, stubby, subhedral crystals of pleochroic green hornblende forming at the expense of slightly foliated biotite. Plagioclase, with a composition of An40, is present as small anhedral grains. Quartz when found is in the form of recrystallized layers associated with the biotite. Late forming actinolite and epidote are prevalent.

Other than the metadiorite, basic dikes that might give rise to an amphibolite during metamorphism were not found. One chemical analysis (sample 12-6, Table 5) compares favourably with Nockolds (1954) average tholeiitic basalt. A normative Or-An-Ab plot falls in the potassum-rich basalt range (Fig. 5). This sample is of the massive variety and was taken from a rather thin band 1.5 m wide, intercalating and conformable with quartzo-feldspathic gneisses. The minor amounts, the thin intercalating conformable layers, a basaltic chemistry and the absence of dikes seem to indicate the possibility of a pyroclastic origin for this amphibolite, the only such volcanic rocks found in the Pilot Lake area.

TABLE 5

Results of chemical and normative analysis for an amphibolite sample

SAMPLE NUMBER		12-6	AVG THOLEIITIC BASALT (NOCKOLDS, 1954)
SiO_2		49.7	50.83
Al_2O_3		15.0	14.07
CaO		10.9	10.42
MgO		8.4	6.34
Na_2O		1.85	2.23
K_2O		1.10	0.82
FeO		6.41	9.06
Fe_2O_3		2.80	2.88
MnO		0.32	0.18
TiO_2		0.62	2.03
LOI		1.83	0.91
Uppm		1.16	0.6
Thppm		5.98	2.2
Total		98.93	99.78
CIPW NORMATIVE MINERAL PERCENTAGES (IN WT %)	Q	---	3.4
	Cor	---	---
	Or	6.7	5.0
	Ab	16.1	19.1
	An	30.3	22.2
	Di	14.2	13.1
	He	6.4	8.2
	En	13.2	9.9
	Fs	6.8	7.0
	Fo	1.2	---
	Fa	0.7	---
	Mt	3.2	4.2
	Il	1.2	3.9

CHAPTER III

RADIOACTIVITY

Methods and Data Used

"Gamma-ray spectrometry is a physical method which provides geochemical information from which geological conclusions can be drawn." (Darnley *et al.* 1971, p. 2.) The use of sophisticated airborne techniques provides the most economical way of gathering this information over large surface areas in the minimum amount of time. Airborne surveys are usually the first phase of work in an area to be newly explored.

In the summer of 1969, the Geological Survey of Canada using a high-sensitivity airborne gamma-ray spectrometer system designed and constructed by Atomic Energy of Canada Limited (Darnley *et al.* 1971), flew a survey to obtain a continuous radiometric profile across the Canadian Shield between Ottawa, Ontario and Yellowknife, Northwest Territories. The main features of this spectrometry system have been described by Darnley (1970, 1972).

According to Darnley *et al.* (1971) the purpose of this survey was:

1. To look for broad scale variations in radioactivity level;
2. To look for previously unreported areas of high radioactivty;
3. To look for correlations between known geology and the radioelement content; and
4. To investigate the problems involved in

collecting and presenting data of this type. The results of the reconnaissance profiles flown in 1969 prompted a follow-up survey in the region between Fort Smith and Great Slave Lake in 1970 (Darnley and Grasty 1970). The 39,000 km² (15,000 sq. miles) covered by this survey are bounded approximately by latitudes 59° 45'N and 62° 25'N and longitudes 110° 00'W and 112° 00'W. Data is corrected for atmospheric background, deviation from the mean terrain clearance and the Compton scattering of radiation into the lower energy channels. The count rates then plotted are thus directly proportional to the mean ground level radioelement abundances. An outline of the correcton and computation procedure has been given in Darnley and Grasty (1971), Grasty and Darnley (1971) and Darnley (1972). The Geological Survey of Canada then computer plotted the corrected data as flight profiles following a standard format, as outlined by Darnley (1972), with the distance in statute miles from some arbitrary base line plotted from left to right. Irregularly spaced fiducial or ground reference points, using bodies of water, topographical features or structural lineaments such as faults are also plotted.

The integral (total radiation), potassium, uranium and thorium corrected counts per unit counting time are plotted, as are also the U/Th, U/K, Th/K ratios and terrain clearance. (See Fig. 7 as an example). The sample counting time for the Fort Smith survey was: integral 0.5 s, other channels 2.5 s. The nominal terrain clearance for all these results, and the value to which they have been normalized is 123 m (400 feet). The data is then compiled on computer enhanced, machine drawn contour maps (isorad maps) at a scale of 1 to 250,000.

Darnley and Grasty (1971) suggest that approximate ground concentrations may be obtained from their maps using the following relations;

1 ppm uranium = 26 counts
1 ppm thorium = 11 counts
1 % potassium = 170 counts

Groundwork using portable gamma-ray spectrometers was undertaken by the Geological Survey of Canada at several of the more interesting anomalies during July and August, 1970 (Charbonneau, 1971). The main purpose of this work was to provide ground values for confirming airborne sensitivities and to provide some insight into the geological cause of the anomaly pattern.

After the release of the Fort Smith survey as Open File Report Number 101 (1971), Richardson and Charbonneau (1973) carried out ground investigations at several localities in 1973. This work was to further aid in the interpretation of the airborne data and to evaluate the potential economic significance of different types of variations in radioelement concentrations and ratios.

During June of 1975 ground investigations were carried out by the author in the Pilot Lake area. All rock types were monitored for their total radioactivity using a SRAT

Spp2 portable scintillometer. Where it was necessary and possible, detailed grid measurements were conducted over anomalous zones.

Outcrop samples were taken from all major lithologies with as wide a range of scintillometer values as possible. Over 100 samples have been analysed in detail for their uranium and thorium content by delayed neutron activation, (see Appendex I for method).

Thin sections for all samples analysed were carefully inspected for the identification of radioactive minerals. Several autoradiographs were prepared when it became evident that standard petrological identification of the U and Th bearing minerals was difficult. A heavy mineral separate of the most radioactive sample (8-5C) helped confirm the thin section and autoradiograph results, (See Appendex II).

Results of the Airborne Radiometric Surveys

The results of the cross-country gamma-ray spectrometer survey in 1969 are both interesting and plentiful. Several of the more important results and the ones of particular interest that prefaced this study are:

1. The northwestern section of the Churchill province has the highest base level radioactivity in every case (integral, U, Th, K) in the Canadian Shield. The base level is equivalent to about 3.2% K, 2.5 ppm U and 20 ppm Th, (Darnley 1971). This was seen after dividing the shield into areas based solely on radiometric similarities;
2. The potassium content is greater than was observed elsewhere over any area of comparable size;
3. Two radiometric 'highs' occur in the northwest

Churchill section-the principal one being the north striking Fort Smith-Great Slave Lake 'high', the second and lesser one in the Uranium City-Eldorado area;

4. The Fort Smith - Great Slave Lake 'high' is a thorium rich belt. Using the count rates the equivalent of 5% K, 5 ppm U and 50 ppm Th is commonly exceeded. The U to Th ratio is usually very low with Th to K higher than anywhere else; U to K is average;

5. The large complex Fort Smith - Great Slave Lake 'high' coincides with a prominent magnetic low shown on the 1 to 5,000,000 Magnetic Anomaly Map of Canada (G.S.C., Map 1255A).

As previously mentioned these results prompted a follow-up survey flown in greater detail in the Fort Smith-Great Slave Lake region, which substantiated the above results and proved the existence of a prominent high over 260 km long averaging 48 km in width.

Darnley (1972) indicates the radiation level over much of this area to be three times greater than the average level for the Canadian Shield.

Using the integral (total radioactivity) isorad map of the second survey (G.S.C. Open File Report No. 101), inspection of the results shows that the area can be subdivided on the basis of radioactivity into three principal forms. The first is a relatively flat base level that covers the majority of the eastern half of the surveyed area. The second form shows as broad swells usually rising 1.5 to 2 times above the base level. The outline of these swells defines the large regional 'high' termed the Fort Smith-Great Slave Lake 'high'. It can easily be seen on the integral map to extend northward from below the surveyed area in northeastern Alberta, to just south of LaLoche Lake where it begins to strike northeast. This northeasterly trend parallels the McDonald fault system and no doubt reflects the movements of this major structural break.

The third and most prominent forms are narrow groups of highs with peak levels three or four times the regional base level. A system of prominent peaks defines a zone of apparent extreme radioactivity in the core of the regional high. Since the area has already been defined as a thorium rich belt this major high is seen very distinctly on the thorium isorad map (Fig. 6). It extends from just south of Pilot Lake to just north of latitude 61°N, a distance of 100 km (62 miles) with a maximum width of 40 km (25 miles).

The uranium isorad map is less specific in defining the 'high' than the thorium map. Broad uranium anomalies are seen to correspond with the majority of the thorium peaks. However, they overlap the thorium peaks producing narrow isolated U to Th ratio anomalies on the flanks of the main thorium high. This is particularly true to the east of the main anomaly between Pilot Lake and latitude 61°N. Darnley (1972) suggests that the location of uranium highs and U to Th ratio anomalies on the margin of or just outside, major regional radioactive highs is quite typical of many uranium occurrences encountered in the Canadian Shield. He uses the Fort Smith situation and a flight profile in Mont Laurier, Quebec as examples.

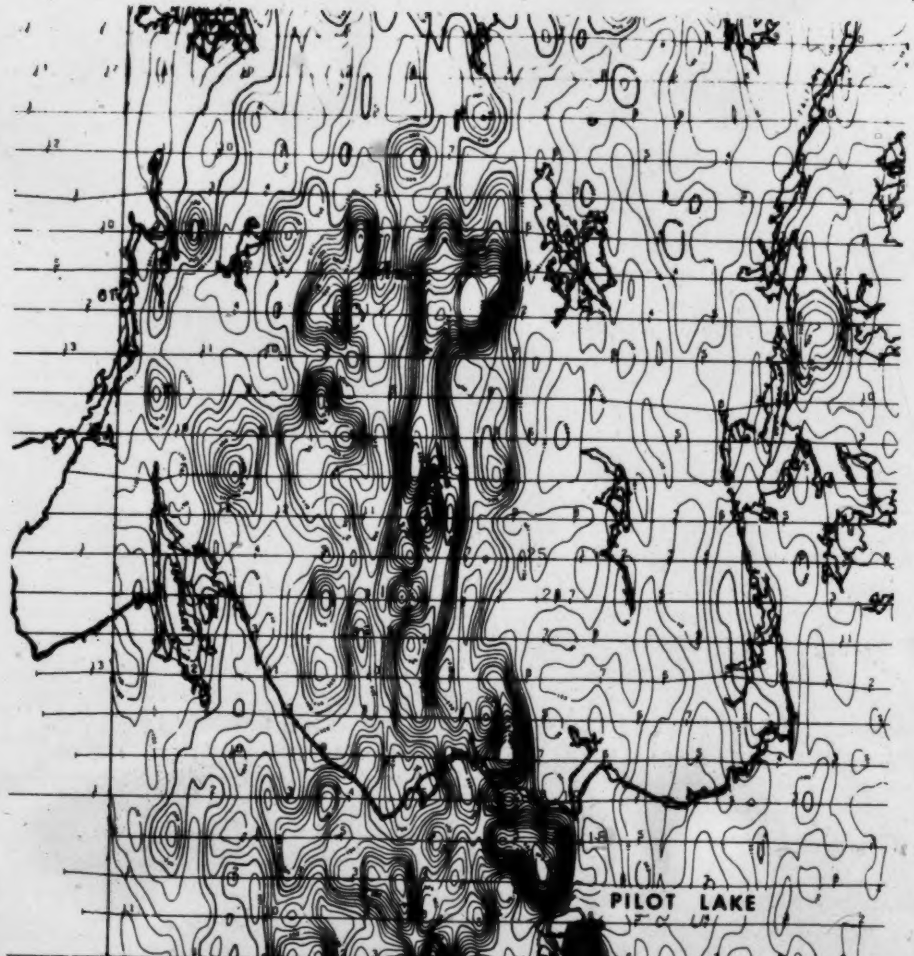

Fig. 6. Thorium isorad map from G.S.C.'s Open File Report Number 101 (Darnley and Grasty 1970), showing the core of the Fort Smith-Great Slave Lake 'high'.

The area covered by the main radioactive core is a large one, some 4,000 km², (1550 sq. miles). To investigate the cause for the above average radioactivity in such a large area would be very costly and time consuming. It was decided, therefore to choose a small and relatively accessible area showing anomalous radioactivity and as many features of the regional 'high' as possible. The Pilot Lake region appeared to be perhaps the best area to investigate in this regard for the following reasons (not necessarily in order of importance):

1. Accessibilty and proximity to a centre of population and supply, (Fort Smith, N.W.T.);
2. The best defined radioactive anomaly and perhaps the highest regional radioactivity found in the area exists here. Peak values in excess of 6 ppm U, 80 ppm Th, and 4.5% K are indicated by the isorad maps;
3. The flight profiles indicate the existence of both base level radioactivity and peak radioactivity and a very abrupt change between the two over a very short distance, (see Fig. 7);
4. Location of the anomaly on the margin of the regional high with slight overlap of the thorium anomaly by the uranium high resulting in a mild U to Th ratio anomaly on the flank, (see Fig. 7, Flight lines 17 and 18, also see Fig. 18);
5. The existence of sharp narrow uranium peaks as opposed to the very broad and extensive thorium peaks, (see Fig. 7, Flight Lines 15 and 18);
6. Apparent correlation between the beginning of the radioactive high and the beginning of a magnetic low, (see Fig. 18 and 19); and
7. The existence of a previously known uranium showing on the north shore of Pilot Lake, (Charbonneau, 1971).

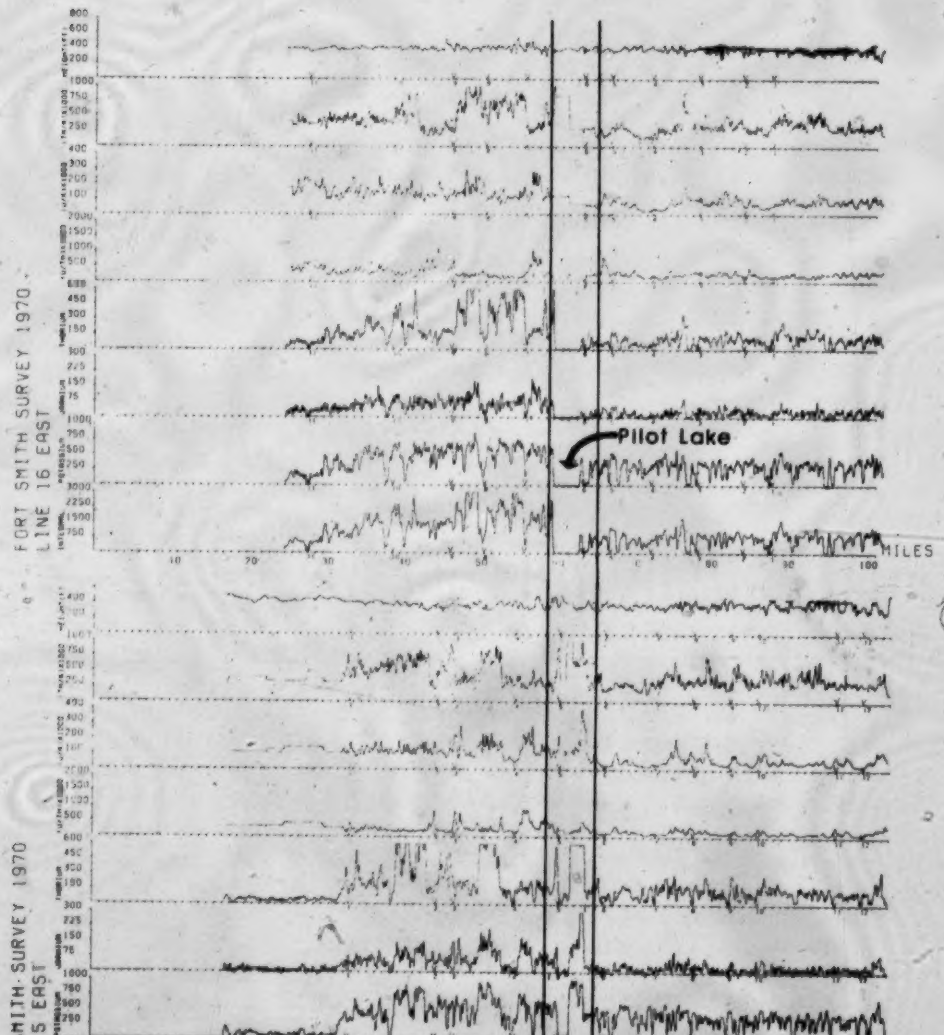

Fig. 7. Flight profiles for the Pilot Lake area from G.S.C.'s Open File Report Number 101 (Darnley and Grasty 1970). Extent of study area is marked by parallel lines.

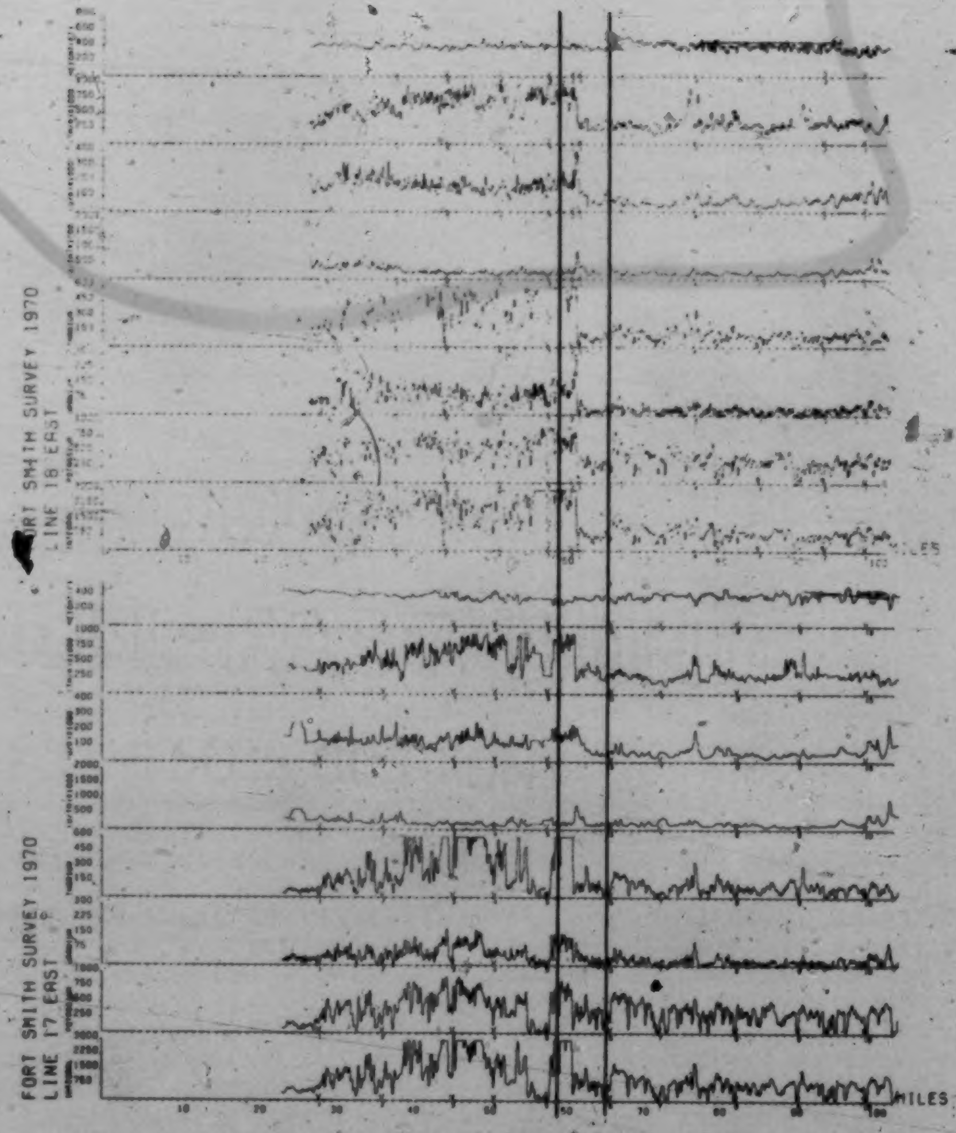

Fig. 7. Continued.

Poor copy

Investigations in the Pilot Lake area

Outcrop Scintillometer Results

The field studies in the Pilot Lake region in June of 1975 revealed excellent correlation between the main lithologies previously described and radioactivity. In general, it was found that the granitic augen gneiss (Pilot Lake Gneiss) was on average four to five times more radioactive than the paragneisses. Several anomalous situations were also found but are on a smaller scale and will be discussed later in detail.

Total radioactivity measurements revealed average count rates of 450 and 100 cps for the Pilot Lake Gneiss and paragneiss respectively. The change in count rates between these two rock types was so abrupt and noticeable that scintillometer measurements were actually used to delineate geological contacts when they were obscured by a cover of light vegetation or by tectonism. Count rates for the Pilot Lake Gneiss were remarkably consistent varying little more than 100 cps. The only exception to this was near the border with the eastern paragneisses. Count rates dropped slightly but consistently towards the metasediments until a sudden change in radioactivity at the actual contact was experienced.

The radioactivity of the paragneisses was slightly more variable as could expected from their differing chemical and mineralogical compositions. There was no apparent correlation between the amount of radioactivity and the type of metasedimentary rock encountered. The amphibolites all appeared to have very low radioelement contents.

Because the scintillometer readings were total radioactivity measurements very little was revealed in the field about the type or cause of radioactivity on a regional scale, except that the two main rock types differed greatly.

Results of U and Th Determinations

The results of the individual analyses of uranium and thorium for 32 samples of paragneiss (including 3 amphibolite) and 36 samples of Pilot Lake Gneiss are given in Tables 6 and 7 respectively. Arithmetic means for uranium in ppm are 1.64 for the paragneisses and 11.21 for the Pilot Lake Gneiss. Thorium means in ppm are 14.94 and 105.21 respectively. In calculating the mean values for the paragneisses, sample 9-9 which has an abnormally high uranium content has been excluded.

Histogram plots of uranium contents in ppm (Figs. 8 and 9) show the results for the paragneisses and the Pilot Lake Gneiss falling into two distinct populations. The histogram plots of thorium in ppm (Figs. 10 and 11) have the same general shapes. The anomalous situations (site locations 5-6, 5-7, 8-1 and 13-3) are also indicated on these plots resulting in the much higher mean values for all 103 samples. It can be noted that since 103 samples have been plotted the histograms closely approximate a plot of

TABLE 6

Uranium and thorium contents and Th to U ratios for selected Pilot Lake area paragneisses and amphibolite.

SAMPLE NUMBER	SITE LOCATION	URANIUM PPM	THORIUM PPM	TH/U	UNIT
7-1	7-1	6.28	21.78	3.5	IMPURE QUARTZITE
7-6	7-5	2.50	24.04	9.6	
9-14A	9-8	0.41	2.41	5.8	
9-17	9-12	0.85	4.09	4.8	
12-9	12-5	1.21	2.86	2.4	
4-6	4-6	2.35	23.75	10.1 *	GARNET-CORDIERITE-ANDALUSITE-GNEISS
7-2	7-2	1.12	12.46	11.1	
8-10	8-2	1.13	6.48	5.7	
9-4	9-1	0.66	2.04	3.1	
15-2	15-2	1.19	19.22	16.1	
6-5	6-3	1.02	39.16	38.5	MUSCOVITE-BIOTITE SCHIST
7-8	7-7	1.64	15.40	9.4	
7-9	7-7	1.40	28.92	20.6	
9-7	9-3	0.61	2.33	3.8	
9-11	9-5C	0.89	5.06	5.7	
14-1	14-1	0.68	4.16	6.1	
14-2	14-2	2.55	17.08	6.7	
15-1	15-1	1.58	20.12	12.7	
6-4	6-3	0.81	2.90	3.6	QUARTZO-FELDSPATHIC GNEISS
6-6	6-3	2.41	4.75	2.2	
6-7	6-4	1.26	36.90	29.3	
7-4	7-4	2.22	81.85	36.9	
7-5	7-5	1.91	21.69	11.3	
9-9	9-5a	29.21	53.21	1.8	
9-10	9-5b	1.04	1.85	1.8	
12-4	12-3	0.93	5.02	5.4	
12-8	12-5	6.87	8.82	1.3	
16-1	16-1	0.97	30.46	31.4 *	
16-3	16-2	0.34	4.72	13.8 *	
6-3	6-2	0.99	1.05	1.1	AMPHIBOLITE
12-6	12-5	1.16	5.98	5.2 *	
12-7	12-5	2.1	6.15	2.9	
AVG. EXCLUDING 9-9		1.64	14.94	9.1	

*DENOTES MAJOR ELEMENT ANALYSIS HAS BEEN DONE

TABLE 7

Uranium and thorium contents and Th to U ratios for selected Pilot Lake Gneiss samples

SAMPLE NUMBER	SITE LOCATION	URANIUM PPM	THORIUM PPM	TH/U	
4-1	4-1	10.82	135.4	12.5	
4-2	4-2	5.45	114.27	21.0	MYLONITE
4-3	4-3	10.86	127.84	11.8	*
4-7	4-7	7.27	111.47	15.3	
5-1	5-1	13.02	140.44	10.8	*
5-2	5-2	5.53	78.51	14.2	
5-4	5-4	4.22	143.32	34.0	
5-5	5-5	19.06	110.33	5.8	
5-6	5-6	14.11	82.57	5.9	* NEXT TO ZONE 1
6-1A	6-1	5.46	39.85	7.3	* CHILLED MARGIN
6-2	6-1	18.39	132.25	7.2	*
6-8	6-5	10.01	60.11	6.0	CHILLED MARGIN
6-9	6-6	17.44	43.1	2.5	
6-10	6-7	27.01	72.90	2.7	
6-11	6-8	15.60	92.24	5.9	
8-1	8-1	7.32	178.31	24.4	NEAR ZONE 3
8-2	8-1	6.2	152.55	25.0	* NEAR ZONE 3
8-6	8-1	6.01	176.88	29.4	NEAR ZONE 3
8-8	8-2	7.20	140.55	19.5	
8-9	8-2	6.83	85.58	12.5	
8-13A	8-4	5.45	150.45	27.6	
8-14	8-6	9.46	122.25	12.9	
9-1	9-1	2.04	23.15	11.4	*
9-6	9-2	29.65	51.08	1.7	* HEAVILY SHEARED
9-15	9-10	16.61	58.63	3.5	
9-16	9-11	4.76	155.71	32.7	
9-18	9-13	7.84	113.93	14.5	*
12-1	12-1	9.59	133.94	14.0	
12-2	12-2	9.09	160.43	17.6	
12-3	12-2	13.79	133.78	9.7	MYLONITE
12-10	12-5	18.36	10.59	0.6	*
12-11	12-5	28.24	63.97	2.3	*
12-13	12-7	8.1	116.96	14.4	
13-1	13-1	6.4	71.77	11.2	
13-2	13-2	9.83	105.99	10.8	*
13-6	13-5	6.78	96.75	14.3	
AVERAGE		11.21	105.21	9.39	

* DENOTES MAJOR ELEMENT ANALYSIS

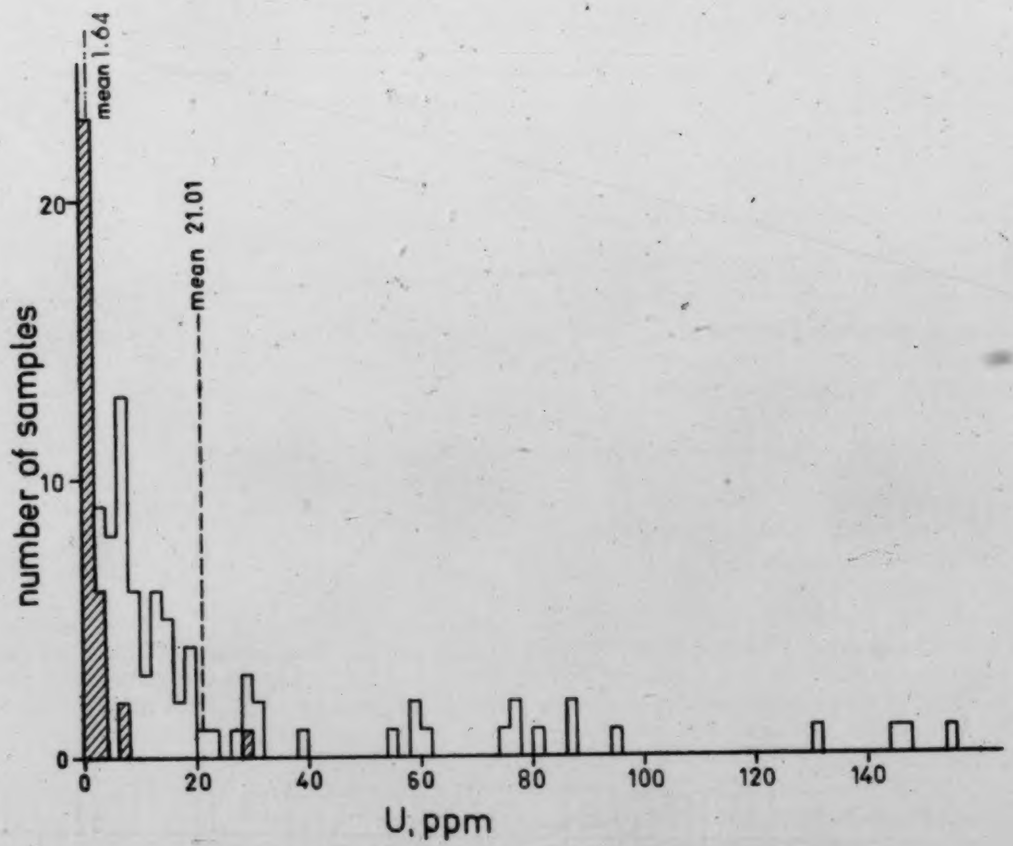

Fig. 8. Histogram showing the distribution of uranium for the Pilot Lake area paragneisses (lined) plotted with all samples analysed. Median value for the paragneisses is 1.16 ppm.

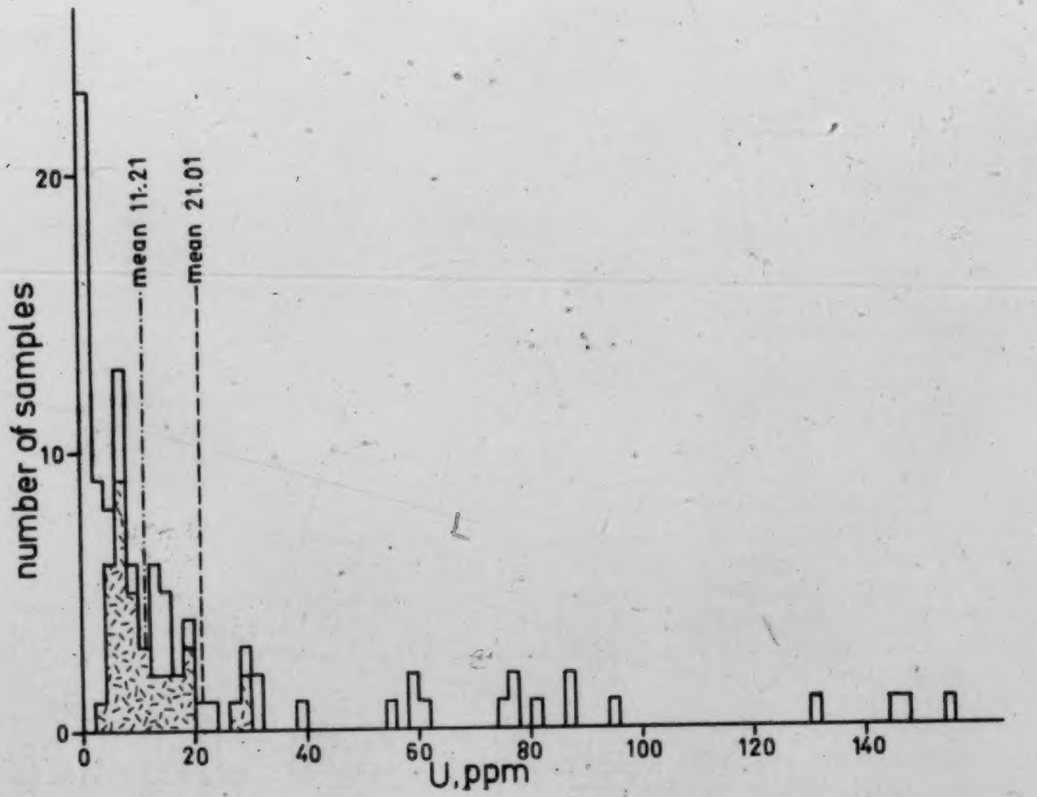

Fig. 9. Histogram showing the distribution of uranium for the Pilot Lake Gneiss (pattern) plotted with all samples analysed. Median value for the Pilot Lake Gneiss is 9.27 ppm.

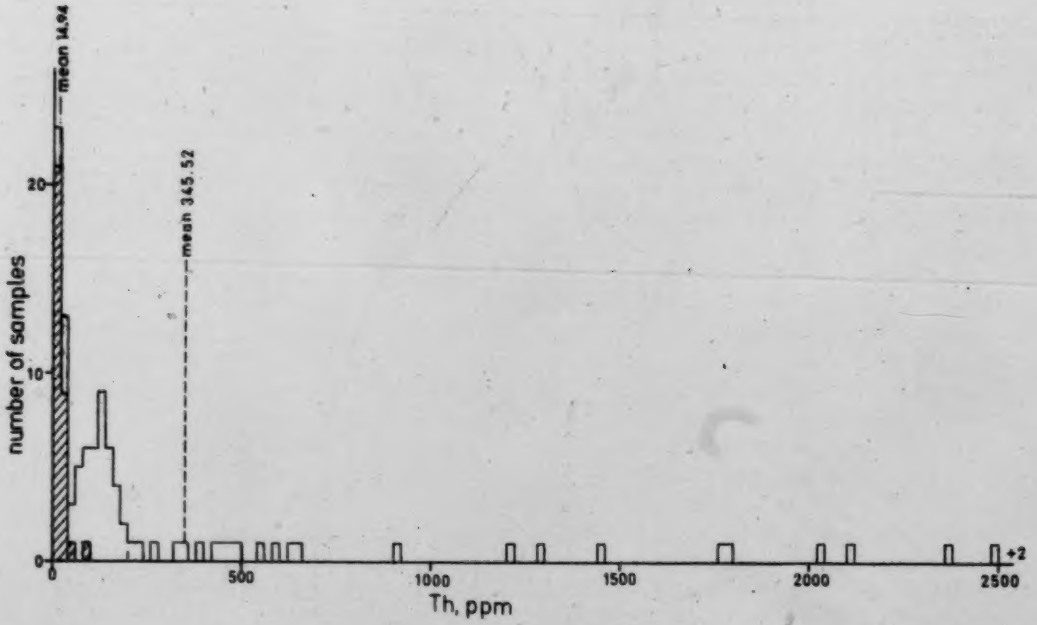

Fig. 10. Histogram showing the distribution of thorium for the Pilot Lake paragneisses (lined) plotted with all samples analysed. Median value for the paragneisses is 6.48 ppm.

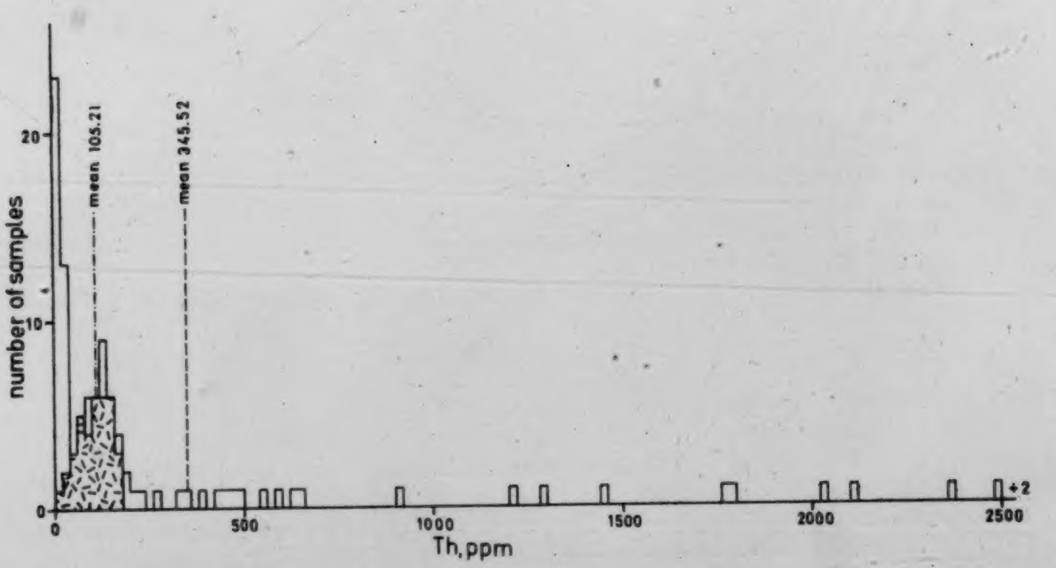

Fig. 11. Histgram showing the distribution of thorium for the Pilot Lake Gneiss (pattern) plotted with all samples analysed. Median value for the Pilot Lake Gneiss 112.7 ppm.

percentages of samples vs. content.

Variable Paragneiss

As was the case with the total scintillometer readings detailed analysis has revealed little about the distribution of uranium and thorium in the metasediments.

Uranium values (excluding sample 9-9) range from a low of 0.34 ppm, to a high of 6.87 ppm. More than 70 percent of the samples analysed have a value of less than 2 ppm. Thorium values range from 1.05 to 81.85 ppm with 66 percent of the results less than 20 ppm and 53 percent less than 10 ppm. There is a great range of Th to U ratios with a mean of 9.1 using the uranium and thorium averages. A histogram plot of the ratios (Fig. 12) shows a skewness with a bias in the range less than the mean.

Other than the consistently low results for the amphibolites, confirming the scintillometer readings, there seems to be no correlation between uranium and thorium abundances and metasedimentary rock type. Turekian and Wedepohl (1961) have listed uranium and thorium averages for common shales and sandstones (Table 8). They designate these two rock types as end members with most other clastic sediments falling in between. Comparison of their results with the paragneisses of the Pilot Lake region (assuming the Pilot Lake metasediments are all originally clastic sediments, no chemical carbonate rock types were found) shows the average uranium value for the study suite (1.64

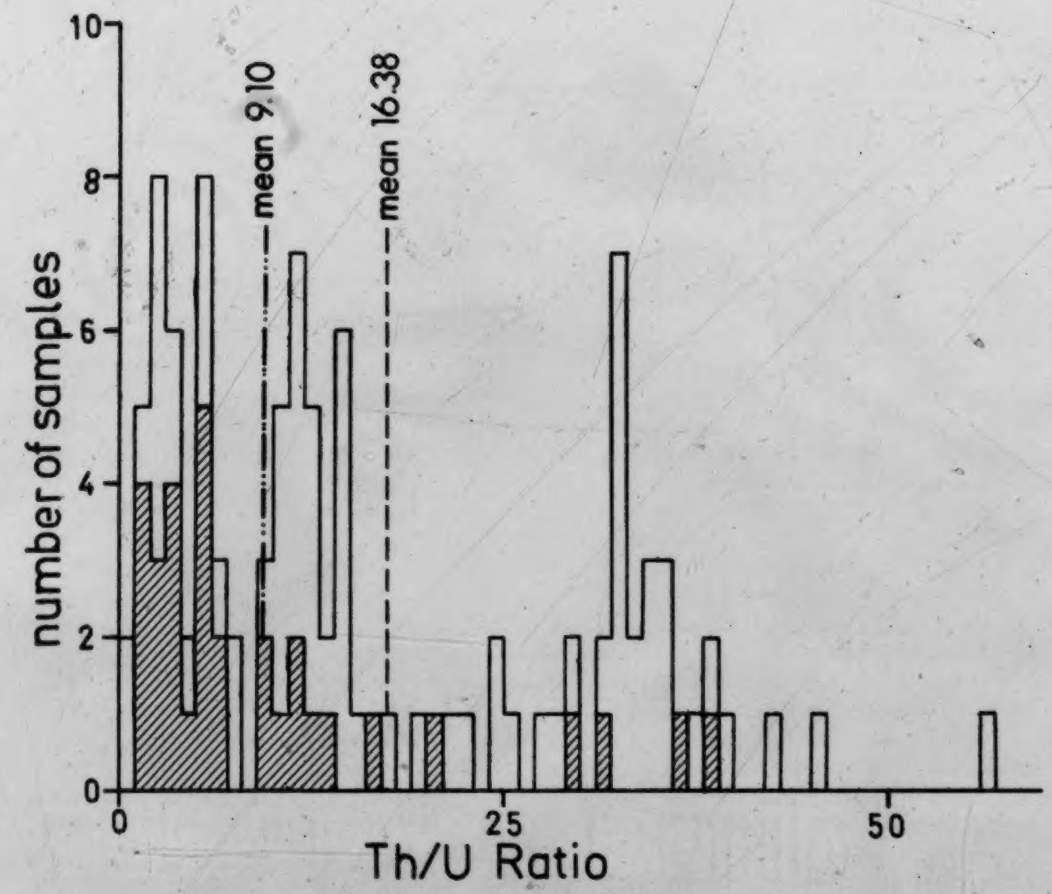

Fig. 12. Histogram showing the distribution of Th to U ratios for the Pilot Lake paragneisses (lined) plotted with all samples analysed.

ppm) to fall between the shale (3.7 ppm) and sandstone (0.45 ppm) average. The thorium average (14.94 ppm) is slightly above that for a common shale (12 ppm) producing a Th to U ratio almost 3 times the norm. This is consistent with the fact that the area is a thorium rich belt.

The average uranium and thorium values for the Pilot Lake metasediments also compare quite closely to average values reported for the Canadian Shield. Shaw (1967) reports values of 2.45 ppm and 10.3 ppm for uranium and thorium respectively. A much closer comparison is obtained by using the average of Eade and Fahrig (1971). They reported values of 2.1 ppm for uranium and 13 ppm for thorium when weighting their results according to the size of the structural provinces of the Canadian Shield.

Pilot Lake Gneiss

Radioelement values for the Pilot Lake Gneiss are significantly more important and interesting than those for the metasediments. Uranium values for the 36 samples analysed range from 2.04 ppm to 29.65 ppm with a mean of 11.21 ppm. Thorium values, with a mean of 105.21 ppm, range from a low of 10.59 ppm to a high of 178.31 ppm.

Although a true metamorphic rock the Pilot Lake Gneiss possesses a mineralogical and chemical composition similar to many granitic rocks. Comparison of uranium and thorium values to those in the literature for rocks with a granitic chemistry is therefore necessary to aid in a petrogenetic interpretation.

Several averages for granitic rocks are presented in Table 8. They group closely together, at approximately 4.0 ppm for uranium and 17.0 ppm for thorium. The average value for the Pilot Lake Gneiss is over 2.5 times that for uranium and 6 times that for thorium in average granites. In fact very few studies of radioelement contents in granitic rocks report values as high as those of the Pilot Lake Gneiss. The Conway granite for example, an alkalic, Triassic intrusive in New Hampshire (Rogers *et al*. 1965) has a reported average value of 15 ppm for uranium but only 56 ppm for thorium.

Heier and Rhodes (1966) report arithmetic means of 10.3 ppm U and 45.7 ppm Th for granites and gneisses of the Rum Jungle Complex in Australia, with thorium values similar to the Pilot Lake Gneiss in only two samples of a leucocratic granite.

Variations in U and Th Content and Their Geographical Distribution. It is interesting to note that the histogram plots of uranium and thorium for the Pilot Lake Gneiss are skewed differently. The median value for uranium is substantially less than the mean (9.27 ppm vs. 11.21 ppm), skewing the population to the left (Fig. 9). The thorium values on the other hand are slightly skewed to the right with a median value (112.7 ppm) greater than the mean (105.21 ppm, Fig. 11). This results in the Th to U ratios showing a bias greater than the mean of 9.39 (Fig. 13). These results are different than the paragneiss which had

TABLE 8

Average uranium and thorium abundances for common sedimentary rocks, granites and the Canadian Shield

ROCK TYPE OR REGION	U ppm	Th ppm	Th/U	REFERENCE
Common Shales	3.7	12	3.2	Turekian and Wedepohl, 1961
Sandstones	0.45	1.7	3.8	Turekian and Wedepohl, 1961
Granite	4.75	17.36	3.6	Killeen and Heier, 1975
Granite Low Ca	3.0	17.0	5.7	Turekian and Wedepohl, 1961
Granite	4.8	17.0	3.5	Taylor, 1964
Canadian Shield	2.45	10.3	4.2	Shaw, 1967
Canadian Shield Weighted according to size of structural province	2.1	13.0	6.2	Eade and Fahrig, 1971
Western Can. Basin (Basement)	4.13	21.1	5.1	Burwash and Cumming, 1976

median values less than the mean for both thorium and uranium.

A plot of uranium vs. thorium for the Pilot Lake Gneiss (Fig. 1[illegible] indicates the reason for this variation in the histogram plots. The large extension of the field and its shape testify to the low degree of mutual dependence of the two radioelements within the gneiss. The correlation in fact is a negative 0.376 (i.e. an increase in Th corresponds to a slight decrease in U). This is in contradistinction to their well known positive interdependence in the evolution of granitic rocks. Whitfield et al. (1959) and Rogers and Ragland (1961) for example show good positive correlations between uranium and thorium in granitic rocks.

Plots of U vs. Th/U and Th vs. Th/U are further indication of the independent action of uranium and thorium during the development of the Pilot Lake Gneiss. Fig. 15 shows the rather large field of Th to U ratios plotting against U, with a high degree of negative correlation. There is a tendency towards a steep rise in uranium values corresponding to a low Th/U. Conversely a plot of Th vs. Th/U (Fig. 16) displays a positive correlation of equally high degree.

On the U vs. Th plot a line representing the average Th to U ratio (9.39) divides the values into two fields; one with samples essentially high in thorium with a high Th/U and the other showing high uranium values with a lower than

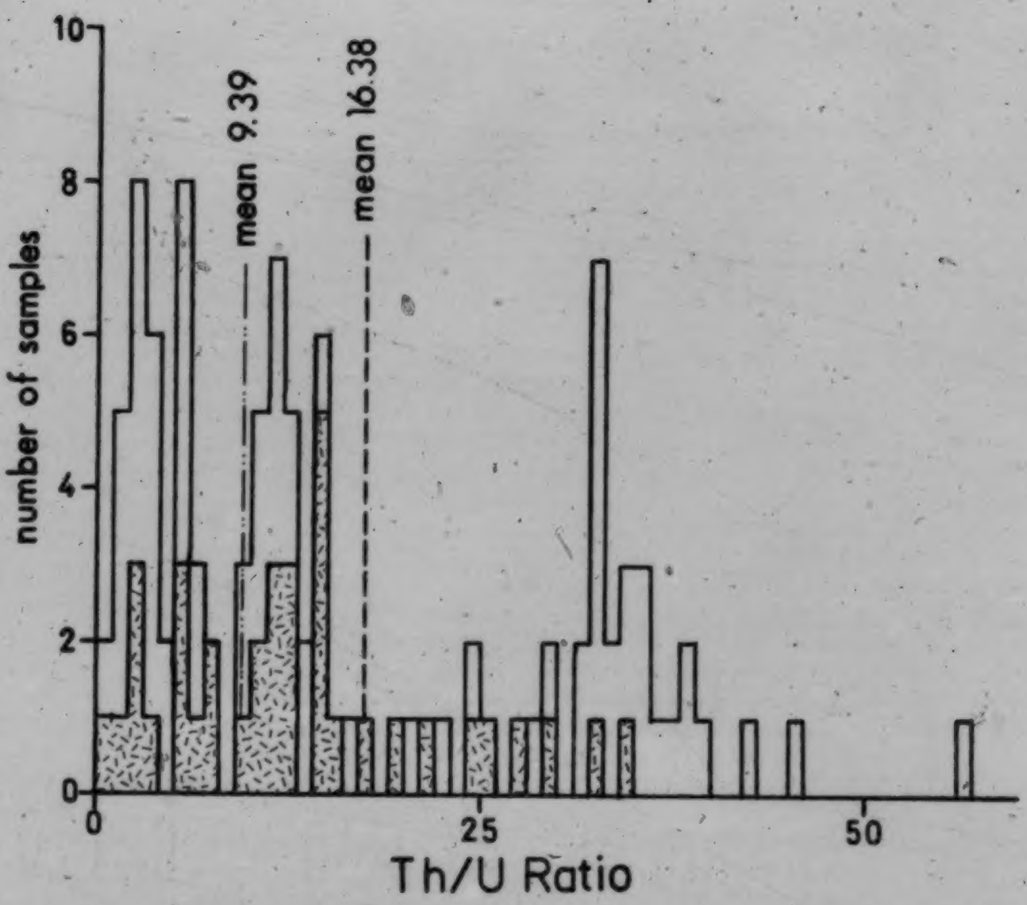

Fig. 13. Histogram showing the distribution of Th to U ratios for the Pilot Lake Gneiss (pattern) plotted with all samples analysed.

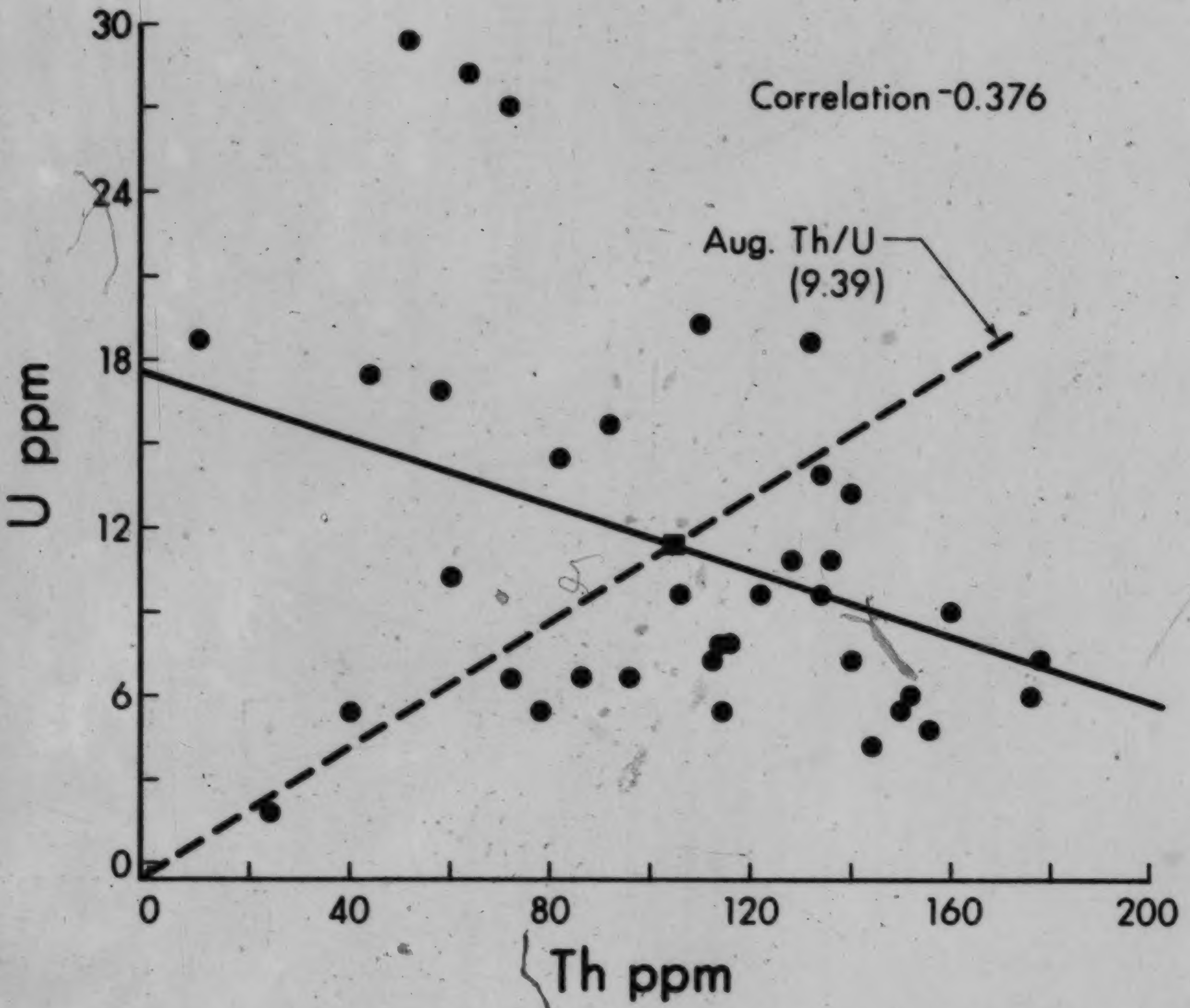

Fig. 14. Uranium content vs. thorium content for the Pilot Lake Gneiss. Square represents the average of all values.

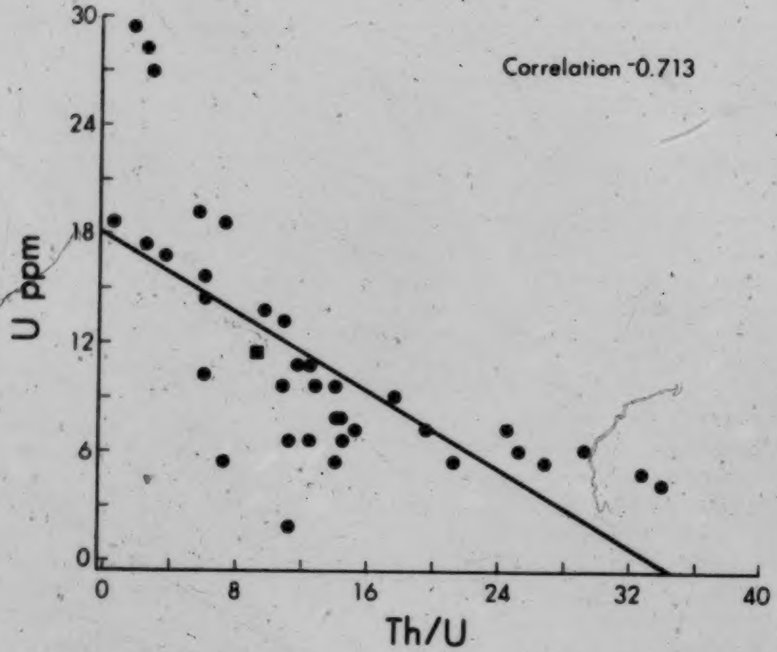

Fig. 15. Uranium content vs. Th to U ratios for the Pilot Lake Gneiss.

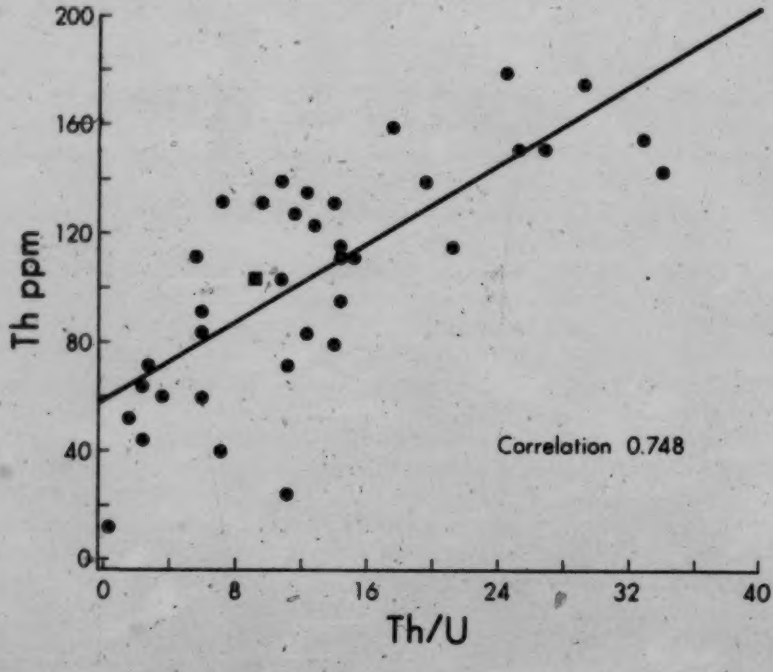

Fig. 16. Thorium content vs. Th to U ratios for the Pilot Lake Gneiss.

average Th to U ratio. Sixty-seven percent of the samples plot in the field with a higher than average Th to U ratio. The closing of the scatter towards the high thorium end also serves to indicate that the high Th to U ratio is the more normal situation. The samples falling in the field of higher than average uranium and lower than average thorium become very significant when we see where they occur in the geological setting. When studying the site locations listed in Table 7 with the sample collection site map (Fig. 17), we find that all 12 samples with Th to U ratios less than the mean fall at or very near the borders between the Pilot Lake Gneiss and paragneisses. This is especially true along the boundary between the granitic augen gneiss and eastern paragneiss where 10 of the 12 samples are located. These samples, with the exception of samples 6-1A and 6-8 which may be part of a chilled contact, have uranium values considerably higher than the average. Thorium values are usually much lower than the average. The averages of these eight samples are 19.78 ppm uranium and 76.00 ppm thorium.

These results illustrate why a mild U/Th anomaly exists on the flank of the regional 'high' in the Pilot Lake area. Fig. 18 is a map showing the trends of the peak uranium and thorium values in the Pilot Lake area from G.S.C. Report Number 101. Flight line 16 crosses a large portion of Pilot Lake where values near zero make correlation across the lake difficult. However, a strong aeromagnetic high, found just to the east, closely following the gneiss-metasedimentary contact, has been plotted to aid in the extrapolation of the radioelement peaks. It should also be noted that the magnetic high is sharp and defines the edge of the previously mentioned broad magnetic low that coincides with the regional radiometric 'high' (Fig. 19).

The thorium peaks are broad but have their highest readings over the core of the Pilot Lake Gneiss. The uranium peaks are sharp and narrow and definitely offset from the thorium high. Their trend coincides with the Pilot Lake Gneiss at the contact with the eastern paragneisses. It is therefore, the high uranium values corresponding with lower thorium, at the eastern margins of the Pilot Lake Gneiss, that is responsible for the U/Th anomaly established by G.S.C. Open File Report Number 101, (1971) on the flanks of the 'high', in the Pilot Lake area.

Anomalous Radioactivity

Scintillometer investigations revealed anomalous radioactivity at four localities in the Pilot Lake region. As previously mentioned these highly radioactive areas are very local in extent. However, they are extremely important in a geologic interpretation of the cause of the regional radioactivity in the Pilot Lake area and perhaps for all of the Fort Smith-Great Slave Lake 'high'. For descriptive purposes and ease of identification, these radioactive areas have been termed Zones 1,2,3 and 4.

Scintillometer measurements indicate radioactivity at

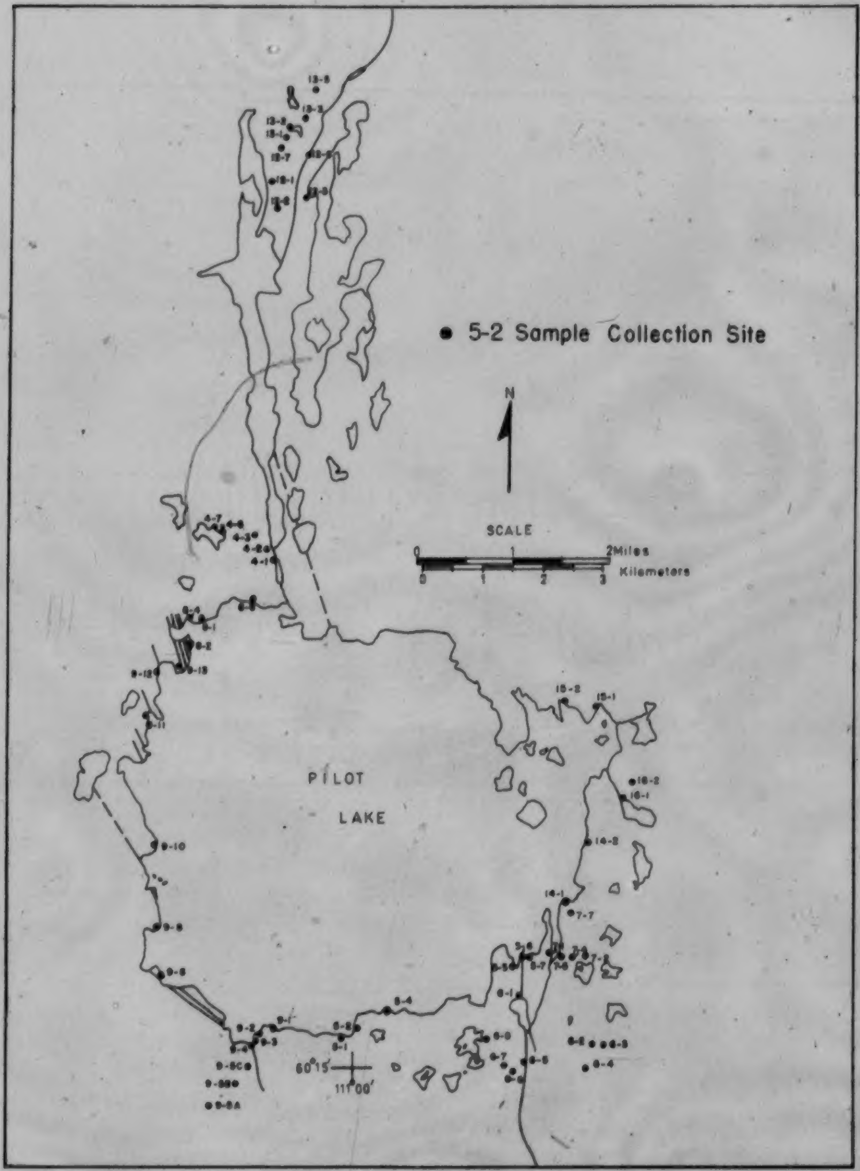

Fig. 17. Sample collection site map.

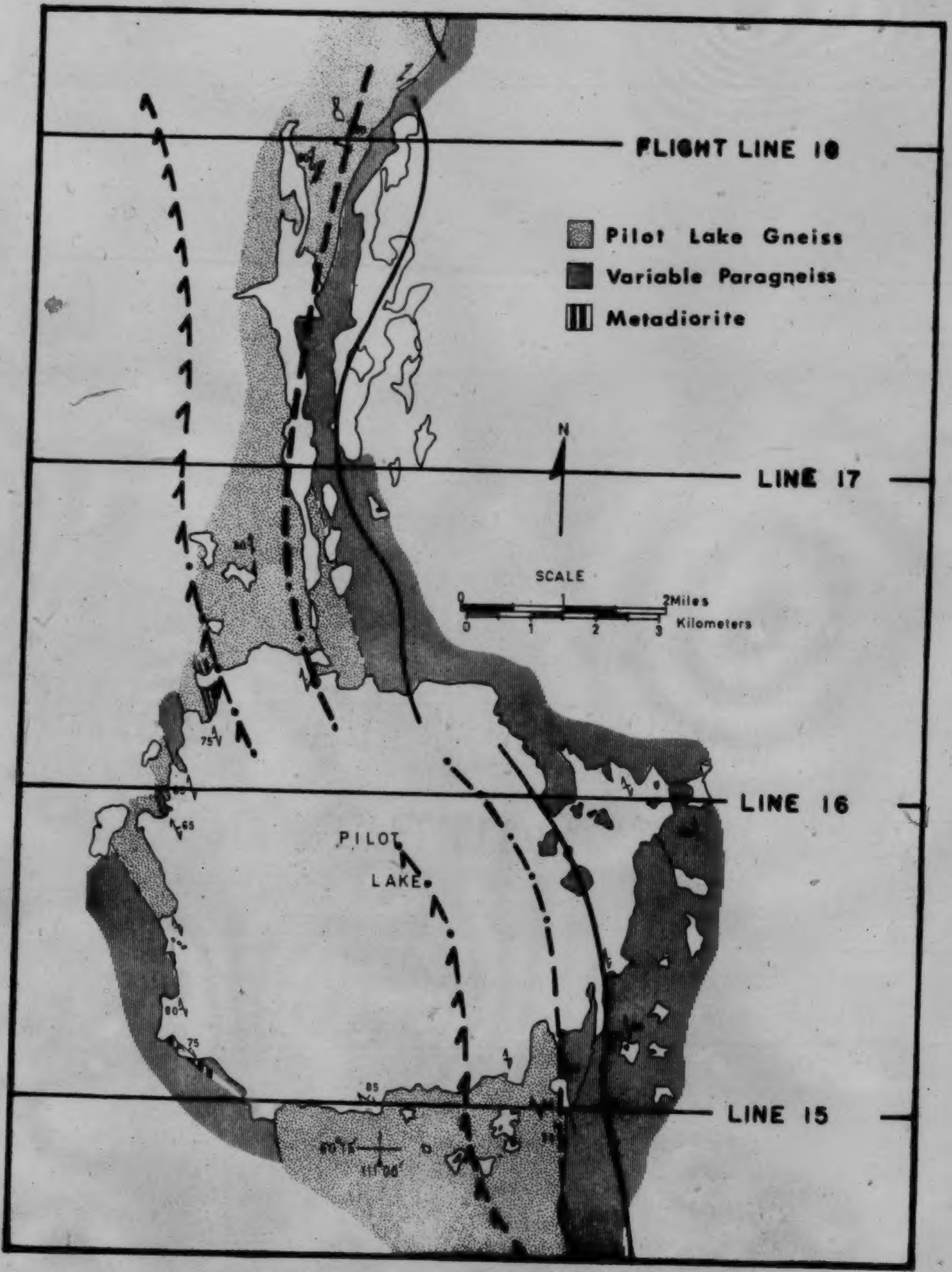

Fig. 18. Trends of peak thorium values (arrowed line), peak uranium values (dashed line) and an aeromagnetic high (solid line). Radiometric data from Darnley and Grasty 1970.

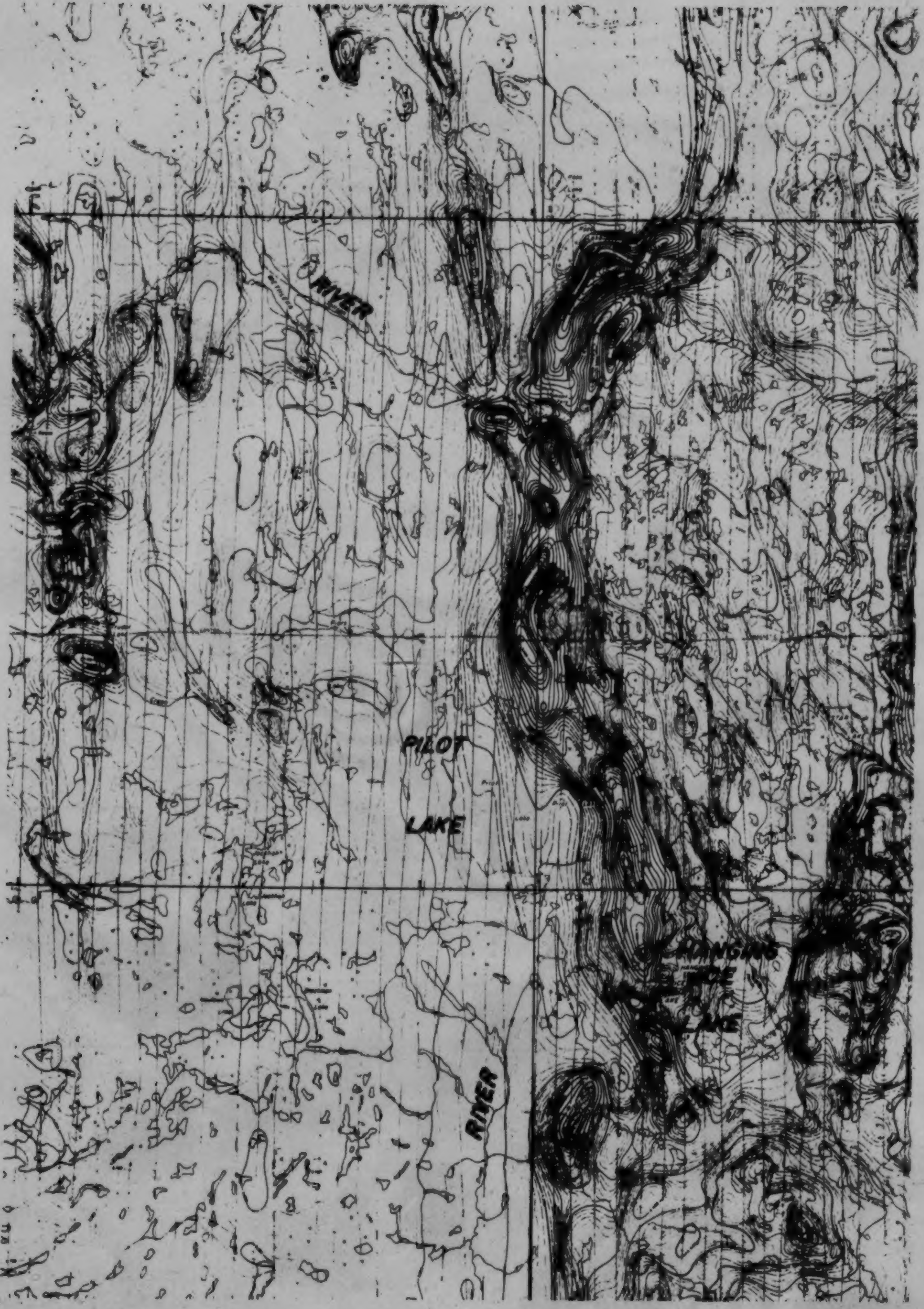

Fig. 19. Aeromagnetic map of the Pilot Lake area.

least twice the average of the Pilot Lake Gneiss, with one zone having values 10 times the gneiss and 50 times the paragneisses or base level of the region.

Detailed grids were set up over each radioactive zone with baselines running roughly parallel to their long axes. Total radioactivity measurements were taken at intervals of 1 ft. along lines 2 or 5 ft. apart, perpendicular to the baseline, until the whole zone was covered. Several samples were taken from each zone for petrographic study and detailed uranium and thorium analysis. In total, 30 samples have been analysed for their uranium and thorium contents and are listed together in Table 9. Ten bulk chemical analyses on selected samples from the four zones are listed separately as each zone is described.

Zone One

Zone 1, with scintillometer values as high as 4000 cps is found trending N 30° W on a very small point of land on the southeast shore of Pilot Lake. Exposed dimensions are approximately 3.5 by 1.5 m with the south end covered by vegetation and the north end by Pilot Lake. The extreme radioactivity is confined to a narrow core 20 to 30 cm wide (Fig. 20). It is considered doubtful that the zone continues any great distance either under the lake or beneath the vegetation cover. This zone is found at the contact immediately east of Pilot Lake Gneiss sample 5-6. The foliation exhibited by the long axis of the zone is slightly oblique to the foliation trend of the neighbouring Pilot

TABLE 9

Uranium and Thorium contents and Th/U for anomalously radioactive samples

SAMPLE NUMBER	SITE LOCATION	URANIUM PPM	THORIUM PPM	TH/U	
5-7A	5-6	86.76	1215.0	14.0	ZONE 1
5-7D	5-6	144.89	1444.8	10.0	*
5-8A	5-7	131.76	1774.9	13.5	
5-8C	5-7	55.70	584.7	10.5	*
5-8D	5-7	80.57	911.4	11.3	ZONE 2
5-8E	5-7	61.23	20.53	0.3	
5-8H	5-7	154.83	1783.8	11.5	*
8-3A	8-1	39.74	1280.2	32.2	
8-3B	8-1	13.76	452.3	32.9	*
8-3C	8-1	76.29	2488.9	32.6	
8-4	8-1	86.09	2108.1	24.5	*
8-5A	8-1	59.26	2024.7	34.2	ZONE 3
8-5C	8-1	95.30	3593.3	37.7	*
8-7	8-1	18.38	655.9	35.7	
11-1	8-1	76.16	2372.9	31.2	
11-3	8-1	75.29	2610.5	34.7	
11-4-2W	8-1	9.32	354.8	38.1	
11-4-1W	8-1	14.15	463.5	32.8	
11-4-00	8-1	14.96	587.2	39.3	* ZONE 3
11-4-1E	8-1	12.38	434.3	35.1	at trench
11-4-2E	8-1	12.78	544.6	42.6	
11-4-3E	8-1	9.06	321.7	35.5	*
11-4-4E	8-1	7.26	244.4	33.7	
11-4-5E	8-1	5.68	186.96	32.9	
11-4-6E	8-1	5.68	162.65	28.6	*
13-20N-1E	13-3	146.54	395.62	2.7	*
13-30N-2E	13-3	59.38	129.55	2.2	ZONE 4
13-90N-7W	13-3	31.02	122.0	3.9	
13-4	13-3	31.08	125.58	4.0	
13-5	13-3	23.55	283.07	12.0	

*DENOTES MAJOR ELEMENT ANALYSIS

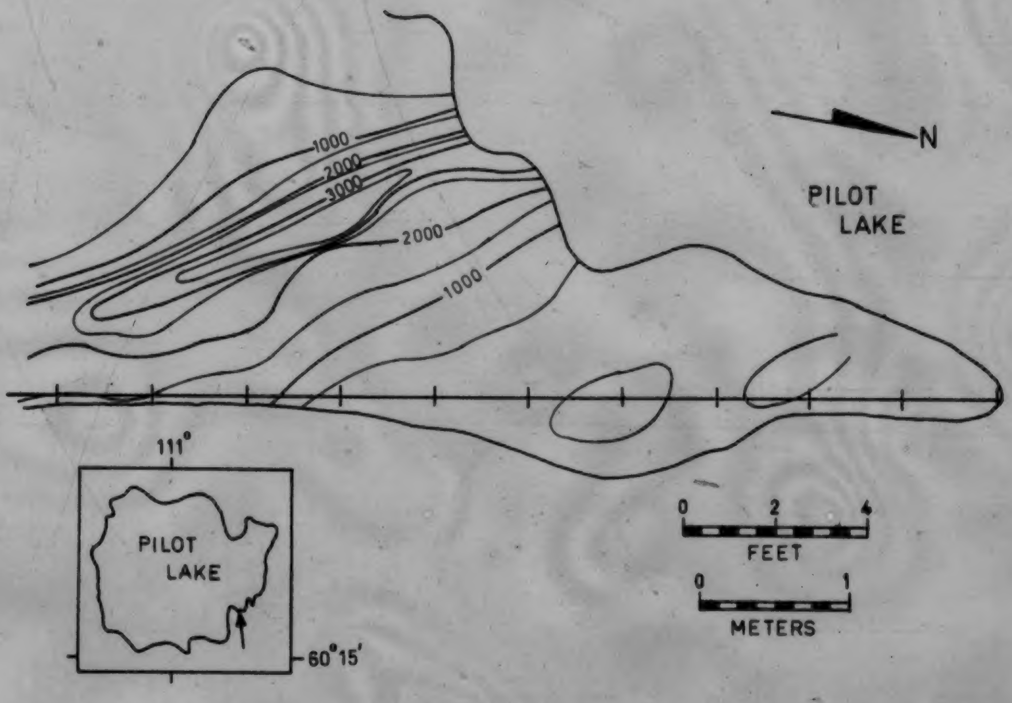

Fig. 20. Scintillometer profile for Zone 1 in counts per second.

Lake Gneiss. Rocks of the variable paragneiss unit are found to the east of the zone.

The extreme radioactive readings are confined to a massive, fine to medium grained, dusky red hornfelsic rock (Plate 5,a). Aggregates of extremely dark red feldspar produce a crude form of layering or banding. Small red feldspars, biotite and a clear, colourless mineral that looks like quartz but proved in thin section to be apatite, give the rock a mosaic or sugary appearance. Late muscovite has crystallized along small fractures.

Petrography and Chemistry. Thin sections show the rock to be composed predominately of plagioclase, mica and apatite, in anhedral subequigranular form. Only muscovite and biotite exhibit subhedral to euhedral habit. Plagioclase, with a composition of An 30, is usually found as irregular or rounded grains 1 mm to 2 mm in size. They are moderately to strongly sericitized and are often fractured and heavily dusted with hematite, giving them a dark red colour in hand specimen. They usually occur as granoblastic-polygonal masses or combine with xenoblastic apatite to form thin layers a few millimeters in width. Dark brown, pleochroic biotite has grown interstial to the plagioclase and apatite or forms masses of interlocking, randomly orientated, subidioblastic crystals. This feature, known as decussate texture is typical of hornfelsic rocks. The biotite is remarkably fresh with only late muscovite formed at its expense.

The most remarkable feature of this zone is the extremely high content of apatite and monazite. The apatite is colourless with a high relief and a weak blotchy birefringence. It usually occurs as xenoblastic grains up to 2 mm in diameter aggregating to form definite layers (Plate 5,b). Very few hexagonal or tabular euhedral crystals were found. The average of four modal analyses (Table 10) shows that apatite exceeds 14 percent of the total. It has grown together with or included many minerals such as: biotite, opaques, monazite and zircon. Fracturing of the apatites is common, often with the infilling of hematite.

Monazite was found to occur as sub-rounded to extremely rounded grains 0.1 mm to 0.2 mm in diameter. It is colourless to pale yellow, with a high relief, an even texture and a strong birefringence. When enclosed or surrounded by colourless feldspar the monazites can be seen to be heavily rimmed with iron oxide (Plate 5,c). When included or abutting against apatite, however, the rim is absent. Smaller rounded zircons are often found included in the monazite cracking the host mineral (Plate 5,c). Autoradiographs showed the extremely radioactive monazite (Plates 5,d and 6,b), averaging 1.5 percent in the zone, to preferentially occur with the apatite layers.

The mineralogy and texture remains quite consistent throughout the zone with an average composition of: 58 percent plagioclase, 2.5 percent potassium feldspar, 13

PLATE 5. ANOMALOUS ZONE 1

a. Field photograph. Site 5-7. Exposure of the fine to medium grained massive to slightly banded hornfelsic rock possessing the anomalous radioactivity at zone 1. The long axis of the zone is parallel to the hammer handle.

b. Zone 1. Photomicrograph. Sample 5-7A. Aggregate of xenoblastic apatite crystals (blotchy high relief) forming a crude layer in plagioclase from center top to center bottom of photograph. Dark minerals are monazite surrounded and dusted by hematite. Plane light. Bar scale is 0.3 mm.

c. Zone 1. Photomicrograph. Sample 5-7B. Rounded grains of monazite heavily rimmed by hematite in plagioclase. Note inclusion of two smaller rounded zircon grains internally fracturing the lower right monazite. Plane light. Bar scale is 0.1 mm.

d. Zone 1. Autoradiograph of monazite grains in Plate 5c. Bar scale is 0.1 mm.

PLATE 5

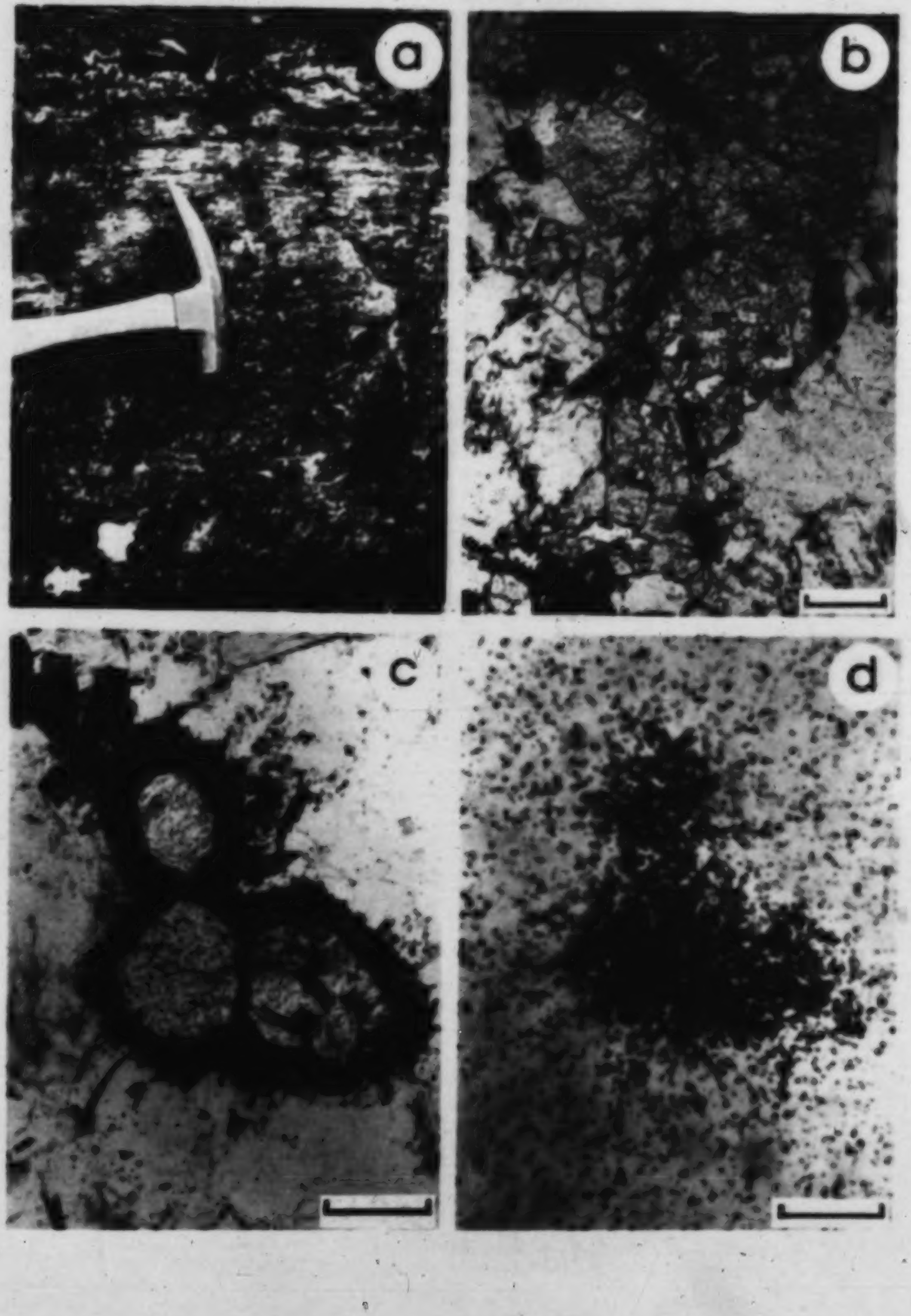

TABLE 10

Results of chemical and modal analysis for zone 1

SAMPLE NUMBER	5-7D	5-7A	5-7B	5-7C	AVG.
SiO_2	45.0				
Al_2O_3	19.4				
CaO	10.6				
MgO	1.16				
Na_2O	4.11				
K_2O	3.14				
FeO	3.47				
Fe_2O_3	1.65				
MnO	0.08				
TiO_2	1.48				
P_2O_5	6.03				
S	Nil				
LOI	2.05				
Total	98.17				
Uppm	148.89	86.76			117.82
Thppm	1444.8	1215.0			1329.9
MODAL ANALYSIS					
Pg	56.65	64.4	55.1	56.8	58.2
Kfel	2.00	2.0	3.8	2.0	2.4
Bi	15.75	8.8	13.2	13.0	12.7
Ap	12.85	12.85	14.4	16.6	14.2
Mu	9.05	7.2	7.6	6.3	7.5
Op	3.60	2.85	3.5	4.0	3.5
Lx	0.15	0.45	1.0	---	0.4
Zr	0.38	1.6	0.32	1.5	0.35
Mz	1.77		1.18		1.47
Total counts	2000	2000	1500	1500	

percent biotite, 14 percent apatite, 7.5 percent muscovite, about 4 percent total opaques and almost 2 percent combined zircon and monazite.

One whole rock chemical analysis and two uranium and thorium determinations are listed in Table 10. The results reflect the high amount of apatite in this zone with just over 6 percent P205 reported. Other striking values are high CaO (10.6%) and high TiO2 (1.48%) and of course high U (average of 2 values 117.82 ppm) and Th (average of 2 values 1329.9 ppm).

Zone Two

Zone 2 is found on the southeast shore of the lake, a few hundred feet to the east of Zone 1, heavily covered with vegetation. As in Zone 1 a profile of the anomaly shows a linear shape roughly 12 by 1.5 m, with scintillometer values as high as 2500 cps (Fig. 21). This zone shows a slight warp with an approximate trend of N 45° W, dipping 75° to the east. The highest radioactivity occurs in two small bands or pockets, one in a cliff face at the shoreline, the other slightly inland. The zone occurs totally within the eastern paragneisses.

Two exposures, one on the cliff face and one stripped of the vegetation cover yielded samples of an extremely biotite-rich schist. The fine, flakey biotite predominates in layers several centimeters thick giving the rock an extremely dark colour on a fresh surface. Small, rounded,

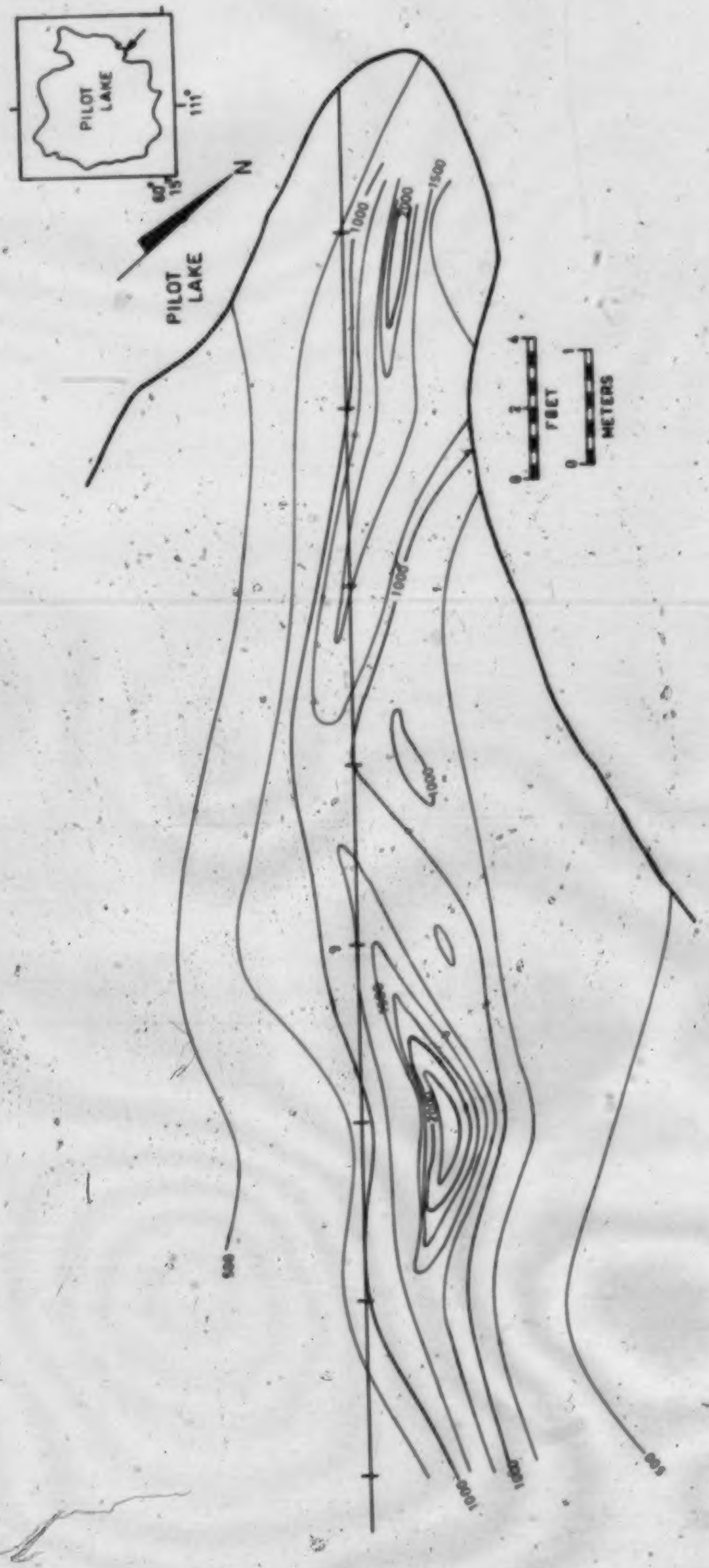

Fig. 21. Scintillometer profile for Zone 2 in counts per second.

pale green to yellow grains (1 mm in diameter), identified as apatite in thin section are found associated with the biotite in varying percentages, to the point where it has been concentrated up to 60 percent in thin bands less than 1 cm wide. Also found scattered throughout the biotite layers are many red feldspar porphyroclasts and dark red garnets up to 1.5 cm in diameter. The biotite-rich layers alternate with dark red feldspar layers or clusters that are generally no more than a couple of centimeters in width. The only exposed contact shows the feldspar layers increasing in frequency over a short distance until the biotite schist gives way to a banded quartzo-feldspathic gneiss with radioactivity consistent with the average paragneiss values.

Petrography and Chemistry. Thin sections taken from the different layers show a variety of mineralogical compositions and textures. The biotite-rich layers have an abundance of the brown mineral in an interlocking array of crystals no more than 1 mm in length. Although many directions of crystal orientation are exhibited the biotites in general do display a preferred orientation. Xenoblastic apatite is scattered widely throughout the biotite network ranging from less than 0.1 mm to greater than 1 mm in diameter. A faint layering of the apatite was often observed as were apatite clusters within the biotite-rich layers. The apatites often include very small grains of zircon and monazite. Extremely broken and altered garnet is sometimes found with a highly irregular growth pattern. Plate 6,c shows an unusual association of garnet growing interstitial

PLATE 6. ANOMALOUS ZONES 1 AND 2

a. Photomicrograph and b. autoradiograph, Zone 1. Sample 5-7B. Characteristics of monazite and zircon. Note the large radioactive monazite in the upper right with a small zircon inclusion. Also the elongated pear-shaped zoned zircon in the lower left with monazite grains on either end. Monazites are recorded on the autoradiograph but the large zircon is not. Dark minerals are opaques and biotite. Light minerals are muscovite. Plane light. Bar scale is 0.1 mm.

c. Zone 2. Photomicrograph. Sample 5-8G. Fractured garnet grown interstitial to and enclosing xenoblastic grains of apatite (light). Plane light. Bar scale is 0.5 mm.

d. Zone 2. Photomicrograph. Sample 5-8E. Irregularly shaped grains of green spinel (dark) interstitial to anhedral feldspar grains (light). Large rounded apatite is in lower left. Plane light. Bar scale is 0.5 mm.

PLATE 6

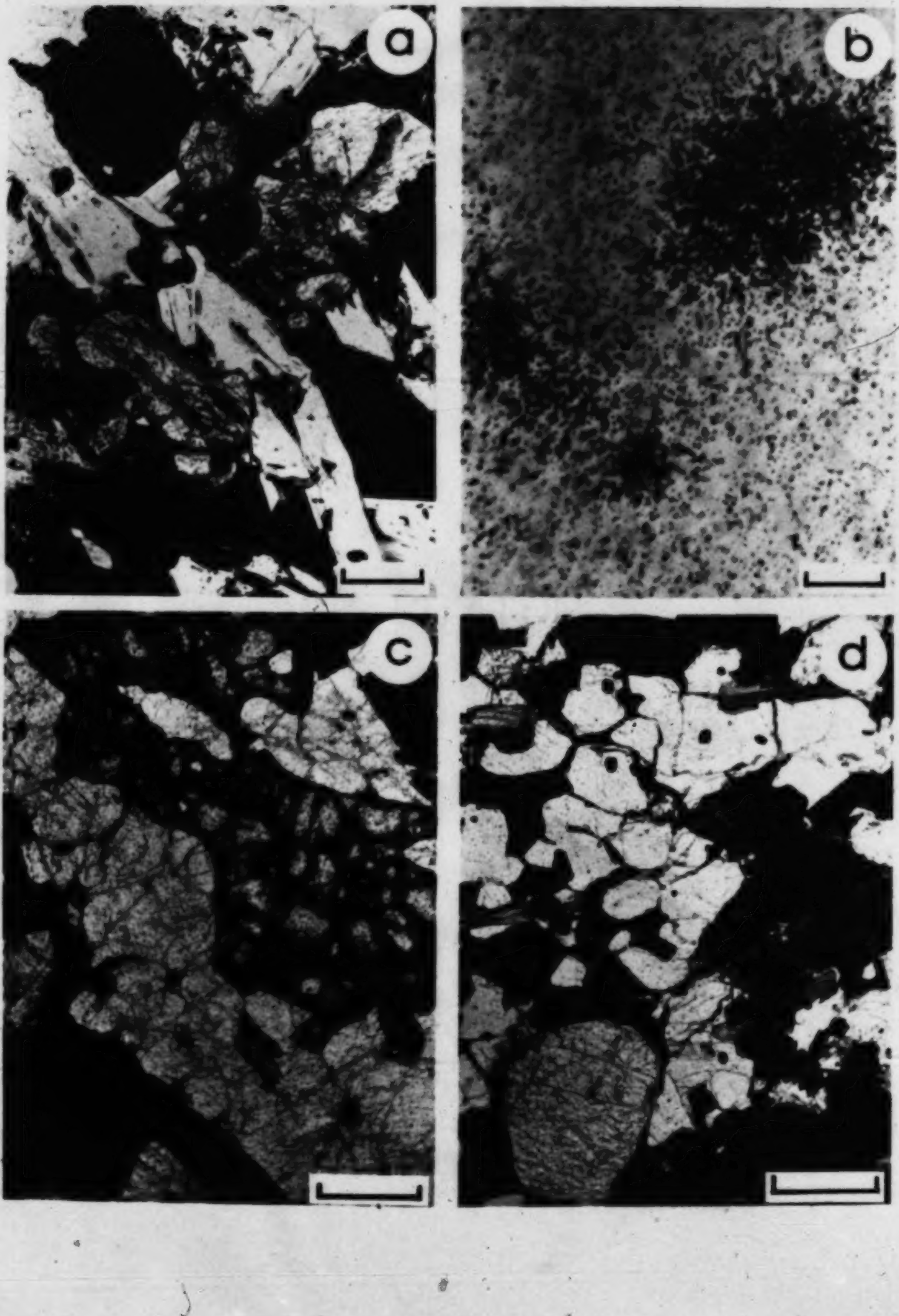

to and enclosing apatite grains. Growth of the garnet has obviously been highly restricted by the apatite. Sericitized and hematite-dusted feldspar porphyroclasts are found randomly distributed throughout the biotite layers. Potassium feldspar has crystallized interstitial to the mica. Many tiny grains of zircon and monazite are also scattered throughout the biotite. A modal analysis of sample 5-8 H (Table 11), representative of the biotite-rich layers, indicates the abundance of biotite (75%) and apatite (13.6%) in this zone. Zircon and monazite were counted with the aid of an autoradiograph and total 1.12 and 1.68 percent respectively.

Thin sections of the feldspar-rich portions show a similarity to the rock type described in Zone one. Slight differences occur in mineral content and abundances but as in Zone 1 the feldspar-rich areas are composed predominately of plagioclase, biotite, and apatite. Large somewhat rounded, anhedral porphyroclasts of plagioclase (An35) are set in a matrix of fine biotite, feldspar and apatite. Zircon and monazite are highly prevalent as small rounded grains. Sample 5-8C represents a feldspar-rich section with the following mineral percentages: plagioclase 63, potassium feldspar 1.4, biotite 31.4, apatite 3.4, zircon plus monazite 0.5, and minor opaques. In general mineral proportions for this zone varied between those listed for 5-8 H and 5-8 C as the biotite and feldspar layers intermix.

Sample 5-8 E displays another interesting mineral

TABLE 11

Results of chemical and modal analysis for Zone 2

SAMPLE NUMBER	5-8C	5-8H	5-8E
SiO_2	39.5	30.0	
Al_2O_3	16.9	13.1	
CaO	8.42	9.42	
MgO	5.25	7.7	
Na_2O	1.56	Nil	
K_2O	5.76	6.35	
FeO	6.72	11.38	
Fe_2O_3	3.23	5.95	
MnO	0.12	0.32	
TiO_2	2.38	4.91	
P_2O_5	4.96	6.98	
S	Nil	Nil	
LOI	2.86	2.48	
Total	97.66	98.99	
Uppm	55.70	154.85	61.23
Thppm	584.74	1783.76	20.53
MODAL ANALYSIS			
Pg	62.8	---	47.2
Kfel	1.4	7.9	
Bi	31.4	75.4	32.2
Ap	3.35	13.6	5.1
Op	0.4	1.3	Tr
Lx	0.2	---	Tr
Zr	0.55	1.12	Tr
Mz		1.68	Tr
Gt	---	---	5.8
Sp	---	---	9.6
Total counts	2000	1500	1500

assemblage from Zone two. Extremely fresh feldspar (47%) and biotite (32%) are the main minerals. Over 5 percent apatite is found, similar to the apatite present elsewhere in this zone. Of interest, however, are spinel, which is almost 10 percent of the total sample and extremely large (1.5 cm) fresh garnets rimmed by large fresh biotite crystals. The black to dark green spinel does not have a euhedral habit. Instead, it is found in very irregular form which seems typical of the Pilot Lake area, interstitial to all other grains or as tiny blebs within the feldspars (Plate 6,d). Also conspicuous in this sample is the absence of the large amounts of monazite and zircon that are found elsewhere in this zone.

The two chemical analyses reported in Table 11 reflect the overall mafic nature of this zone. The analysis of sample 5-8 C includes sections of biotite-rich material and cannot be directly correlated with the mineralogy reported. The zone appears rich in ferromagnesiums and low in SiO_2 and Na_2O. Potassium is slightly anomalous with an average of 6 percent reported. The P_2O_5 contents are high as would be expected from the high apatite contents. TiO_2 is also of interest with 2.4 and 4.9 percent reported for the two samples. It likely is present in the biotite, as only minor opaque minerals occur throughout the zone.

Uranium determinations range from 55.7 ppm to 154.83 ppm and thorium values from 20.5 ppm to 1783.7 ppm. Four samples excluding sample 5-8 E which has the low thorium result give an average of 105.71 ppm uranium and 1263.7 ppm thorium for this zone. The Th/U are quite consistent with an average of 11.9. The range of values, therefore, seems to be a reflection of the mineralogy and the amount of monazite in each sample. The higher values reported are for the biotite-rich material which contains more monazite than the felsic layers. Sample 5-8 E which has a low thorium result appears to have virtually no monazite present. Uranium, a more mobile element than thorium, has likely migrated into this layer during metamorphism from the uranium-rich layers and perhaps is present in the zircon and biotite.

Zone Three

Zone three is found on the northwest shore of Pilot Lake and appears to be the uranium showing referenced by Charbonneau (1971). Some exploratory work in the form of trenching and blasting has been done at the shoreline near the main showing.

The zone is exposed in two sections, a main body near the edge of a rather large high outcrop area and an extension some 25 m (80 ft.) south in a trench.

Scintillometer values of 5000 cps were recorded as the highest readings obtained in the Pilot Lake area. This peak reading is 10 times that of the average Pilot Lake Gneiss and almost 50 times above the paragneisses or base level of the region. Dimensions of the zone are difficult to measure because of extensive drift cover and exploratory work

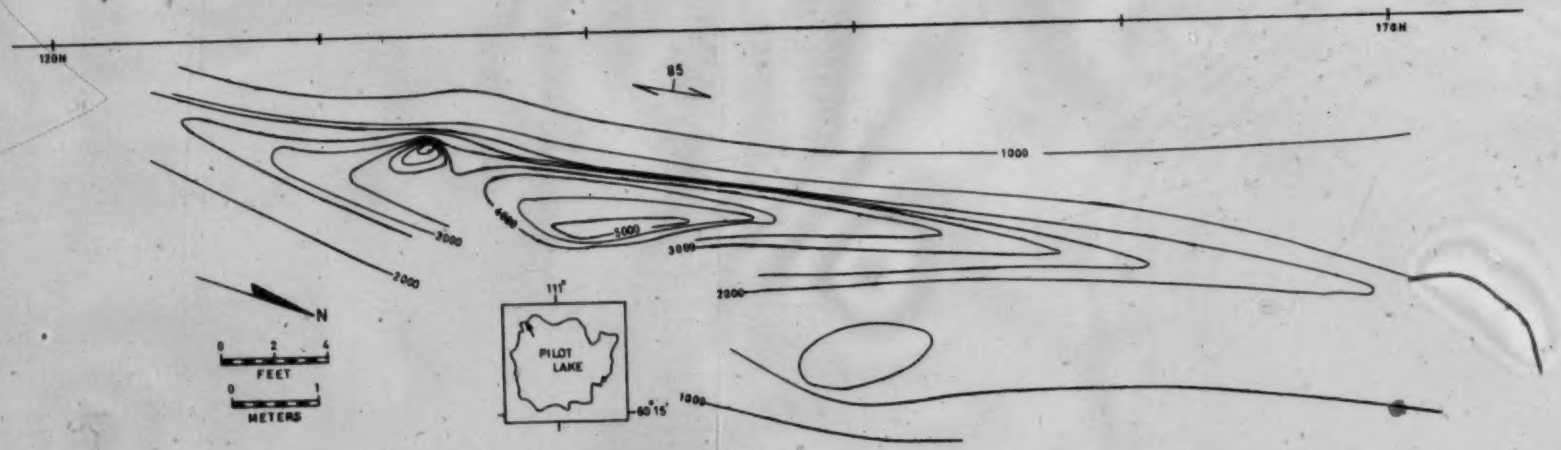

Fig. 22. Scintillometer profile about the main showing in Zone 3 in counts per second.

breaking up sections of the main body. Anomalous radioactivity does occur, however, over a length of at least 42 m (170 ft.) with a maximum exposed width of some 4 m (13 ft). The trend of N 15° W is parallel to the foliation direction of the surrounding rock.

A scintillometer survey indicated the source of the extreme radioactivity to be a brownish black, dense, mafic pod that occurs as an inclusion in the Pilot Lake Gneiss. Plate 7,a shows the radioactive inclusion to be in sharp contact with the gneiss. The highest radioactivity in the pod is found near the contact, with a two fold decrease in values on the Pilot Lake Gneiss side. Readings dropped rapidly at first then gradually until background Pilot Lake Gneiss values are found approximately 3 m (10 ft.) from the inclusion. Fig. 22, a scintillometer profile over the main zone, illustrates the sharp contrast in values about the exposed contact which runs roughly, on the west, along the 2000 cps contour between line 120N and 160N. The profile also shows the linear trend of the zone parallel to the main foliation direction.

The pod is a brownish black, very heavy rock, rich in biotite and black opaques. Banding parallel to the main foliation can be seen in Plate 7,b. A thin (3-5 cm) biotite-opaque mineral band occurs along the contact with the Pilot Lake Gneiss. Garnetiferous zones occur with the biotite and opaques away from the contact. Zones rich in red feldspar porphyroclasts and clusters, the larger of which are broken

PLATE 7. ANOMALOUS ZONE 3

a. Field photograph. Site location 8-1. The main radioactive pod (right) in Zone 3 included in the Pilot Lake Gneiss (left). Note the sharpness of the contact and the long linear trend of the inclusion.

b. Field photograph. Close up of the mafic radioactive pod showing banding parallel to the contact. Bands from the top down consist predominately of: biotite-feldspar-garnet; biotite-opaques; biotite-opaques-garnet; feldspar; and biotite-opaques.

c. Zone 3. Photomicrograph. Sample 8-4. Garnetiferous-biotite-opaque band, Zone 3. Note the garnet (upper left), kinked and bent biotite and the abundance of monazite associated with the opaques. Plane light. Bar scale is 0.5 mm.

d. Zone 3. Photomicrograph. Sample 8-5B. Biotite-opaque band. Note the crude layering of biotite and the opaques. Also the invasion of biotite cleavages and fractures by hematite. A granulated spinel rimmed slightly by chlorite (light) can be seen left center in the opaque layer. Plane light. Bar scale is 0.5 mm.

PLATE 7

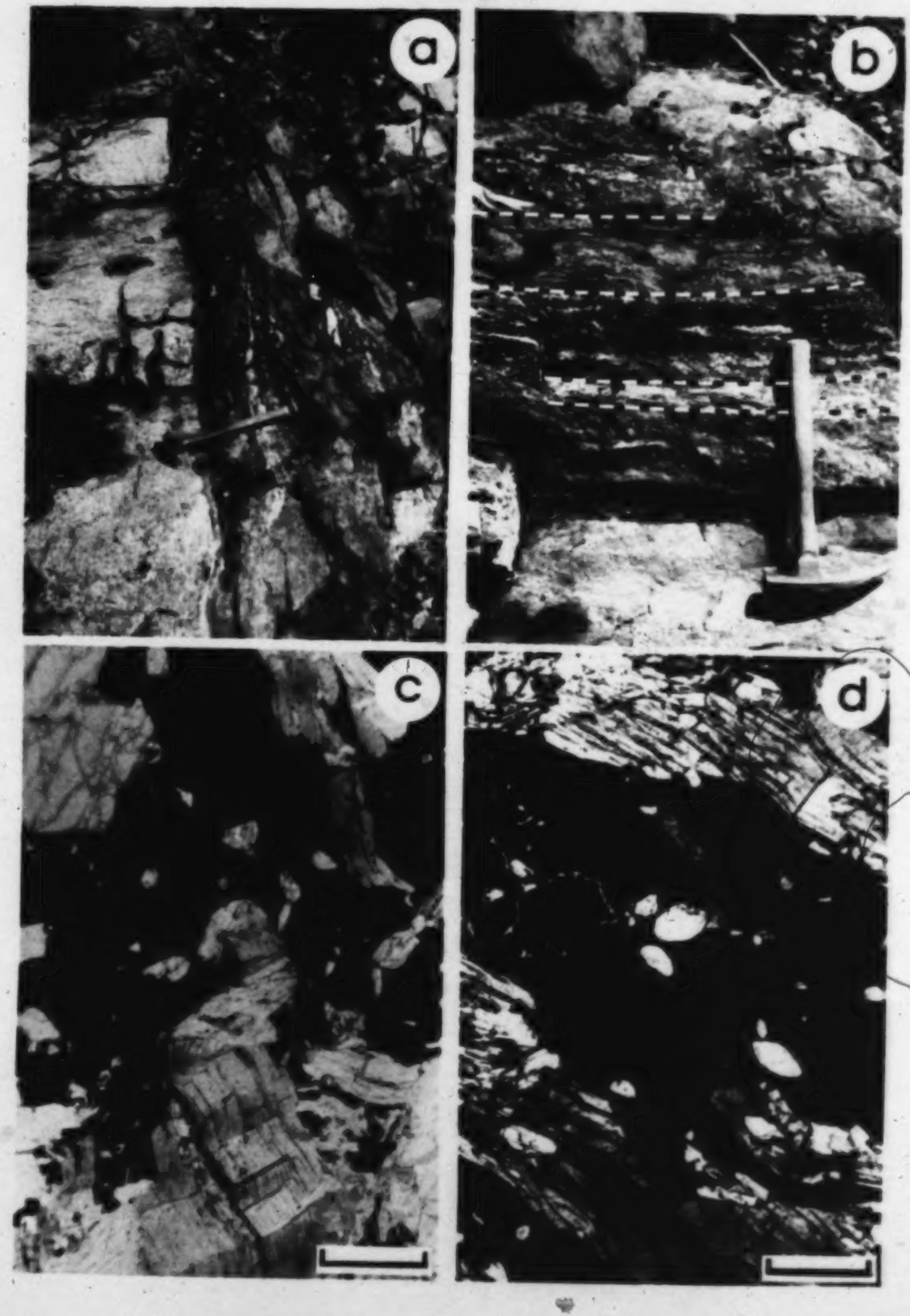

and boudinaged in the direction of the foliation, are prevalent. The high radioactivity readings correspond with the biotite-opaque rich sections. Contamination of the Pilot Lake Gneiss near the contact is demonstrated by the gradual decrease in radioactivity away from the contact and large amounts of opaques and biotite in the gneiss otherwise low in mafic minerals.

The inclusion has undergone severe stress and has been lengthened in the direction of the foliation. To the north the pod thins to biotite and black opaque lenses that disappear into a cliff face. To the south it has been drawn out to thin mafic-rich radioactive lenses, exposed in the trench, which cause the Pilot Lake Gneiss to have above average radioactivity to the shoreline of the lake. The total measurable length of the radioactive zone is some 55 to 60 m (185 to 200 ft.).

Scintillometer readings in the trench are generally less than 1500 cps with a maximum value of 3000 cps (Fig. 23) over the mafic lenses. Several tons of rubble make detailed profiling around the pit difficult.

Petrography. Thin section work confirmed the pod to be mafic-rich and predominately composed of biotite and black opaques in varying proportions. The inclusion comprises approximately 30 to 50 percent pleochroic, light to dark brown biotite that has been extremely frayed, bent and broken (Plate 7,c). The crystals display numerous shapes and sizes and although a weak preferred orientation can be seen

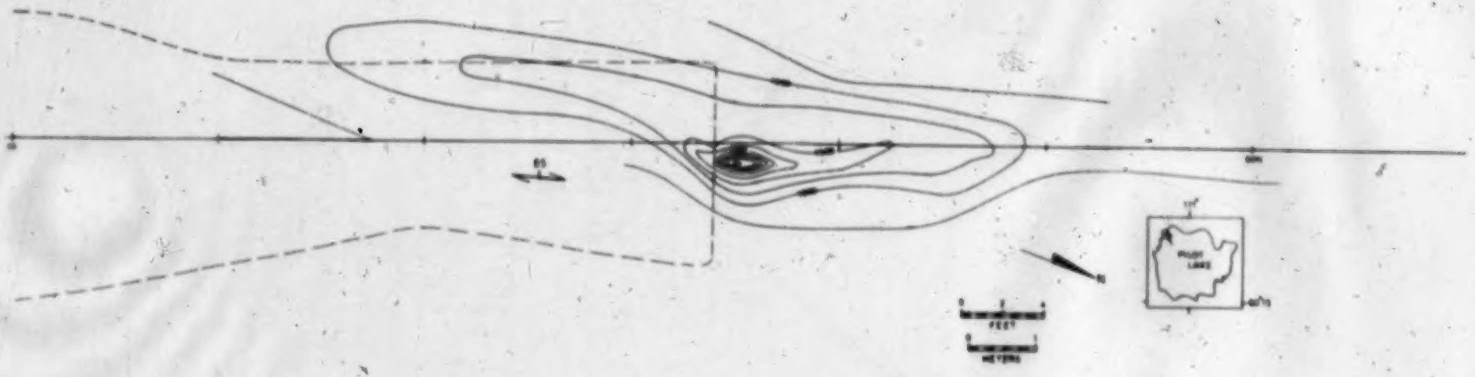

Fig. 23. Scintillometer profile about the trench (dashed line) south of the main showing in Zone 3 in counts per second.

they are often randomly orientated into a decussate texture. The infilling of fractures and cleavages by blood red hematite is very common. Lengths of the crystals seldom exceed 2.0 cm.

Massive, amorphous hematite and ilmenite were identified as the main opaque minerals by polished section work. Cores of ilmenite still exist but the majority has been replaced by the hematite, anatase, leucoxene and sphene. The opaques and their alteration products total about 38 percent of the biotite-opaque rich layers. They are generally found in crude bands, or to have filled many of the openings interstial to the biotite. The bending, breaking and infilling of many fractures and cleavages of the biotite crystals appears due to the opaques becoming mobile during metamorphism.

Pyrite, as small granulated grains scattered throughout the hematite-ilmenite bands, is the only other opaque to have been noted. Minor granulated, irregular shaped green spinel is also associated with the opaques as are the bulk of the important heavy minerals zircon and monazite (Plate 7,d and 8,c).

The titanium mineral anatase was found only after being separated as a heavy mineral during the analysis of sample 8-5 C. When an acid wash removed a heavy coating of iron oxide, the anatase was seen to display excellent euhedral form. The tetragonal, uniaxial, negative crystals were dark

PLATE 8. ANOMALOUS ZONE 3

a. Zone 3. Photomicrograph. Sample 11-1. Close up of zircon and monazite in hematite. Note the zonation of the zircon (top mineral) and the radiating fractures in the monazite (lower mineral) about a small included zircon. Plane light. Bar scale is 0.1 mm.

b. Zone 3. Photomicrograph. Sample 8-3A. Close up using intensified light of a euhedral tetragonal crystal of anatase in hematite. Plane light. Bar scale is 0.1 mm.

c. Zone 3. Photomicrograph. Sample 8-4. Biotite-opaque band. Note the large monazites partially to totally enclosing smaller zircon grains. Also note the fragments or pieces of biotite crystals scattered throughout the opaques (top center). Plane light. Bar scale is 0.5 mm.

d. Zone 3. Photomicrograph. Sample 8-3B. Sample of Pilot Lake Gneiss a few centimeters from the contact with the radioactive pod. Note the high degree of fracturing and impregnation of the rock with hematite especially the large plagioclase grain in the center. Crossed nicols. Bar scale is 0.5 mm.

PLATE 8

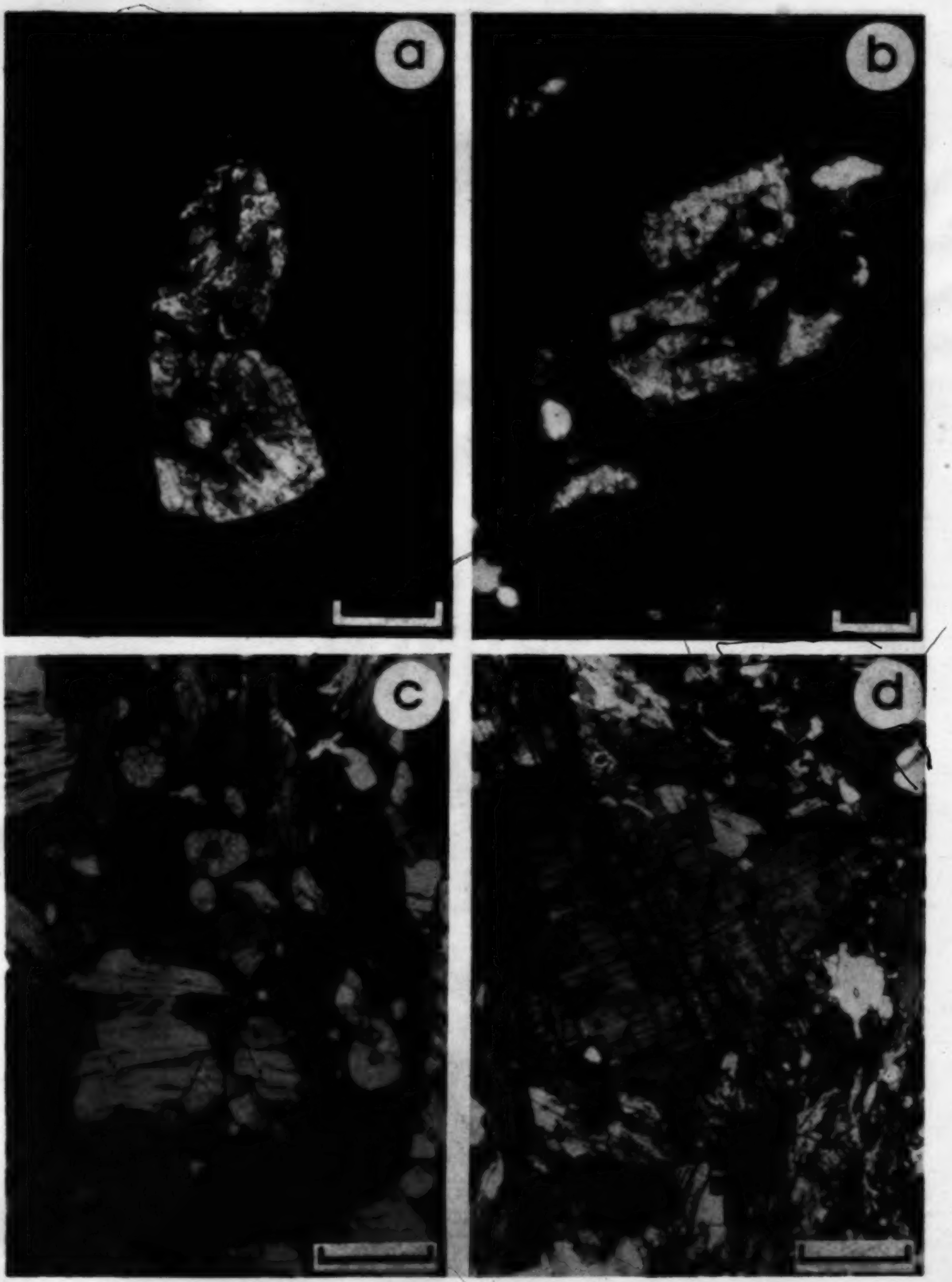

red brown to almost black in colour making identification in their opaque surroundings difficult. The anatase was first thought to be masses of sphene and leucoxene altered from the ilmenite when viewed in thin section. Trace amounts of both these minerals do occur with the anatase. After positive identification further thin section work under intensified light revealed single crystals or clusters of crystals metablastically grown throughout the hematite-ilmenite (Plate 8,b). Over 5 percent anatase was found in one sample (8-5c).

Monazite and zircon were found to be rather abundant as in Zones 1 and 2. Six modal analyses showed zircon and monazite together to total over 4 percent of the inclusion. The highest zircon and monazite contents occur with the highest opaque totals (Table 12). Counts with the aid of autoradiographs showed a high of 3.19 percent monazite (sample 8-4) and a high of 3.25 percent zircon (sample 8-5c). The autoradiographs, as in the other zones described, indicated the monazite to be the only radioactive mineral encountered.

Zircons are typically round to well rounded but can be angular if they have been fractured and broken by internal expansion. They occur in a variety of sizes with an average diameter of 0.1 mm, although grains in excess of 0.4 mm were noted. High relief, fractures filled with hematite, strong birefringence and zoning are characteristic features (Plate 8,d). Tiny rounded zircons are also scattered throughout the biotite but are minor in proportion to the amount found included in the opaque layers.

Colourless to pale yellow monazite is found in the same association as the zircon. It displays a strong birefringence and an even texture with much less fracturing than the zircon. Hematite staining however, is common. On average, the monazite is slightly larger than zircon, 0.1 to 0.2 mm in diameter and although well rounded grains are found the monazite is slightly more irregular in form. There are many cases of monazite growing around or including small zircon grains, a phenomena attributed to some recrystallization of the monazite (Plate 8,d and c). Two other features associated with the zircon and monazite are noteworthy: one is the almost total absence of metamict grains of either zircon or monazite, the other is the absence or very minor occurrences of light pleochroic halos in the biotite around the included zircons and monazite. Both features are interesting and unexplainable considering the large amounts of radioactivity present in these samples.

Garnet up to 1 cm in diameter in certain biotite-hematite layers is extremely fresh, and massive, with very irregular but smooth grain boundaries. Inclusions and embayments along the margins by hematite is common. Other included minerals are biotite and rare monazite and zircon. Most samples show at least traces of garnet with some sections containing greater than 20 percent.

TABLE 12

Results of chemical and modal analysis for Zone 3

SAMPLE NUMBER	8-3B	8-5C	8-4
SiO_2	55.8	16.72	19.9
Al_2O_3	16.9	5.43	8.91
CaO	2.83	0.17	0.35
MgO	3.65	4.96	4.40
Na_2O	2.29	0.13	0.01
K_2O	3.95	3.37	2.64
FeO	5.17	7.52	34.00
Fe_2O_3	2.55	19.64	
MnO	0.06	0.06	0.11
TiO_2	2.86	30.5	24.7
P_2O_5	0.82	0.98	0.72
S	Tr	0.32	0.51
LOI	1.42	3.0	1.43
Total	99.00	92.80	97.17
Uppm	13.76	95.30	86.09
Thppm	452.3	3593.3	2108.1
MODAL ANALYSIS			
Kfel	2.79	8.72	0.74
Pg	54.02	---	---
Q	15.29	---	---
Bi	22.36	42.68	37.44
Gt	0.37	0.30	15.4
Op	4.37	34.64	34.37
Lx	Tr	Tr	Tr
Ant	---	5.23	4.94
Zr	0.29	3.25	1.92
Mz	0.51	2.65	3.19
Ch	---	0.86	0.51
Sp	---	0.40	0.23
Py	---	1.26	1.25
Total counts	2150	2000	2000

TABLE 12 (cont'd)

Results of chemical and modal analysis for Zone 3

SAMPLE NUMBER	8-5A	8-5B	11-1	11-3
Kfel	25.1	9.0	26.7	1.25
Pg	11.75	---	0.2	---
Bi	34.35	53.0	44.7	28.65
Gt	5.5	---	4.3	23.8
Op	19.45	32.4	19.9	34.2
Lx	Tr	Tr	Tr	Tr
Ant	0.8	0.8	0.4	3.75
Zr	2.7	4.3	2.34	2.15
Mz				2.35
Ch	---	---	0.97	1.95
Sp	0.15	0.3	0.58	0.2
Py	0.2	0.2	---	1.75
Total counts	2000	1500	1500	2000

Percentages of feldspar in the zone are difficult to estimate because of their irregular distribution throughout the inclusion. Most samples contain potassium feldspar but not all contain plagioclase. The potassium feldspar has formed in small interstitial pockets between most other minerals including plagioclase. It is anhedral in form and has often broken up plagioclase clusters by infiltrating between grains.

Plagioclase is generally absent from the biotite-hematite rich sections, unless it is found as single grains or clusters of subhedral to anhedral crystals surrounding biotite-opaque-monazite islands. The plagioclase, with a composition of An36 has been highly sericitized and impregnated with hematite.

Chemistry. Chemical analysis of samples from this zone proved to be very unique and difficult to do. Xral Laboratories analysed samples 8-5c and 8-4 a total of three times each before satisfactory results were obtained by calibration against methods and standards used for Ti-Fe ores. Total iron and titanium were repeated by A. Stelmach at the University of Alberta giving results that confirmed Xral's analyses. The main problem was apparently getting the titanium bearing minerals, mainly anatase which is insoluable in acid, into solution.

Results of the analysis of sample 8-5c and 8-4 are given in Table 12 and clearly indicate the mafic nature of this rock type.

Sample 8-5c was taken from a biotite-opaque rich layer with a combination of over 80 pecent of these minerals and their alteration products. Sample 8-4 was taken from a similar section that included over 15 percent garnet. Both samples were devoid of large plagioclase clusters. The SiO_2 content was most unique with less than 20 percent in both samples. It was considered to be contained primarily in the biotite, garnet and minor potassium feldspar. Total iron values are extremely high and titanium results are above most economic deposits for that mineral (Rose 1969).

A value of 7.52 percent FeO vs. 19.64 percent Fe_2O_3 in the one determination completed indicates that much of the opaque is now present in the form of hematite. The original ilmenite has therefore been oxidized liberating much of the titanium to perhaps the biotite and the formation of anatase. Na_2O is almost nil as would be expected from the total absence of plagioclase. Sulphur is present in the minor pyrite found in both samples.

Totals much less than 100 percent were obtained for both analyses. A general qualitative spectrographic analysis revealed the presence of the additional elements :chromium, 0.07 percent; Nb_2O_5, 0.07 percent and zirconium, 1.13 percent for sample 8-4 and 1.46 percent for sample 8-5c. The addition of these elements plus U, Th and the rare earths that are expected to be found in monazite (Ce_2O_3, La_2O_3, Y_2O_3) would account for an additional 3.5 to 4.0 percent.

PLATE 9. MINERAL SEPARATES AND METAMORPHIC MINERAL RELATIONSHIPS

a. Mounted monazite separate from sample 8-5c, Zone 3. Note size and roundness of some grains. Many grains have been broken during crushing. Bar scale is 0.5 mm.

b. Mounted zircon separate from sample 8-5C, Zone 3. Note size and many well rounded grains. Bar scale is 0.5 mm.

c. Photomicrograph. Sample 13-6. Metamorphic mineral relationships in an inclusion in the Pilot Lake Gneiss. A lenticular crystal of kyanite (upper center) has grown across a network of sillimanite blades. Crossed nicols. Bar scale is 0.1 mm.

d. Photomicrograph. Sample 9-2. Metamorphic mineral relationships in an inclusion in the Pilot Lake Gneiss. An orthpyroxene crystal-hypersthene (upper left) partially replaced by chlorite in a matrix of polygonally recrystallized plagioclase. Crossed nicols. Bar scale is 0.5 mm.

PLATE 9

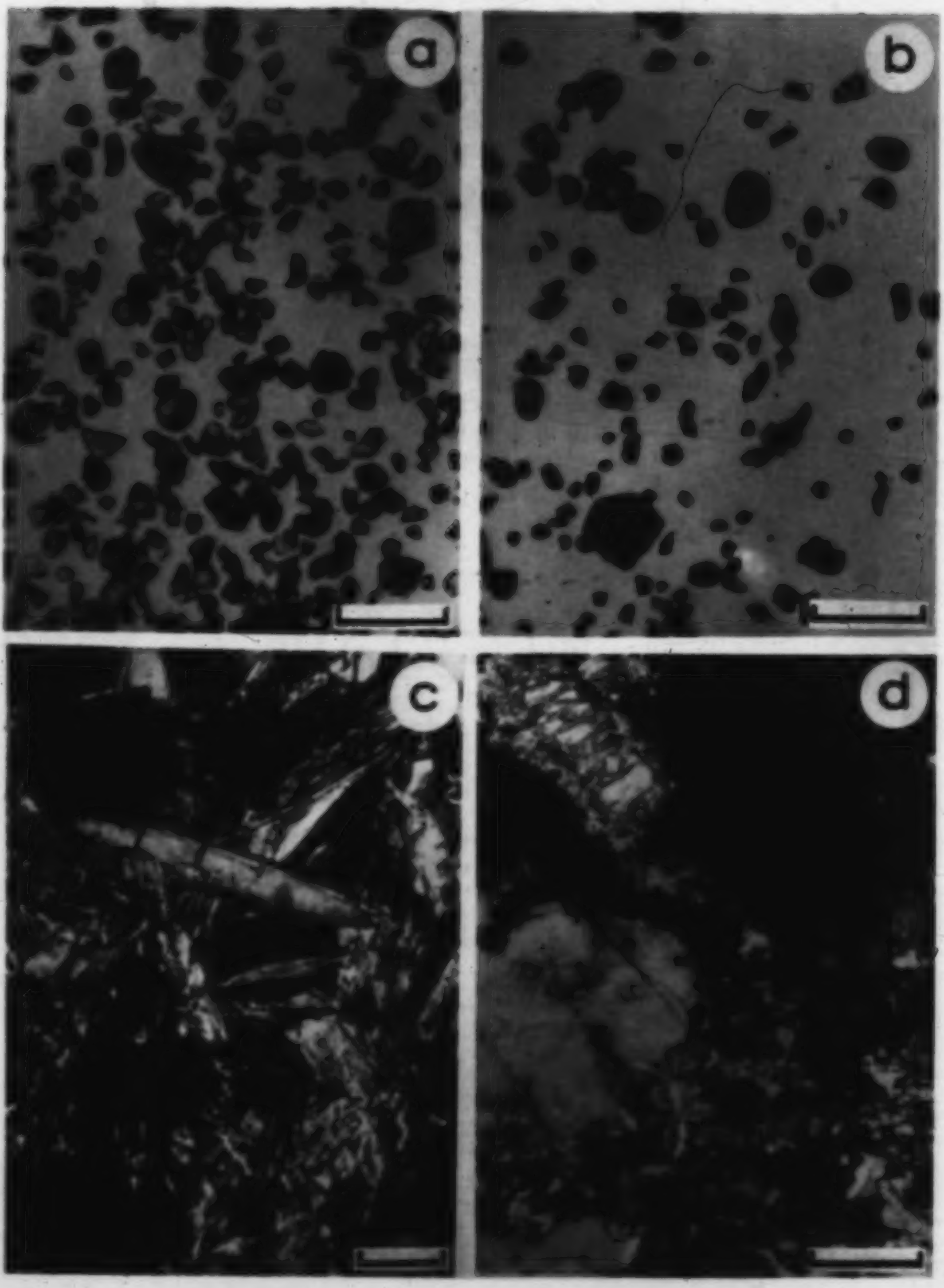

Sample 8-5c would still fall some 3.0 to 4.0 percent short of 100 percent. Additional elements and unidentified mineralogy in this rare assemblage still remain a problem at this stage.

All the uranium and thorium determinations from this zone are included in Table 9. The averages of these samples (8-3A, 8-3C, 8-4, 8-5A, 8-5C, 11-1, 11-3) are 72.59 ppm for uranium and 2354.1 ppm for thorium giving a Th/U of 32.4. This value is extremely high but remarkably consistent throughout the entire zone reflecting the high percentages of the thorium mineral monazite.

Chemical and Mineralogical Changes About Zone 3. The effects on the Pilot Lake Gneiss by the inclusion responsible for the radioactivity in Zone 3 are considerable on a small scale. As previously mentioned, the stretching of the inclusion in the direction of the foliation during a period of severe stress has been great. However, migration of elements perpendicular to the structural trend is also seen within centimeters of the edges of the pod. The Pilot Lake Gneiss at the contact with the inclusion has above normal radioactivity and an increased amount of mafic minerals. Sample 8-3B was taken from the Pilot Lake Gneiss within 2 cm of the contact with the inclusion. It has been highly fractured and invaded by hematite and biotite carrying an excess of zircon and monazite (Plate 8,d). Plagioclase is now abundant instead of the normally high percentages of potassium feldspar. This sample as a result, possesses a chemical composition much different than the Pilot Lake Gneiss some 9 m (30 ft.) to the west (sample 8-2, Table 1). SiO2 and K2O contents are much lower and the total mafic (Mg, Fe, Ti) U and Th values are considerably higher than the normal Pilot Lake Gneiss.

To further illustrate some of these effects, samples were collected about the radioactive lens exposed in the trench some 25 m (80 ft.) to the south of the main pod. Nine samples collected at intervals of approximately 30 cm (12 in.) along a line perpendicular to the lens were analysed for their U and Th contents (Table 9). In addition, 3 samples (11-4-00,-3E,-6E) were chemically analysed and were point counted to reveal changes in mineralogy (Table 13).

Sample 11-4-00 taken nearest the radioactive lens, is dark red with a fairly high mafic content and a scintillometer reading of almost 1500 cps. Values after peaking at 2000 cps, centimeters to the east decreased through 900 cps (sample 11-4-3E) to 650 cps (sample 11-4-6E) 1.8 m (6 ft.) away. Here sample 11-4-6E exhibits in outcrop, all the characteristics of the Pilot Lake Gneiss. Fig. 24 graphically illustrates the changes in chemistry between the most radioactive sample in the trench and the host Pilot Lake Gneiss. Only SiO2 and to some extent K2O have been depleted in the Pilot Lake Gneiss about the radioactive material. SiO2, especially has decreased from 67 percent (sample 11-4-6E) to below 50 percent, (sample 11-4-00) nearest the lens. The 13 percent change in SiO2 is

TABLE 13

Results of chemical and modal analysis for trench, Zone 3

SAMPLE NUMBER	11-4-00	11-4-3E	11-4-6E
SiO_2	49.5	64.1	67.0
Al_2O_3	19.3	15.8	14.7
CaO	3.32	2.83	1.2
MgO	4.42	2.19	1.45
Na_2O	3.16	2.77	1.90
K_2O	4.85	3.27	6.34
FeO	5.42	4.55	4.17
Fe_2O_3	2.02	0.82	0.11
MnO	0.05	0.05	0.04
TiO_2	4.23	1.52	0.92
LOI	1.80	0.76	0.80
Total	98.07	98.66	98.63
Uppm	14.96	9.06	5.68
Thppm	587.2	321.7	162.65
MODAL ANALYSIS			
Kfel	2.82	8.13	52.78
Pg	67.83	47.86	16.25
Q	0.18	24.30	22.87
Bi	24.94	15.38	5.73
Mu	---	0.15	1.18
Gt	0.06	1.23	---
Op	2.76	1.87	0.47
Lx	0.43	0.44	0.41
Mz	0.67	0.39	Tr
Zr	0.31	0.25	0.12
Total counts	2000	2000	2000

enough to offset the increases in the Pilot Lake Gneiss about the pod shown by all the other major elements. These higher values decreasing outward to values normal for the Pilot Lake Gneiss are similar to the trend shown by U and Th. Uranium values are the highest at the radioactive lens (14.96ppm-sample 11-4-00) and the lowest 1.8 m (6 ft.) into the Pilot Lake Gneiss (5.68ppm-sample 11-4-6E). High and low thorium values (587.2 and 162.6 ppm) correspond to the high and low uranium results.

Mineralogical variations are concurrent with the chemical differences. Fig. 25 shows quartz to increase from 0.18 percent to above 20 percent moving away from the mafic lens. Reversals in feldspar content are quite striking. Plagioclase has taken the place of the depleted quartz and potassium feldspar nearest the lens.

The higher biotite, opaque mineral, zircon and monazite contents about the radioactive material reflect the higher Ti total Fe, U and Th contents.

The chemical and resultant mineralogical variations in the Pilot Lake Gneiss about the inclusion, appear to be the result a physical transfer of material from the pod outward into the Pilot Lake Gneiss, by assimilation and subsequent metamorphism. All thin sections studied about the inclusion exhibit deformational features such as strained, fractured and granulated grains of quartz, plagioclase and potassium feldspar. Fractures now filled with biotite, opaques and an

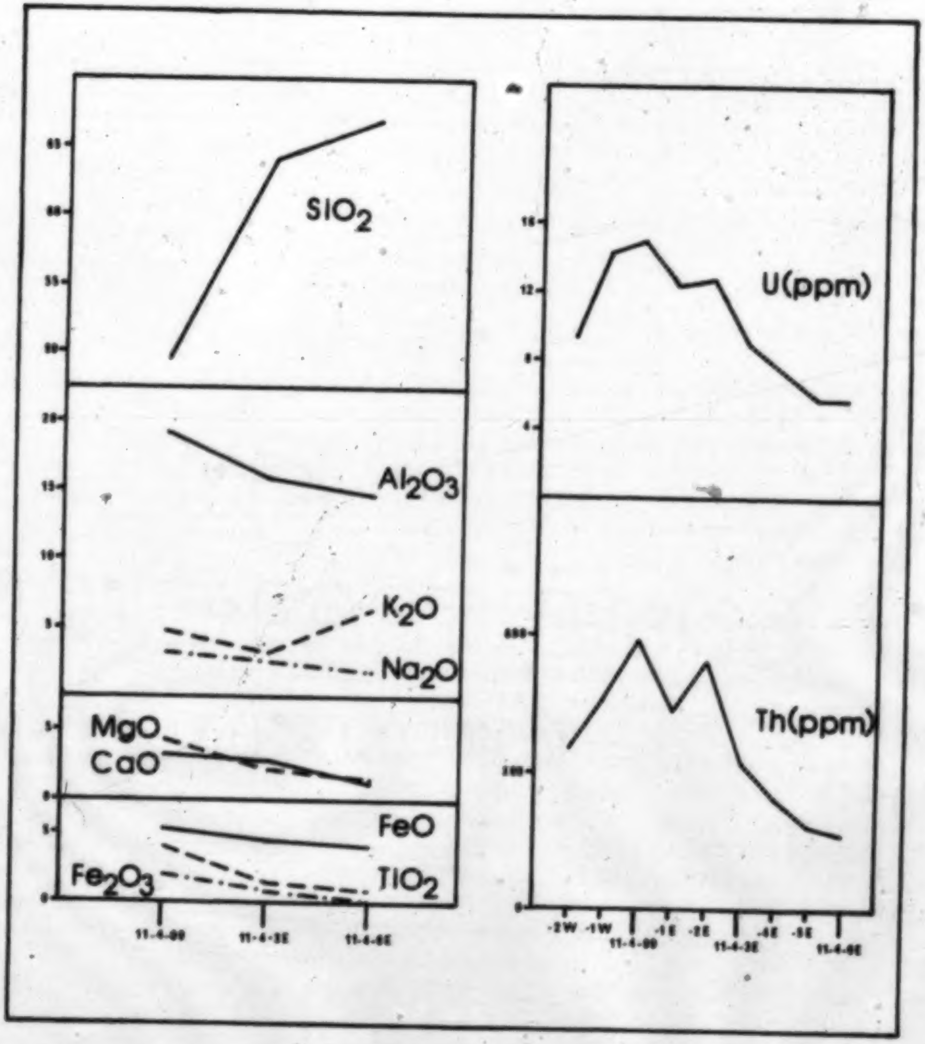

Fig. 24. Chemical variations in the Pilot Lake Gneiss about a radioactive lens in Zone 3. Samples taken at the head of the trench shown in Fig. 23. Major oxides in wt.%.

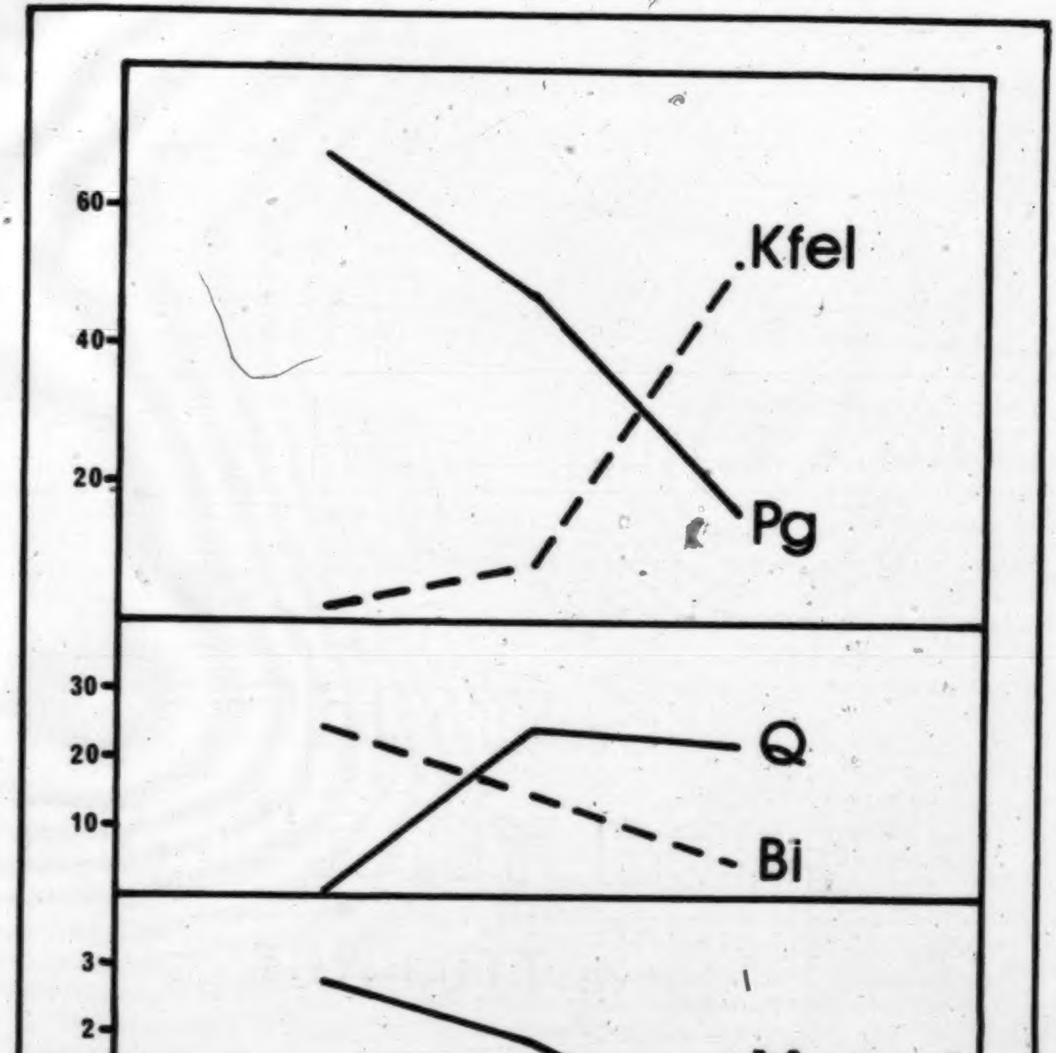

Fig. 25. Mineralogical variations in the Pilot Lake Gneiss about a radioactive lens in Zone 3. Minerals in volume %.

excess of zircon and monazite are greatest nearest the inclusion (Plate 8,d).

Zone Four

Zone 4 is found in the Pilot Lake Gneiss some 8 km north of Pilot Lake near the eastern contact with the paragneisses. A scintillometer grid showed the radioactivity to be much less defined than the three previously described zones. Values range from normal Pilot Lake Gneiss readings (550 cps) to a high of 1400 cps, sporadically distributed over an area some 30 m (100 ft) long and 4.5 m (15 ft) wide. As a result a contoured profile was impossible to obtain.

The zone has a core that is fine grained, deep red brown and laced with a network of thin parallel quartz stringers or rods. The core, which contains the anomalous radioactivity passes gradationally outward into well foliated Pilot Lake Gneiss.

Petrography and Chemistry. In thin section the core rocks are predominately composed of quartz and potassium feldspar. The feldspars are extremely fine and mass together as crystals with highly irregular and granulated margins. Grain boundaries are often marked by rims of hematite and muscovite. Overall, hematite dusting is heavy giving rise to the deep red colour of the rock. Plagioclase is of minor proportion. Accessories include opaque minerals, apatite, small monazite and zircon and rare calcite.

The quartz in these rocks is atypical of the quartz

TABLE 14

Results of chemical and normative analysis for a sample from Zone 4

SAMPLE NUMBER	13-20N-1E
SiO_2	70.6
Al_2O_3	13.8
CaO	0.33
MgO	0.88
Na_2O	2.09
K_2O	8.03
FeO	1.81
Fe_2O_3	1.51
MnO	0.03
TiO_2	0.2
LOI	0.76
Total	99.95
Uppm	146.54
Thppm	395.6

NORMATIVE ANALYSIS	
Q	25.16
Cor	1.07
Or	47.88
Ab	17.83
An	1.65
En	2.01
Fs	1.82
Mt	2.19
Il	0.38

generally found throughout the Pilot Lake area. It is not heavily strained or recrystallized with sutured polygonal grain boundaries. Instead it cuts the rock in a rod-like fashion and contains many inclusions. A 20 cm (8 in.) wide quartz vein (sample 13-5) containing abundant monazite grains at the boundaries between quartz crystals was found to cut the Pilot Lake Gneiss a few meters from the zone. Quartz veining is a relatively rare feature in the Pilot Lake Gneiss.

One chemical analysis (sample 13-20N-1E, Table 14) compares closely with the average Pilot Lake Gneiss (Table 1). Slight differences occur in K2O; 8.03 vs. 6.35 percent and Fe2O3; 1.51 vs. 0.24 percent. The higher K2O results in a normative orthoclase value approaching 50 percent, considerably greater than the average Pilot Lake Gneiss value of 31 percent.

One of the highest uranium values in the entire Pilot Lake area, 146.54 ppm was found in sample 13-20N-1E with a corresponding thorium value of 395.62 ppm. Three other samples average 40.5 ppm U and 125.73 ppm Th. These values are 3.5 times the average Pilot Lake Gneiss uranium value but just minimally above the thorium average.

CHAPTER IV

DISCUSSION OF RESULTS

Structure and Metamorphism

The characteristic northerly and vertical orientation of structural features, such as foliation and the elongate outline of the Pilot Lake Gneiss and metasedimentary inclusions, all point toward a deep seated plastic deformation, with maximum stress on an east-west axis early in the development of the area.

Post and syncrystalline deformation are evidenced by the blurred nature of textural boundaries in hand-specimen and the very irregular diffuse grain boundaries in thin section, absence of crystal forms and the hiatal grain-size variation and rolled out lenses, streaks or bands. Most of the rocks in the Pilot Lake area can be classed as blasto-cataclastic according to Burwash and Krupicka (1969). The dominant texture is porphyroclastic with quartz fully crushed and the feldspars and garnet porphyroclasts surrounded by mortar. Locally, mylonitic bands have developed in the later stages of early deformation. The change from a plastic phase to a brittle phase is further evidenced by the one upper crustal level breccia found on the southeastern shore of Pilot Lake (on the point of land north of site 7-1, Fig. 17). However, evidence for a continuous cycle from a plastic to a brittle phase deformation is inconclusive. The two events are most certainly, widely separated in time. A regional study of aerial photographs and aeromagnetic data indicates the presence of many large scale postcrystalline fault systems generally trending in a northerly direction. One such structural break passes to the east of the study area and appears to affect only the rocks in the extreme northeast corner of the lake (sites 16-1 and 2).

The metamorphic history of the Pilot Lake area is very complex and certainly polyphase. Correlation between defomational events, and metamorphic phases no doubt exists, but a detailed investigation of these relationships is beyond the scope of this study. However, a discussion of certain metamorphic conditions reached during the development of the area is of consequence.

The metasedimentary rocks, which are more sensitive indicators of metamorphic grade commonly show the mineral assemblage garnet-cordierite-andalusite. This assemblage is transitional between the lower to high pressure subfacies of amphibolite facies metamorphism (Turner 1968). The presence of spinel and corundum which predate the garnet-cordierite-andalusite assemblage (Plate 3, and c and 4,c) and the isolated cases of sillimanite (Plate 4,d and 9,c) are an indication that at least higher temperatures if not higher pressures existed early in the metamophic history (Fyfe et al. 1958 p. 213). Occurrences of corundum-spinel-andalusite in the Pilot Lake Gneiss showing the same textural sequences as in the metasediments is indicative of an early high temperature regional metamorphic event rather than purely a thermal event at the edges of the Pilot Lake Gneiss.

Ultimately, occurrences of both hypersthene and kyanite were observed in inclusions within the Pilot Lake Gneiss. Hypersthene altering to chlorite (Plate 9,d) was found in a coarse grained xenolith perhaps of igneous origin on the south shore of Pilot Lake (sample 9-2, site 9-1). Results of major element and uranium and thorium analysis for two hypersthene bearing rocks are presented in Table 15 to complete the chemical data.

Kyanite as lens shaped crystals was found to cross-cut sillimanite mats (Plate 9,c) in an inclusion some 15 km to the north of the hypersthene bearing rocks. (sample 13-6, site 13-5).

Evidence of an early very high grade (granulite facies) regional metamorphism, perhaps Kenoran in age is therefore recorded sporadically throughout the Pilot Lake area. The most clearly recognizable event, high grade metamorphism of the amphibolite facies, overprints the entire area and possibly marks the beginning of the Hudsonian orogeny.

Retrogressive metamorphism to greenschist facies conditions, synonymous with post-cataclastic recrystallization, is responsible for the development of biotite, chlorite and muscovite. This latter stage of development is recorded by the numerous 1800 m.y. K-Ar dates south of the study area (Baadsgaard and Godfrey 1966,1972).

TABLE 15

Results of chemical and modal analysis for two granulite samples

SAMPLE NUMBER	9-2	9-3
SiO_2	66.8	57.1
Al_2O_3	15.2	18.3
CaO	2.1	4.09
MgO	1.66	2.96
Na_2O	2.47	3.46
K_2O	4.68	2.04
FeO	4.92	5.64
Fe_2O_3	0.22	1.7
MnO	0.05	0.08
TiO_2	1.28	2.3
LOI	0.6	1.42
Total	98.98	99.09
Uppm	6.16	14.53
Thppm	197.92	485.07
Th/u	32.1	33.4
MODAL ANALYSIS		
Q		11.43
Kfel		4.12
Pg		53.70
Bi		9.56
Hy		Tr
Ch		11.34
Gt		5.90
Op		3.56
Zr		0.16
Mz		0.22

Chemical Correlations

A study of chemical considerations through the correlation of all major elements and uranium and thorium was attempted, to aid in an understanding of the above average radioactivity in the Pilot Lake area. Several of the more important correlations have been presented in Figs. 26 to 37. The results of the normal variable paragneisses were not used because they do not seem to be excessively enriched in uranium or thorium. Samples 8-5c and 8-4 from Zone 3 were also omitted because their anomalous chemical compositions affected the correlation coefficients for most of the data beyond acceptable limits. Some correlations (Th vs. SiO2, total Fe and TiO2) were actually enhanced with the inclusion of samples 8-5c and 8-4.

On the diagrams the Pilot Lake Gneiss (including sample 13-20N-1E because of its similar chemistry) are marked by closed circles; the metadiorite by a triangle and samples taken from the anomalously radioactive zones as well as the granulites by open circles.

From a correlation of all elements the following generalities can be made:

1. Uranium correlates poorly with all major elements.
2. Thorium shows excellent positive correlations with total iron, titanium, calcium and magnesium, excellent negative correlation with silica and poor correlations with aluminum, potassium and sodium.
3. Uranium correlates favourably and positively with thorium when the anomalous occurrences are included.

Diagrams of silica content vs. uranium, thorium, total iron and titanium are shown in Figs. 26 to 29. Uranium correlates poorly, showing if anything a decrease with an increase in silica. Thorium, total iron and titanium, however show pronounced decreases with increasing silica. The total iron and titanium trends are typical of the normal felsic vs. mafic element relationships. However, the uranium and most certainly the thorium trends are in contradiction to the popular opinion that uranium and even more so thorium increase regularly with an increase in silica (Rogers and Adams 1969 and Whitfield _et al_. 1959).

Plots of potassium vs. uranium and thorium (Figs. 30 and 31) show virtually no correlations. In fact the coefficient for potassium vs. uranium was the lowest of all the correlations. In normal petrologically differentiated sequences the trends of thorium against potassium are almost invariably quite linear, exhibiting a marked thorium increase with increasing potassium (Rogers and Adams 1969). Also the tendencey for potassium and uranium to occur together have led to the presumption that uranium is highly involved in metasomatic activity (Whitfield _et al_. 1959). The relationships between uranium, thorium, silica and potassium in the Pilot Lake area clearly negate the radioelement enrichment by either a normal differentiated or metasomatic process. The only exception is possibly Zone 4 which shows an increase in both potassium and uranium but a minimal increase in thorium.

As previously documented, especially for Zones 2 and 3 the higher the mafic content in a sample the higher its radioactivity. Plots of uranium and thorium against total iron and titanium (Figs. 32 and 35) show this relationship to be chemically valid. Although the uranium plots show poor correlations, the coefficients are positive (ie. an increase in uranium with slight increases in total iron and titanium). Thorium plots, as might be expected from the relationships with silica, show good positive correlations with both total iron and titanium. A definite increase in thorium with an increase in total iron and titanium is even shown by the Pilot Lake Gneiss. Fig. 36 shows the expected normal trend of total iron increasing with titanium.

The relationship between uranium and thorium has been influenced greatly by the anomalous occurrences. A correlation for these data shows an increase in uranium corresponding to an increase in thorium (Fig. 37). In fact the same correlation coefficient (+0.777) is found when all 103 analyses are used.

In summary normal magmatic differentiation or the process of metasomatism is not responsible for the overall above average radioactivity in the Pilot Lake area. However as will be shown in the next section magmatic and metasomatic processes may be responsible for slight distributional differences in uranium and thorium, as in the Pilot Lake Gneiss or local enrichment, as in Zone 4.

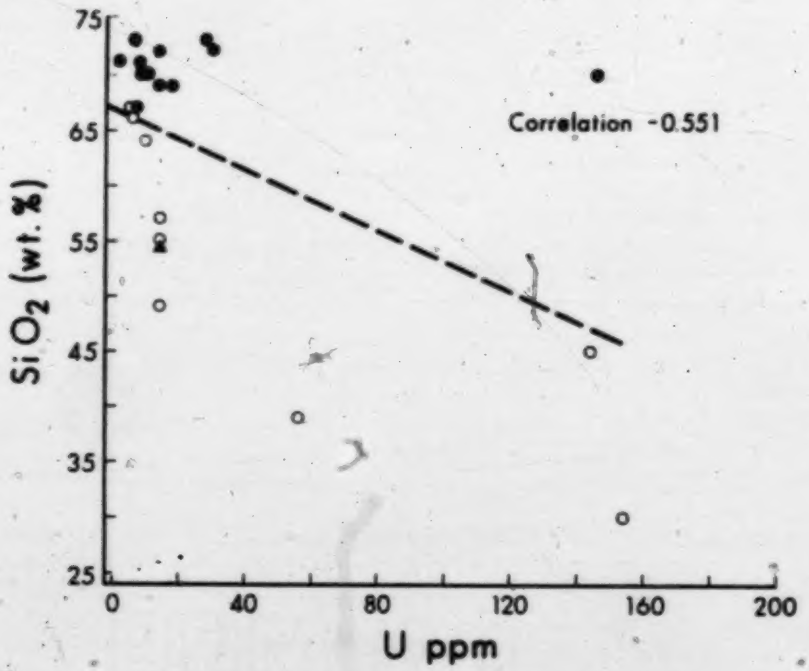

Fig. 26. Relation of uranium to SiO2.

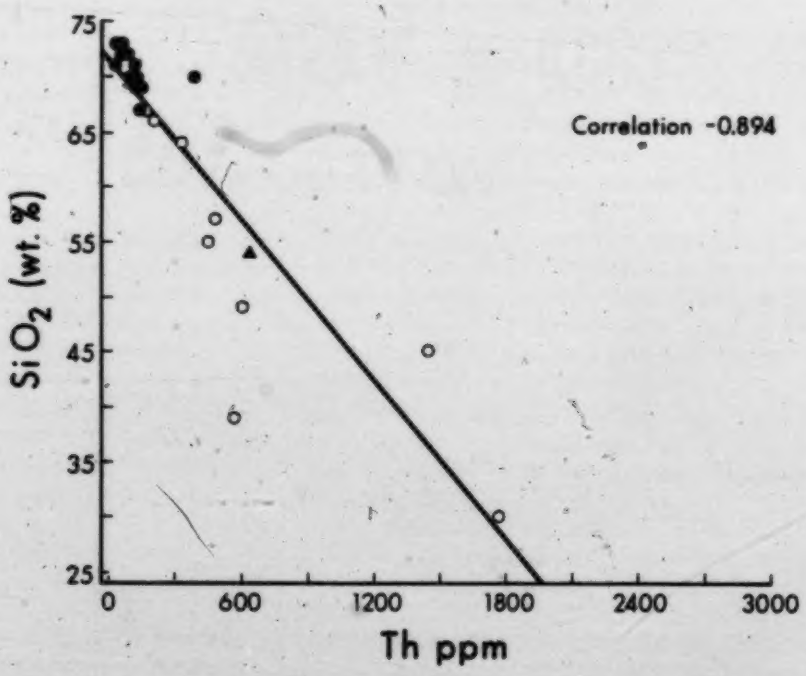

Fig. 27. Relation of thorium to SiO2.

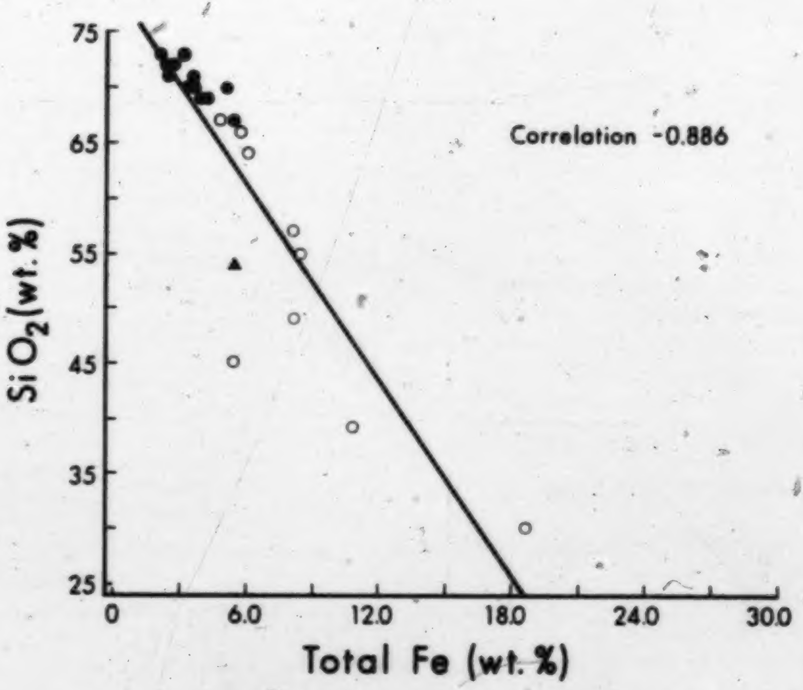

Fig. 28. Relation of total iron to SiO2.

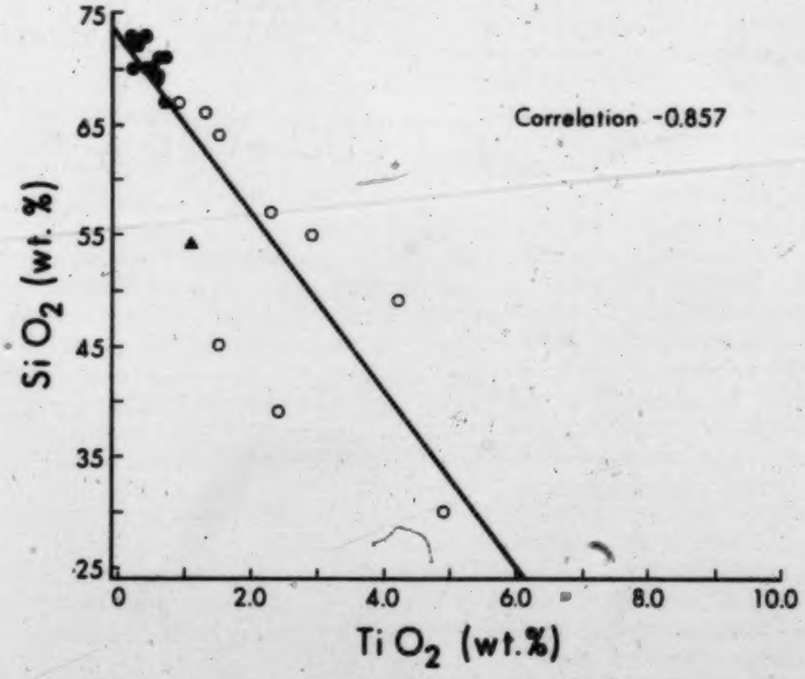

Fig. 29. Relation of TiO2 to SiO2.

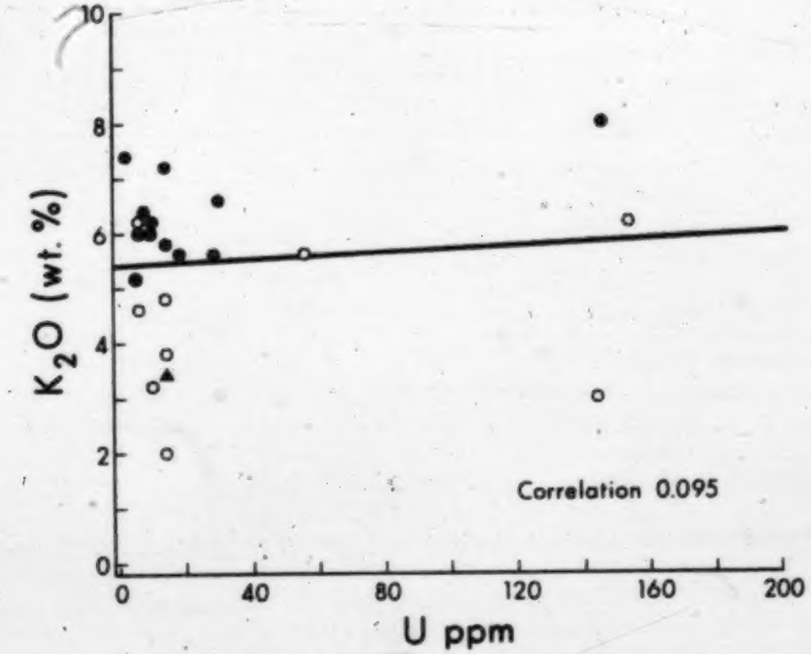

Fig. 30. Relation of uranium to K20.

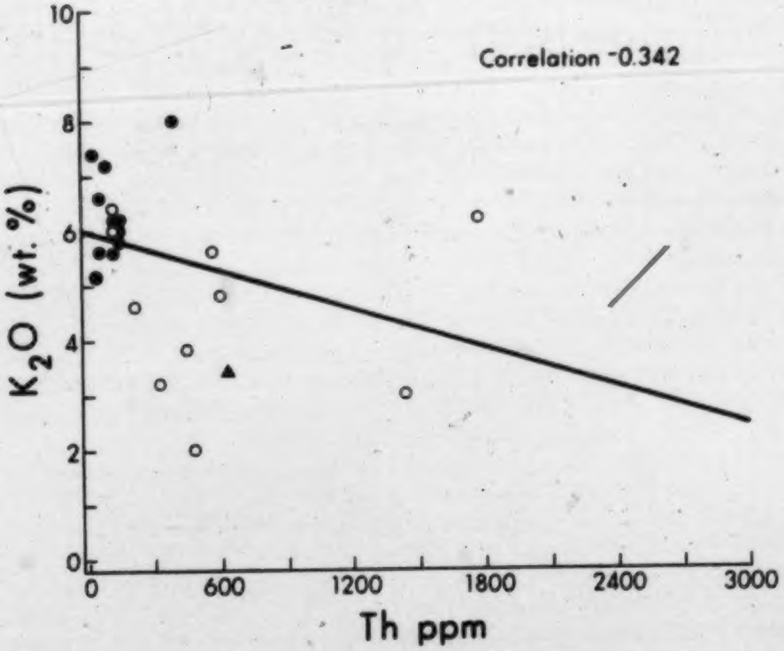

Fig. 31. Relation of thorium to K20.

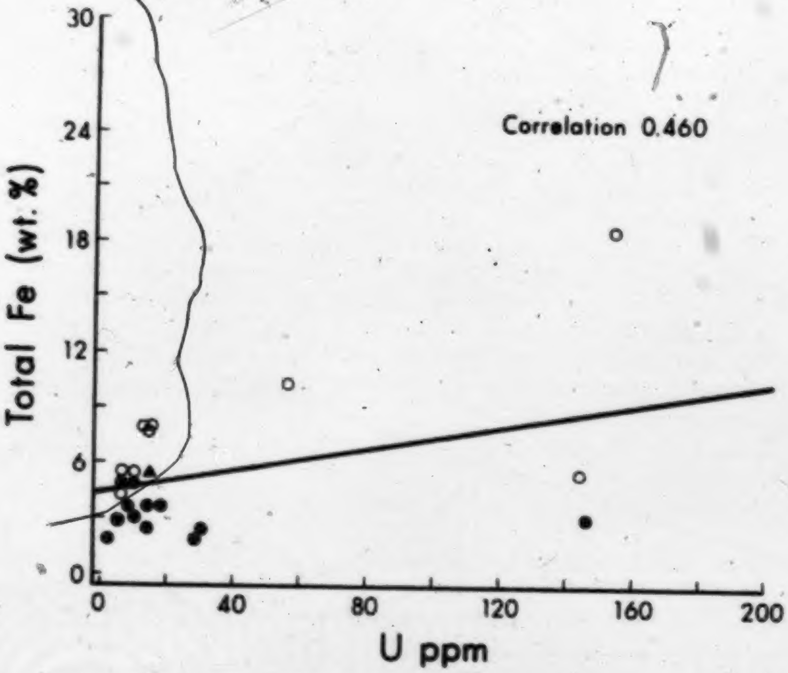

Fig. 32. Relation of uranium to total iron.

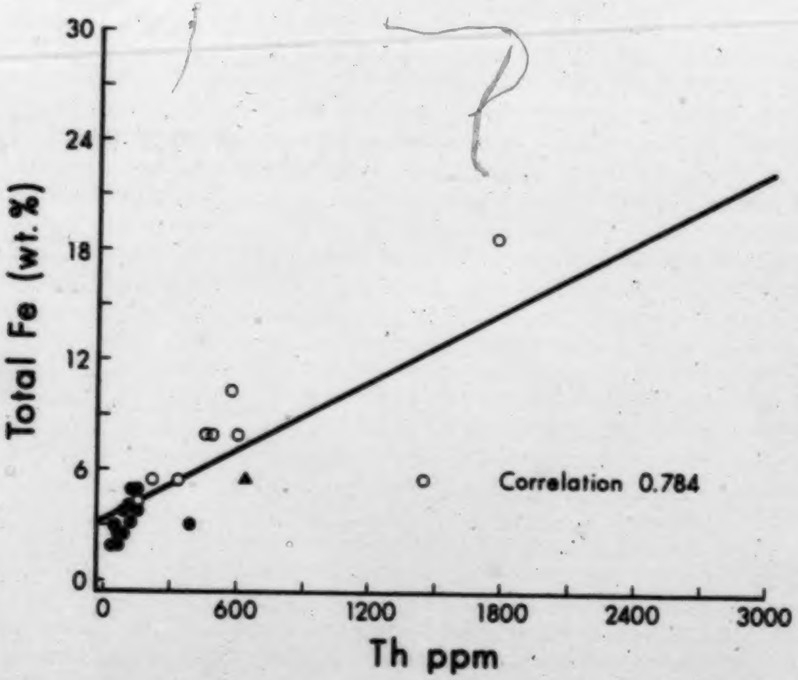

Fig. 33. Relation of thorium to total iron.

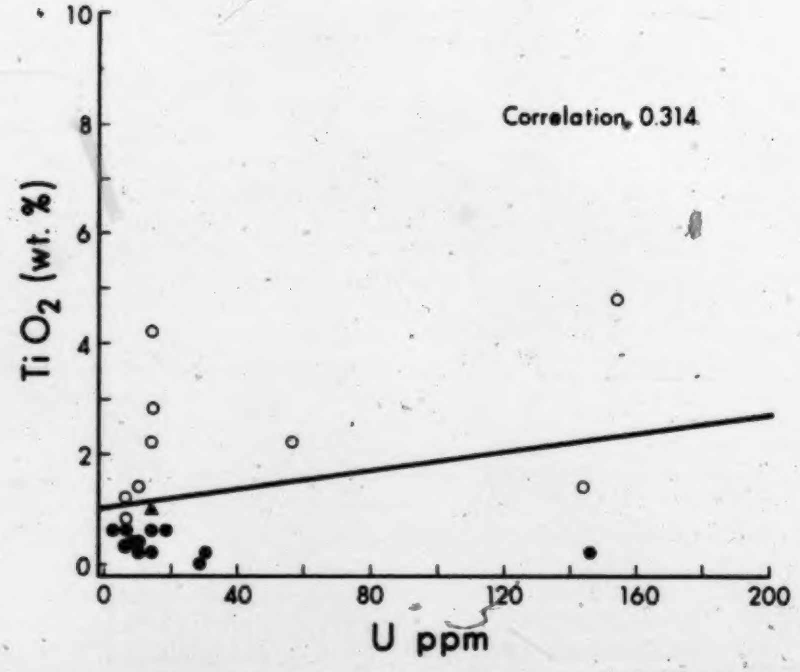

Fig. 34. Relation of uranium to TiO2.

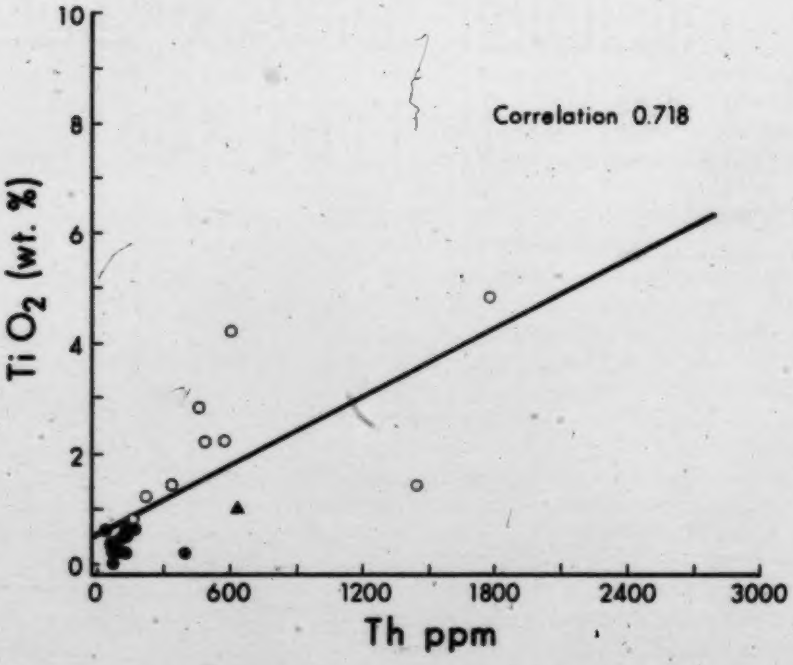

Fig. 35. Relation of thorium to TiO2.

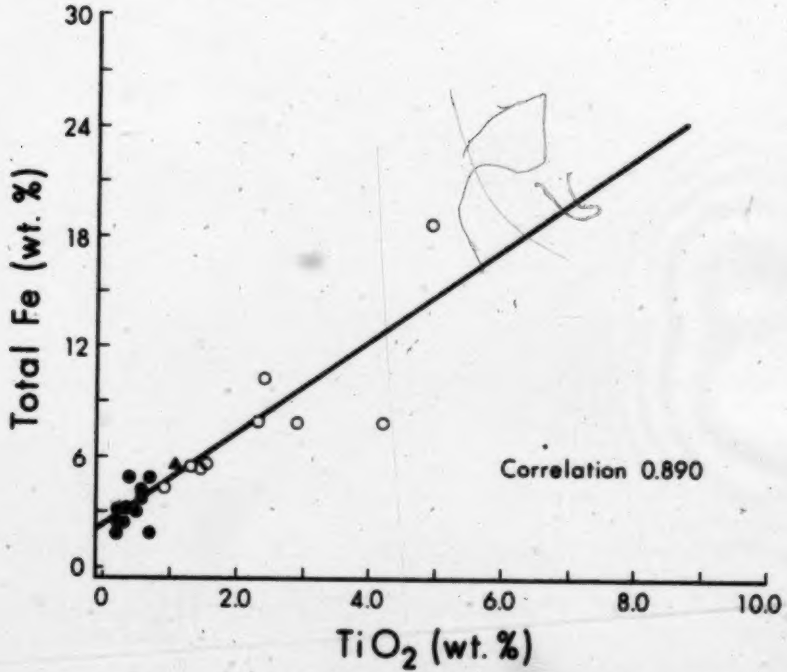

Fig. 36. Relation of TiO2 to total iron.

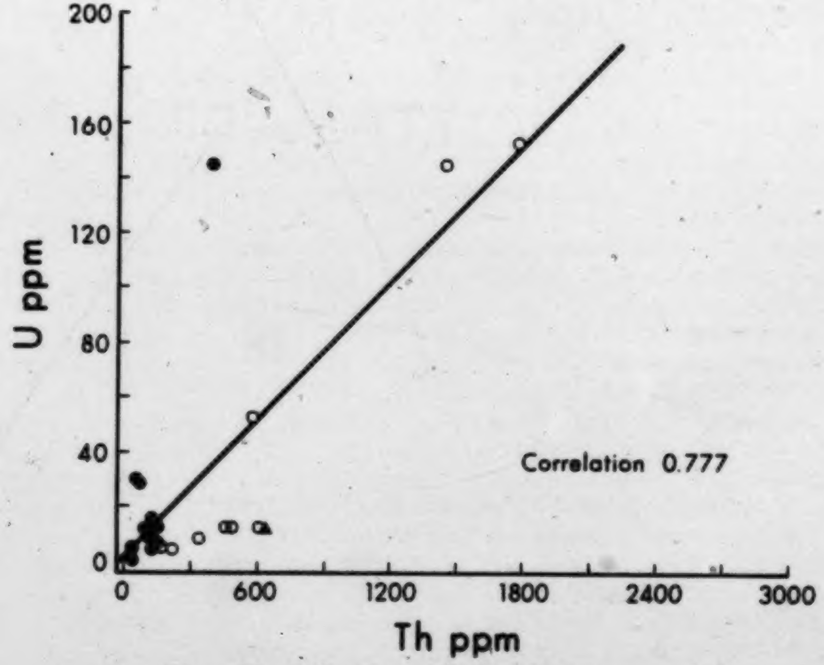

Fig. 37. Relation of thorium to uranium.

Petrogenesis of Uranium and Thorium Rich Rocks

Any explanation proposed for the cause of the above average radioactivity in the Pilot Lake area must explain the following:

1. Monazite as the only highly radioactive mineral;
2. The occurrences of local anomalously high values of uranium and thorium and concentrations of monazite;
3. The association of monazite with mafic minerals and thorium with titanium and total iron;
4. The poor correlations of uranium with all major oxides;
5. The high contents of uranium and thorium in the Pilot Lake Gneiss and the abrupt changes at the contacts with the variable paragneiss; and
6. The behaviour and distribution of uranium and thorium in the Pilot Lake Gneiss.

Zones One, Two and Three

Monazite, through careful petrographic and autoradiation work, has been established as the only highly radioactive mineral in the Pilot Lake area. It was found to be in abundance in all major rock types except the variable paragneisses. The presence of this thorium phosphate mineral in the Pilot Lake Gneiss and the high accumulations in Zones 1, 2 and 3 are perhaps reasons enough to account for the fact that the area is a thorium-rich belt.

Textural patterns, mineralogical associations and certain chemical correlations and compositions all contribute evidence suggesting a gravity accumulation of monazite in Zones 1, 2 and especially 3.

In Zone 3 small monazite grains are found in a heavy mineral association with zircons and abundant opaque minerals and their alteration products. The monazite grains show signs of recrystallization and the opaque minerals have been mobile during metamorphism, but the zircons appear to be most certainly of detrital origin. They are well rounded and although many are zoned, outer concentric growth rings have often been severed and worn, a feature that can only be attributed to the mechanical abrasion of the zircon during transportation and deposition in a sedimentary environment. Baadsgaard and Godfrey (1966) also indicate that the zircons in the gneisses of the Andrew Lake domain in northeastern Alberta are stable detrital pre-gneissic remnants.

Placer deposits of monazite of Recent age have been well documented in the literature. The concentration of monazite with other resistant heavy minerals such as ilmenite, magnetite, zircon, rutite, anatase and garnet in heavy sands is almost universal. The important concentrations in India, Brazil and the United States have yielded thousands of tons of monazite over the years (Overstreet 1967). Fossil placers have been recognized in Cretaceous formations in Colorado, Montana and New Mexico and Precambrian strata in Virginia, Michigan and the Blind River-Elliot Lake district of Ontario (Overstreet 1967). More recently Watkinson and Mainwaring (1975) suggest that premetamorphic placer deposits of monazite, oxides and apatite might have been the source for the Precambrian monazite occurrence at Kulyk Lake, Saskatchewan.

A heavy mineral detrital accumulation as an origin for the inclusion at Zone 3 would account for monazite occurring with heavy opaque minerals and zircon. The original opaques being predominately ilmenite would account for the extremely high titanium contents and the relationships between thorium, titanium, and total iron. The fact that monazite is the only radioactive mineral can possibly be attributed to an original source deficient in other uranium and thorium bearing minerals. However, the tendency for uranium to be oxidized to the comparatively soluble uranyl ion permitting uranium to be mobilized easily in surficial processes, allows for the loss of uranium-rich minerals during erosion, transportation and diagenesis. The absence of quartz and the extremely low silica content of the inclusion might be attributed to the maturity of the original placer.

It is interesting to note that Bell (1954, p. 104) says:

> "The monazite content of placer deposits is rarely more than 3 percent. It appears that the maximum concentrations of uranium and thorium in placer-type deposits are about 70 and 3000 ppm of sediment respectively."

The monazite concentration and uranium and thorium contents of the most radioactive parts of the inclusion in Zone 3 almost exactly match these figures.

In Zone 1 monazite preferentially occurs with apatite and in Zone 2 with apatite and biotite. Both zones occur exclusively within the paragneiss sequence although they have been affected through their proximity with the Pilot Lake Gneiss. The accumulation of apatite in these zones does present somewhat of a problem. Apatite is not particularly noted for its resistance to attrition during transportation with clastics. However, under favourable conditions it has become enriched with monazite in sands and gravels which have been transported short distances (Bell 1954). Apatite is known to occur widely as a heavy mineral in most Recent placer deposits (Overstreet 1967). Although a small occurrence, the mineralogical and chemical composition of Zone 2 suggests that it was perhaps originally a mud that had monazite and apatite deposited into it. Metamorphic segregation and recrystallization might account for some of the layering and difference in grain sizes of apatite and monazite within this zone.

Pilot Lake Gneiss and Zone Four

Certain field relationships suggest that the Pilot Lake Gneiss was emplaced as a magma into a superstructure of predominately clastic sediments. The inclusion of numerous large xenoliths of sedimentary origin and evidence of an original finer grained chilled contact on the eastern margins are suggestive of the emplacement of a magma.

The abrupt changes in radioactivity between the Pilot Lake Gneiss and both the bordering and included paragneissic material is evidence enough to prove the intrusive relationship. No process of insitu granitization of pre-existing sedimentary rocks could account for a selective enrichment of uranium and thorium in the Pilot Lake Gneiss in sharp contact with rocks either low or extremely high in radioactivity. The Pilot Lake Gneiss magma must have been anomalously high in uranium and thorium prior to emplacement.

The high contents of uranium and thorium in the Pilot Lake Gneiss must be accounted for through an original external source, as the processes of magmatic differentiation and late metasomatism have been ruled out. Such a source is available in situations similar to Zones 1, 2 and 3. That is, the incorporation of large amounts of uranium and especially thorium rich sediments into a magma, by total assimilation or anatexis of sediments containing uranium and thorium rich minerals, to produce a granitic melt.

The high Th/U in the Pilot Lake Gneiss (average 9.39) and the abundance of the mineral monazite are indication that monazite bearing sediments such as Zones 1, 2 and 3 have been incorporated into a magma prior to or during emplacement.

In chapter three the effects of partial assimilation and subsequent deformation were seen on a very local basis about the inclusion in Zone 3. If incorporation of larger amounts of material like that found in Zone 3 is responsible for the bulk of the uranium and more so the thorium in the

Pilot Lake Gneiss, similar effects on a regional basis should be evident. In fact the important chemical correlations that were found for all the data are the same for the Pilot Lake Gneiss itself. These are: thorium in excellent negative correlation with silica (Fig. 27), thorium in good positive correlation with total iron (Fig. 33) and titanium (Fig. 35).

One exception is the correlation between uranium and thorium which was shown in chapter two to be negative in the Pilot Lake Gneiss rather than positive for all data. Although magmatic differentiation is not responsible for the enrichment of uranium and thorium in the gneiss, magmatic processes have brought about a slight redistribution of uranium. Whitfield et al. (1959) have explained the independent action of uranium and thorium and the subsequent loss of uranium in granites through the ability of uranium to be oxidized to the more soluble hexavalent state during magmatic activity. Oxidized uranium could then enter the volatile phases and have migrated outward to its present position at the edges of the Pilot Lake Gneiss, as seen in Fig. 18. The overall red colour of the Pilot Lake Gneiss may indicate oxidizing conditions during magmatic activity. Oxidized uranium and subsequent redistribution and perhaps some eventual loss will account for uranium correlating poorly with all major oxides.

The process of metasomatism has been ruled out only as the cause for the overall above average radioactivity in the

Pilot Lake Gneiss. It however may be responsible for some of the present features noted in the Pilot Lake area. One such feature is the occurrence of Zone 4. As previously mentioned this zone is enriched in uranium but minimally enriched in thorium. The potassium content (8.03%) is the highest of all samples analysed. Thin sections indicate low contents of monazite compared to the other zones and the invasion of post-cataclastic quartz veins and rods into the heavily crushed rock. Therefore, it seems that uranium and potassium have migrated into this zone, perhaps a small shear, with silica, on a very local basis.

The development of large potassium feldspar porphyroclasts in granitic augen gneisses has long been a source for great debate. The potash feldspar in the Pilot Lake Gneiss is strongly perthitic and its relatively large size tends to give the rock a porphyroblastic aspect. However, thin sections reveal the large feldspars to be undulose and marginally granulated with crushed layers wrapping around their ends. Protected quartz and biotite inclusions are also features suggesting at least a pre-cataclastic origin. The elongated northerly trend of the Pilot Lake Gneiss indicates deformation with a compressional east-west axis at the time of emplacement. Potassium feldspar growth and alignment is perhaps contemporaneous with emplacement (trachytoid texture) resulting in true phenocrysts rather than porphyroblasts.

Summary

The Pilot Lake area was found to consist of an original superstructure of clastic sediments intruded by a granitic magma during a time of severe stress. Most rock types show the effects of polyphase metamorphism and cataclastic activity.

Detailed uranium and thorium analysis by delayed neutron activation confirmed the area to be part of a thorium-rich belt as indicated by a gamma-ray spectrometer survey flown by the Geological Survey of Canada (Darnley and Grasty 1970). Metasedimentary lithologies averaged 1.64 ppm uranium and 14.94 ppm thorium, slightly thorium-rich but fairly consistent with the average sedimentary rock and Precambrian Shield values. A granitic augen gneiss (the Pilot Lake Gneiss) averages 11.21 ppm uranium and 105.21 ppm thorium, considerably above most rocks possessing a granitic chemistry. Small, lenticular shaped zones containing abundant monazite which accumulated as placer deposits, often exceed 100 ppm uranium and 2000 ppm thorium. Assimilaton of these and similar deposits are responsible for the Pilot Lake Gneiss being monazite and thorium-rich.

The rather large granitic augen gneiss pluton is responsible for the broad anomalies disclosed by the airborne survey in the Pilot Lake area. Redistribution of uranium by magmatic activity within the Pilot Lake Gneiss has given rise to the narrow overlapping uranium anomaly at the edge of the broad thorium high. Small highly anomalous bodies of rock such as those found in Zones 1,2,3 and 4 may result in sharp thorium peaks on the flight profiles if involved in the coverage of a particular flight line.

SELECTED BIBLIOGRAPHY

Allan, J.A.S., and Weaver, C.E.
1958: Th to U ratios as indicators of sedimentary processes: Example of concept of Geochemical facies; Am. Assoc. Pet. Geol., Bull., v. 42, No. 2, p. 387-430.

Baadsgaard, H., and Godfrey, J.D.
1966: Geochronology of the Canadian Shield in northeastern Alberta, I. Andrew Lake area; Can. J. Earth Sci., v. 4, p. 541-563.

1972: Geochronology of the Canadian Shield in northeastern Alberta, II. Charles-Andrew-Colin Lakes area; Can. J. Earth Sci., v. 9, p. 863-881.

Bell, K.G.
1954: Uranium and thorium in sedimentary rocks; in Nuclear Geology, a symposium on nuclear phenomena in the earth sciences, ed. Henry Faul; John Wiley and Sons, Inc., New York, 414 p.

Burwash, R.A., and Cumming, G.L.
1976: Uranium and thorium in the Precambrian Basement of Western Canada I. Abundance and Distribution; Can. J. Earth Sci., v. 13. No. 2, p. 284-293.

Burwash, R.A., and Krupicka, J.
1969: Cratonic reactivation in the Precambrian basement of western Canada, I. Deformation and chemistry; Can. J. Earth Sci., v. 5, p. 1381-1396.

1970: Cratonic reactivation in the Precambrian basement of western Canada, II, Metasomatism and isostosy; Can. J. Earth Sci., v. 7, p. 1275-1294.

Burwash, R.A., Krupicka, J. and Culbert, R.R.
1973: Cratonic reactivation in the Precambrian basement of western Canada, III, crustal evolution; v. 10, p. 283-291.

Camsell, C.
1916: An exploration of the Tazin and Taltston Rivers, N.W.T; Geol. Surv. Can., Memoir 84.

Charbonneau, B.W.
1972: Gamma-ray support, District of Mackenzie, Geol. Surv. Can., Paper 71-1A, p. 40-46.

Charbonneau, B.W., Killeen, P.G., Carson, J.M., Cameron, G.W., and Richardson, K.A.
1976: Significance of radioelement concentration measurements made by airborne gamma-ray spectrometry over the Canadian Shield; in Exploration for Uranium Ore Deposits, Panel of a sym., Vienna, p. 35-53.

Cumming, G.L.
1974: Determination of uranium and thorium in meteorites by the delayed neutron method; Chem-Geol., v. 13, p. 257-267.

Darnley, A.G.
1970: Airborne gamma-ray spectrometry; Can. Inst. Min. Met., Trans., v. 73, p. 20-29.

1972: Airborne gamma-ray survey techniques-present and furture; in Uranium Exploration Methods, I.A.E.A. Panel. Proc. Ser., Vienna, p. 67-108.

1972: Airborne gamma spectrometry surveys in the areas of Elliot Lake, Ontario and Fort Smith, N.W.T.; Geol. Surv. Can., Paper 71-1A, p. 48-49.

Darnley, A.G., and Grasty, R.L.
1970: Geol. Surv. Can., Open File Report No. 101.

1971: Mapping from the air by gamma-ray spectrometry; Can. Inst. Min. Met., Spec. Vol. II, p. 485-500.

Darnley, A.G., Grasty, R.L. and Charbonneau, B.W.
1971: A radiometric profile across part of the Canadian Shield; Geol. Sur. Can., Paper 70-46, 42 p.

Day, W.
1975: Zircon Geochronology of Northeastern Alberta; unpublished MSc thesis, 50 p.

Eade, K.E. and Fahrig, W.G.
1971: Geochemical evolutionary trends of continental plates-A preliminary study of the Canadian Shield; Geol. Surv. Can., Bul. 179, 55 p.

Fyfe, W.S., Turner, F.J. and Verhoogen, J.
1958: Metamorphic reactions and metamorphic facies; Geol. Soc. Am., Mem. 73, 259 p.

Gabelman, J.
1977: Migration of uranium and thorium - exploration significance; Am. Assoc. Pet. Geol., Studies in Geology No. 3, 168 p.

Gale, N.H.

1967: Development of delayed neutron technique as rapid and precise method for deterinaton of uranium and thorium at trace levels in rocks and minerals with applicatons to isotope geochronology; Radioactive Dating and Methods of Low-level Counting, I.A.E.A. Vienna, p. 431-452.

Geol. Surv. Can.

1970: Geology and economic minerals of Canada; Economic Geology Report No. 1, ed. R.J.W. Douglas, 838 p.

Godfrey, J.D.

1961: Geology of the Andrew Lake, north district, Alberta; Res. Counc. Alta, Prelim. Rep. 58-3, 32 p.

1963: Geology of the Andrew Lake, South district, Alberta; Res. Counc. Alta, Prelim. Rep. 61-2 30 p.

1966: Geology of the Bayonet, Ashton, Potts, and Charles Lake district, Alberta; Res. Counc. Alta., Prelim Rep 65-6, 45 p.

Godfrey, J.D. and Peikert, E.W.

1963: Geology of the St. Agnes Lake district, Alberta; Res. Counc. Alta., Prelim. Rep. 62-1, 31 p.

1964: Geology of the Colin Lake district; Res. Counc. Alta., Prelim. Rep. 62-2, 28 p.

Godfrey, J.D. and Langenberg, C.W.

(in press): Metamorphism in the Precambrian Shield of northeastern Alberta.

Grasty, R.L. and Darnley, A.G.

1971: Calibration of gamma-ray spectrometers for ground and airborne use; Geol. Sur. Can., Paper 71-17.

Heier, K.S. and Rhodes, J.M.

1966: Thorium, uranium and potassium concentrations in granites and gneisses of the Rum Jungle Complex, Northern Territory, Australia; Econ. Geol., v. 61, p. 563-671.

Irvine, T.N. and Baragar, W.R.A.

1971: A guide to the chemical classification of the ccmmon volcanic rocks; Can. J. Earth Sci., v. 8, p. 523-548.

Kerr, P.F.
1959: Optical Mineralogy; Third edition, McGraw-Hill Book Co., New York, 442 p.

Killeen, P.G. and Heier, K.S.
1975: Trend surface analysis of Th, U, and K and heat production in three related granitic plutons, Farsund area, South Norway; Chem. Geol., 15, p. 163-176.

Krauskopf, K.B.
1967: Introduction to geochemistry; McGraw-Hill Book Co., New York, 721 p.

Krupicka, J. and Sassano, G.P.
1972: Multiple deformaton of crystalline rocks in the Tazin Group, Eldorado Fay Mine, N.W. Saskatchewan; Can. J Earth Sci., v. 9, p. 422-432.

Lambert, I.B. and Heier, K.S.
1967: The vertical distribution of uranium, thorium and potassium in the continental crust; Geochim. Cosmochim Acta, v. 31, p. 377-390.

Moorhouse, W.W.
1959: The Study of Rocks in Thin Section; Harper and Row Publishers, New York, 514 p.

Nockolds, S.R.
1954: Average chemical compositions of some igneous rocks; Geol. Soc. Am. Bull., v. 65, p. 1007-1032.

Overstreet, W.C.
1967: The geologic occurrence of monazite, U.S. Geol. Surv., Prof. Paper 530, 327 p.

Richardson, K.A. and Charbonneau, B.W.
1974: Gamma-ray spectrometry Investigatons, 1973; Geol. Surv. Can., Paper 74-1, Pt. A, p. 371-372.

Riley, G.C.
1960: Geology, Fort Fitzgerald, Alberta; Geol. Surv. Can. Map 12-1960, scale 1 in. to 4 miles.

Rodgers, J.J.W. and Adams, J.A.S.
1969: Uranium in Handbook of Geochemistry, V. II, ed. K.H. Wedepohl, Springer-Verlag, New York.

1969: Thorium in Handbook of Geochemistry, V. II, ed. K.H. Wedepohl, Springer-Verlag, New York.

Rogers, J.J.W., and Adams, J.A.S. and Gatlin B.
1965: Distribution of thorium, uranium, and potassium concentraton in three cores from the Conway granite, New Hampshire, U.S.A.; Am. J. Sci., 263, p. 817.

Rodger, J.J.W. and Raglan, P.C.
1961: Variation of thorium and uranium in selected granitic rocks; Geochim. Cosmochim. Acta, v. 25, p. 99-109.

Rose, E.R.
1969: Geology of titanium and titaniferous deposits of Canada; Geol. Surv. Can., Ec. Geol. Rep. 25, 177 p.

Ruzicka, V.
1971: Geological comparison between East European and Canadian uranium deposits, Geol-Sur. Can. Paper 70-48, 196 p.

Shaw, D.M.
1967: U, Th and K in the Canadian Precambrian Shield and possible mantle compositions; Geochim. Cosmochin. Acta, 31, p. 1111-1113.

Smith, T.E.
1974: The geochemistry of the granitic rocks of Halifax County, N.S.; Can. J. Earth Sci., v. 11, p. 650.

Spry, A.
1969: Metamorphic Textures; Pergamon Press, Oxford, 350 p.

Taylor, S.R.
1964: Abundance of chemical elements in the continental crust; Geochim. Cosmochim. Acta, v. 28, p. 1280-1281.

Tremblay, L.P.
1968: Geology of the Beaverlodge mining area; Geol. Surv. Can., Mem. 367, 468 p.

1970: The significance of uranium in quartzite in the Beaverlodge area, Saskatchewan; Can. J. Earth Sci., v. 7 p. 280-305.

Turekian, K.K. and Wedepohl, K.H.
1961: Distribution of elements in some major units of the earth's crust; Geol. Soc. Am. Bull. 72, p. 175-192.

Turner, F.J.
1968: Metamorphic Petrology, Mineralogical and Field Aspects; McGraw-Hill Book Co., New York, 403 p.

Watanabe, R.Y.
1966: Petrology of Cataclastic Rocks of Northeastern Alberta; unpublished Phd thesis, Univ. of Alberta, 219 p.

Watkinson, D.H. and Mainwaring, P.R.
1976: The Kulyk Lake monazite deposit, northern, Saskatchewan; Can. J. Earth Sci., v. 13, p. 470-475.

Whitfield, J.M., Rodgers, J.J.W. and Adams, J.A.S.
1959: The relationship between the petrology and the thorium and uranium contents of some granitic rocks; Geochim. Cosmochim. Acta, v. 17, p. 248-271.

Wilson, J.T.
1941: Geology, Fort Smith, N.W.T.; Geol, Surv. Can. Map 607A, scale 1 in. to 4 mile.

APPENDIX I

METHOD FOR DELAYED NEUTRON ACTIVATION ANALYSIS

APPENDIX I

METHOD FOR DELAYED NEUTRON ACTIVATION ANALYSIS

Uranium and thorium determination on 103 rock samples from the Pilot Lake area were carried out by delayed neutron activation analysis during two working sessions, (Nov. 1975 and March 1976) at the McMaster University Nuclear Reactor. The method of delayed neutron activation analysis described by Gale (1967) was adapted by Cumming (1974) for use at the McMaster swimming pool reactor. The theory underlying the method is given in these two papers.

In preparation slices of rock samples measuring approximately 3.5 cm in length 2.5 cm in width and 1.0 cm thick and corresponding exactly to a facing slice that was prepared for thin section work, were pulverized to a fine rock powder. Using corresponding rock slices, exact amounts of uranium and thorium could then be directly correlated with the mineralogy giving rise to these abundances. This would be particularly valuable for mineral identification if the radioelements were concentrated in very fine layers or veins or in small radioactive minerals scattered throughout a sample.

Five gram aliquots of the powdered sample are then sealed in polyethylene vials measuring 17 by 55 mm. The vial is placed in a 3 by 9.7 cm cylindrical polyethylene container (rabbit) which has coarse threaded screw caps on each end, so that removal of the sample container from the rabbit may be carried out as quickly as possible, after irradiation. The rabbit is then introduced into the reactor by means of a pneumatic transfer tube. Gale (1967) points out that the only fissionable nuclides are ^{232}Th, ^{235}U and ^{238}U. In a mixed thermal / fast neutron flux the thermal neutrons will fission ^{235}U and the fast neutrons will fission ^{238}U and ^{232}Th. Therefore it is necessary to irradiate each sample twice to obtain enough information to determine both uranium and thorium separately, once in a mixed flux and once with the sample inside a cadmium shield to screen out the thermal neutrons allowing only ^{232}Th and ^{238}U to fission. With the reactor operating at power of 1.5MW an irradiation time of 30 s was sufficient for most samples. However, 6 samples analysed during the first session were found to be considerably more radioactive than the average samples and were irradiated for 15 s to prevent the counters from being overloaded. The rabbit is then automatically returned to the counting area and the sample is rapidly removed, using remote handling apparatus, and dropped into the neutron counter.

Twenty-five seconds after ejection from the reactor, the neutrons emitted during a 64 s counting period were recorded. According to Cumming (1974) the 25 second delay (24 s of precision time delay following approximately 1 s transit time in the pneumatic rabbit system) minimizes the interference of delayed neutron emission by ^{9}Li (T1/2=0.17 s) and ^{17}N (T1/2=4.2 s). The counter is sufficiently shielded from any external neutrons by layers of cadmium and paraffin blocks. This resulted in an average background for the 64 s counting interval of a negligible 2 counts.

The uranium and thorium contents, where calculated by comparison with standard samples prepared by addition of known weights of pure uranium or thorium salts to an inert matrix. The uranium salt was checked for normal isotopic composition by Dr. H. Baadsgard. The formulas used for the calculation given by Gale (1967) and listed by Cumming (1974) are;

$$C = K\,U + k\,Th \qquad 1$$

$$S = K\,U/R + k\,Th/r \qquad 2$$

which on rearrangement become

$$U = \frac{C/r - S}{K(1/r - 1/R)} \qquad 3$$

$$Th = \frac{S - C/R}{k(1/r - 1/R)} \qquad 4$$

Where U and Th are uranium and thorium respectively, C and S are unshield and shielded counts respectively, K and k are the calibration-constants in counts per microgram for natural U and Th respectively. R and r are the cadmium radio in the reactor neutron flux for natural U and Th respectively (ie. unshielded counts/ shielded counts). The following parameters were then applied to the calculations:

Session Irradiation Time	Nov. 1975		March 1976
	30 S	15 S	30 S
K	190.8±0.90 (0.47%)	118.3±1.18 (1.0%)	192.30±4.58 (2.38%)
R	28.35±.45 (1.04%)	26.56±.8 (2.0%)	24.8±1.194 (4.81%)
k	1.535±.016 (1.59%)	0.986±.02 (3.0%)	1.576±.0536 (3.4%)
r	1.003±.022 (2.19%)	1.055±.053 (5.0%)	1.021±.04 (3.97%)

The errors quoted for the 30 s irradiations are the result of 5 standard runs during each session. The errors reflect the unavoidable fluctuations in neutron flux within the reactor as control rods were inserted or withdrawn during the working periods.

As only one standard run was taken during the 15 s irradiation errors of 1.0, 2.0, 3.0 and 5.0% were chosen for K, R, k and r respectively. These values are considerably above the precision limits for the first session and therefore, were deemed appropriate.

It can be seen from the parameters used that the analysis during the first session, when the majority of samples were run (68 samples or 66%), was more precise and accurate then the second session. As a rule precision in analysing uranium was better than that for thorium.

APPENDIX II

IDENTIFICATION OF RADIOACTIVE MINERALS

APPENDIX II

IDENTIFICATION OF RADIOACTIVE MINERALS

When it became apparent that the identification of radioactive minerals was difficult by standard petrographic methods, it was decided to investigate the heavy mineralogy by means of separation and autoradiograph techniques. Sample 8-5c, the most radioactive sample collected, and containing an abundance of heavy minerals, was reduced to a fine rock powder by jaw crushing and the use of a rotary plate mill. Minerals were then separated using standard techniques of magnetic separation; tetrabromoethane, methylene iodide and hot clerici float-sink separation; and nitric acid washing. Individual heavy mineral separates were then studied petrographically and mounted for autoradiograph work. A selected set of thin sections representing all rock types with above average radioactivity were also prepared for autoradiograph work. The autoradiographs were done by exposing individual dental x-ray plates to mounted heavy grain separates and uncovered thin sections. A 6 day exposure was found to give optimum results. These methods allowed for the positive identification of the petrographically similar minerals zircon and monazite and revealed characteristics about each that made further identification without these methods simpler. It was also positively established that monazite was the only radioactive mineral.

Also identified by separation techniques was the titanium mineral anatase, which was almost totally unidentifiable in thin section because of its opaque surroundings. When separated and acid washed anatase was seen to be in excellent euhedral form, dark red brown to black, tetragonal and uniaxial negative.

The following Table indicates some of the differing characteristics of zircon and monazite in the Pilot Lake area.

Characteristic	Zircon	Monazite
Magnetic property	Non magnetic at 1.6A	Magnetic at 0.08A
Form	well rounded	subrounded to rounded
colour	colourless to pale purple	pale yellow
radioactivity	Non radioactive-no photographic plate destruction	Radioactive-photographic plate destruction
average grain size	0.1 mm	0.1-0.2 mm
In thin section		
relief	higher of the two	lower of the two
texture	blotchy	even
internal structure	zoned	none
external structure	fracturing of host minerals	heavy rimming by hematite
inclusions	small rare opaques	zircon